



# QEX

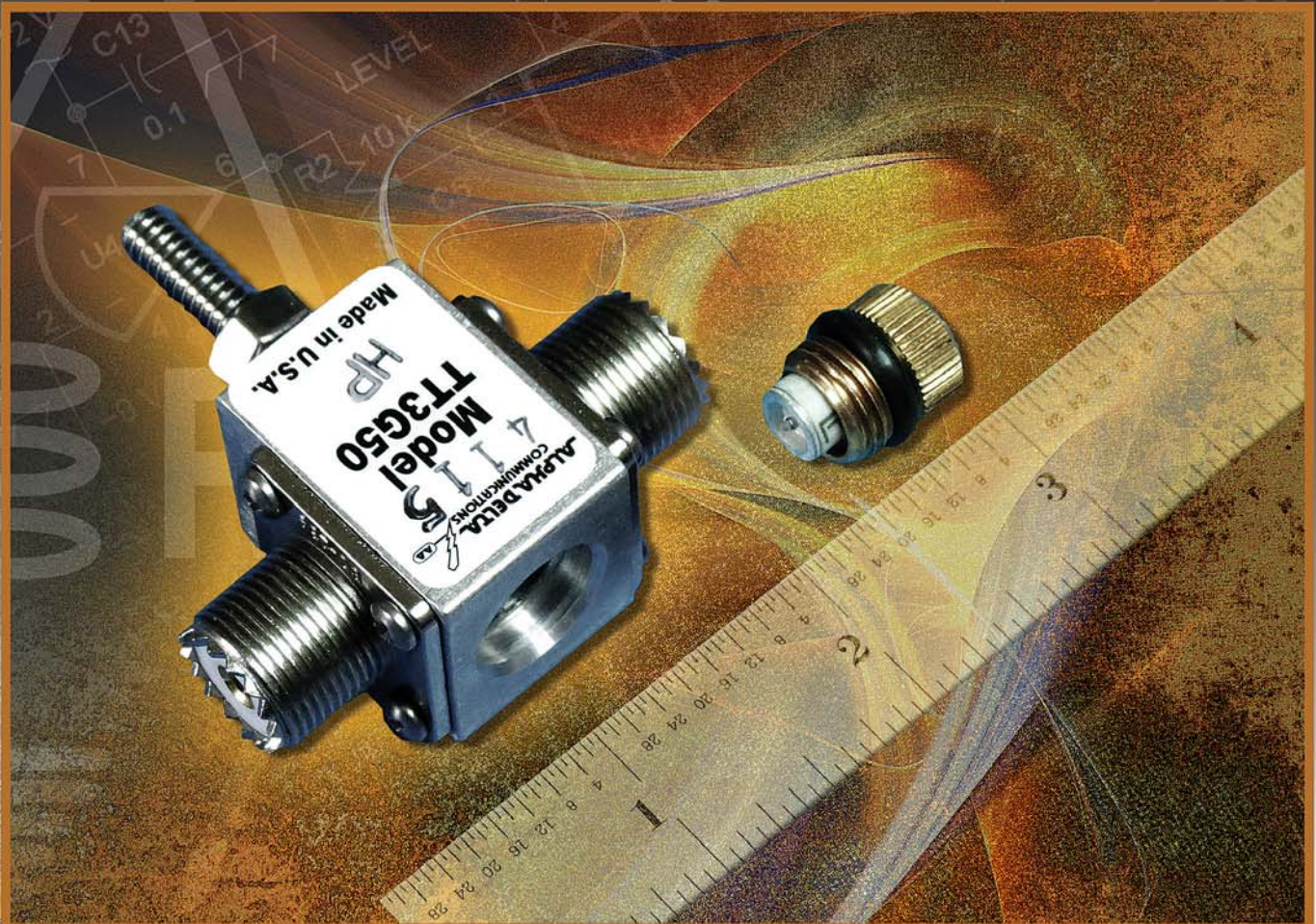
\$5

July/August 2016

[www.arrl.org](http://www.arrl.org)

## A Forum for Communications Experimenters

Issue No. 297



**K5PA** shows how to keep your RF surge suppressor from arcing over on transmitter power peaks.



# Taking HF By Storm



The TS-480HX

**KENWOOD**

Customer Support: (310) 639-4200  
Fax: (310) 537-8235



Scan with your phone to  
download TS-480HX brochure.

[www.kenwood.com/usa](http://www.kenwood.com/usa)



ISO9001 Registered  
JVCENWOOD Corporation

UKAS  
QUALITY SYSTEM  
JQA-1205  
001

ADS#27315





QEX (ISSN: 0886-8093) is published bimonthly in January, March, May, July, September, and November by the American Radio Relay League, 225 Main Street, Newington, CT 06111-1494. Periodicals postage paid at Hartford, CT and at additional mailing offices.

POSTMASTER: Send address changes to: QEX, 225 Main St, Newington, CT 06111-1494 Issue No 297

*Publisher*  
American Radio Relay League

Kazimierz "Kai" Siwiak, KE4PT  
*Editor*

Lori Weinberg, KB1EIB  
*Assistant Editor*

Zack Lau, W1VT  
Ray Mack, W5IFS  
*Contributing Editors*

**Production Department**

Steve Ford, WB8IMY  
*Publications Manager*  
Michelle Bloom, WB1ENT  
*Production Supervisor*  
Sue Fagan, KB1OKW  
*Graphic Design Supervisor*

David Pingree, N1NAS  
*Senior Technical Illustrator*  
Brian Washing  
*Technical Illustrator*

**Advertising Information Contact:**

Janet L. Rocco, W1JLR  
*Business Services*  
860-594-0203 – Direct  
800-243-7768 – ARRL  
860-594-4285 – Fax

**Circulation Department**

Cathy Stepina, QEX Circulation

**Offices**

225 Main St, Newington, CT 06111-1494 USA  
Telephone: 860-594-0200  
Fax: 860-594-0259 (24 hour direct line)  
e-mail: [qex@arrl.org](mailto:qex@arrl.org)

**Subscription rate for 6 issues:**

In the US: ARRL Member \$24, nonmember \$36;

US by First Class Mail: ARRL member \$37, nonmember \$49;

International and Canada by Airmail: ARRL member \$31, nonmember \$43;

Members are asked to include their membership control number or a label from their QST when applying.

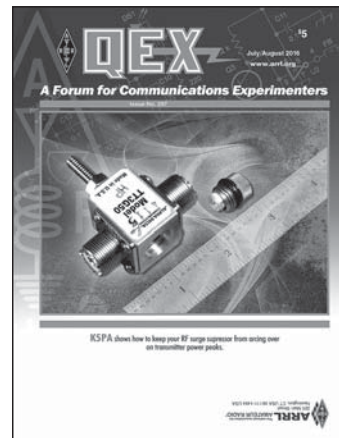
In order to ensure prompt delivery, we ask that you periodically check the address information on your mailing label. If you find any inaccuracies, please contact the Circulation Department immediately. Thank you for your assistance.



Copyright © 2016 by the American Radio Relay League Inc. For permission to quote or reprint material from QEX or any ARRL publication, send a written request including the issue date (or book title), article, page numbers and a description of where you intend to use the reprinted material. Send the request to the office of the Publications Manager ([permission@arrl.org](mailto:permission@arrl.org)).

**About the Cover**

Gene Hinkle, K5PA, provides a methodology to calculate the peak voltage with reactive loads on surge suppression devices that are typically mounted at the base of an antenna or at the coaxial entry point of the radio site. He relates the voltages with reactive loads to suppressor ratings.



**In This Issue**

**Features**

**2 Perspectives**  
Kazimierz "Kai" Siwiak, KE4PT

**3 Radio Frequency (RF) Surge Suppressor Ratings for Transmissions into Reactive Loads**  
Gene Hinkle, K5PA

**7 The Case of Declining Beverage-on-Ground Performance**  
Rudy Severns, N6LF

**20 A PLL Based Stand Alone Signal Generator with I and Q Outputs**  
Charles Templeman, W2EHE

**23 Zolotarev Low-Pass Filter Design**  
Gary Cobb, G3TMG

**30 Hands-On-SDR**  
Scotty Cowling, WA2DFI

**35 Letters to the Editor**

**Index of Advertisers**

ARRL.....	Cover III	Quicksilver Radio Products.....	Cover IV
Down East Microwave Inc:.....	36	RF Parts:.....	33, 35
DX Engineering: .....	19	Roger Palmer, VE7AP .....	22
Kenwood Communications: .....	Cover II	Tucson Amateur Packet Radio: .....	18
Nemal Electronics International, Inc:.....	36		

## The American Radio Relay League



The American Radio Relay League, Inc. is a noncommercial association of radio amateurs, organized for the promotion of interest in Amateur Radio communication and experimentation, for the establishment of networks to provide communications in the event of disasters or other emergencies, for the advancement of the radio art and of the public welfare, for the representation of the radio amateur in legislative matters, and for the maintenance of fraternalism and a high standard of conduct.

ARRL is an incorporated association without capital stock chartered under the laws of the state of Connecticut, and is an exempt organization under Section 501(c)(3) of the Internal Revenue Code of 1986. Its affairs are governed by a Board of Directors, whose voting members are elected every three years by the general membership. The officers are elected or appointed by the Directors. The League is noncommercial, and no one who could gain financially from the shaping of its affairs is eligible for membership on its Board.

"Of, by, and for the radio amateur," ARRL numbers within its ranks the vast majority of active amateurs in the nation and has a proud history of achievement as the standard-bearer in amateur affairs.

A *bona fide* interest in Amateur Radio is the only essential qualification of membership; an Amateur Radio license is not a prerequisite, although full voting membership is granted only to licensed amateurs in the US.

Membership inquiries and general correspondence should be addressed to the administrative headquarters:

ARRL  
225 Main Street  
Newington, CT 06111 USA  
Telephone: 860-594-0200  
FAX: 860-594-0259 (24-hour direct line)

### Officers

**President:** Rick Roderick, K5UR  
PO Box 1463, Little Rock, AR 72203

**Chief Executive Officer:** Tom Gallagher, NY2RF

The purpose of *QEX* is to:

- 1) provide a medium for the exchange of ideas and information among Amateur Radio experimenters,
- 2) document advanced technical work in the Amateur Radio field, and
- 3) support efforts to advance the state of the Amateur Radio art.

All correspondence concerning *QEX* should be addressed to the American Radio Relay League, 225 Main Street, Newington, CT 06111 USA. Envelopes containing manuscripts and letters for publication in *QEX* should be marked Editor, *QEX*.

Both theoretical and practical technical articles are welcomed. Manuscripts should be submitted in word-processor format, if possible. We can redraw any figures as long as their content is clear. Photos should be glossy, color or black-and-white prints of at least the size they are to appear in *QEX* or high-resolution digital images (300 dots per inch or higher at the printed size). Further information for authors can be found on the Web at [www.arrl.org/qex/](http://www.arrl.org/qex/) or by e-mail to [qex@arrl.org](mailto:qex@arrl.org).

Any opinions expressed in *QEX* are those of the authors, not necessarily those of the Editor or the League. While we strive to ensure all material is technically correct, authors are expected to defend their own assertions. Products mentioned are included for your information only; no endorsement is implied. Readers are cautioned to verify the availability of products before sending money to vendors.

Kazimierz "Kai" Siwiak, KE4PT

## Perspectives

### Guest Comment from the CEO

I will be honored to add an editorial contribution to *QEX* from time to time, and I thank Kai for the opportunity in advance. *QEX* is a publication that I have admired for many years. I claim to be an inveterate tinkerer. I have always enjoyed building things if only for the pure satisfaction of actually completing a project. In that pursuit, we probably share a common goal. My interests are eclectic, and they range from tube transmitters to VHF-and-above antennas. In south Florida, having limited space for HF arrays, my transmitter and antenna tinkering is confined to the garage. Of course, the common element is RF burns.

Recently, I have become involved with high-speed multimedia at 2.4 GHz (of the kind described in Glen Popeil's new book recently published by ARRL), experimenting with extended shots down straight, long Florida highways and long shots over water — 16 miles in one case — creating mesh networks utilizing VOIP and slow scan video. I've built specialized antennas for that band, added power amplification and measured the impact on propagation of changing temperature, humidity and vegetation. The latter three items are abundantly available in south Florida! I also enjoy repurposing commercial, off-the-shelf devices to serve Amateur Radio functions.

The highest and best use of our amateur grants lies in experimentation, pushing forward the frontiers of our specialized know-how. Only through this activity can we ensure the preservation of our various spectrum allocations — by using them and determining their possibilities. I urge you to continue exploring the limits of our avocation. Exploration has always been the hallmark of *QEX*'s readers. So please count on my support for your larger efforts. Thanks so much for being a subscriber to *QEX*; and let me know how I can help by writing to me at [ny2rf@arrl.org](mailto:ny2rf@arrl.org).

Kindest personal regards, 73  
Tom Gallagher, NY2RF  
Chief Executive Officer, American Radio Relay League

### In This and Future Issues of *QEX*

Remember that the content of *QEX* is driven by you, the reader and prospective author. If you don't write it, we can't share it with your fellow readers. So please, put your favorite topic or innovative measurement on paper, and share it on these pages. Just follow the details on the [www.arrl.org/qex-author-guide](http://www.arrl.org/qex-author-guide) web page, and contact us at [qex@arrl.org](mailto:qex@arrl.org). We value your feedback, comments and opinions about these pages.

Our *QEX* authors describe and analyze PLLs, oscillators, Beverage antennas, crystals, RF filters and coaxial components. Charles Templeman, W2EHE, features PLLs in this general purpose stand-alone signal generator that produces precise quadrature signals, and can support SDR projects from 160 m to 6 m. Rudy Severns, N6LF, uses measurements to validate NEC analysis, and explains the performance decline of a Beverage-on-the-ground antenna. Fred Brown, W6HPH, built universal oscillators that can test a wide range of fundamental and overtone crystals. Gary Cobb, G3TMG, explains the filter approximation problem relating to the synthesis of Zolotarev low-pass functions with finite zeros. Gary Appel, WA0TFB, shows how to modify staggered LC resonators to implement the filter poles and simplify the tuning of the staggered filter, removing the need for high bandwidth operational amplifiers. Gene Hinkle, K5PA, reviews RF surge suppressor ratings to help keep transmissions into reactive loads from arcing over. Scotty Cowling, WA2DFI, returns this month with his SDR column.

Please continue to support *QEX*, and help it remain a strong technical publication.

73,  
Kazimierz "Kai" Siwiak, KE4PT

# Radio Frequency (RF) Surge Suppressor Ratings for Transmissions into Reactive Loads

*Keep your RF surge suppressor from arcing over on transmitter power peaks.*

Surge suppression devices in RF systems are typically mounted either at the base of an antenna or at the coaxial entry point at the radio site. They provide a direct path across the antenna terminals suppressor control short voltage spikes that should be grounded. One common surge suppressor is the Alpha Delta TT3G50UHP shown in Figure 1.<sup>1</sup> The purpose of this technical note is to provide a methodology to calculate the peak voltage when the impedance and power are known. One software tool useful for the calculation is the *Transmission Line for Windows (TLW)* program provided by the ARRL.<sup>2</sup> TLW is distributed in current editions of *The ARRL Antenna Book*.<sup>3</sup>

## Background

Surge protectors typically have coaxial terminals — Type N, BNC, or UHF connectors — and a removable/replaceable cartridge consisting of a ceramic, vacuum discharge tube. Grounding of the suppressor is provided by using a screw terminal. The surge protector use a removable cartridge — called an Arc-Plug™ by Alpha Delta — consisting of a metal threaded piece housing the vacuum discharge tube whose rating determines the power rating for the unit. The discharge tubes can also be changed out after a high energy surge event. The discharge tubes are considered a consumable device. Therefore, the end-user has an opportunity to tailor the part numbers depending on power capabilities of the surge device.

If an antenna is well matched at the connection point to the coaxial cable, the voltages presented across the connection are calculated using a variation of Ohm's Law,

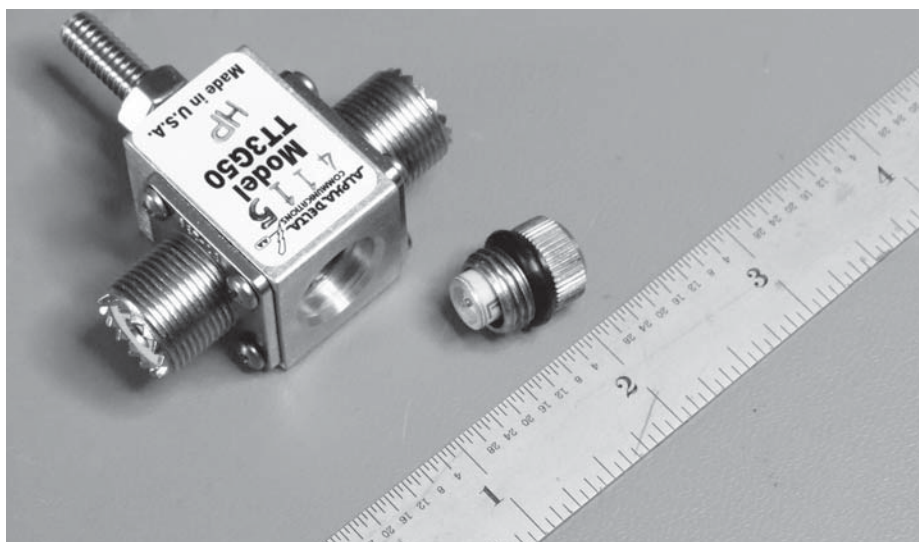


Figure 1 —The model TT3G50UHP surge protector from Alpha Delta.

$$V_{pk} = \sqrt{R \times 2 \times PWR} \quad (1)$$

In 50  $\Omega$  impedance systems this is equal to

$$V_{pk} = 10\sqrt{PWR}$$

For example, with 1000 W at the antenna terminals and a 50  $\Omega$  match, the peak voltage equals 316 V. The surge suppressor must withstand this voltage without arcing over during normal transmissions.

The sporadic shutting down of my medium power amplifier during SSB operation first aroused my interest in the surge suppressor characterization. As my trouble shooting unfolded, I found what appeared to be voltage breakdown events within the antenna system.

Although this could be attributed to a bad coax, connectors, antenna switches, antenna connections or the antenna itself, my final analysis lead me to the RF surge protection device. I discovered that the rating of the surge suppressor was too low for my peak transmitted power and SWR on the transmission line. At the time the voltage breakdown occurred, the amplifier would indicate a high SWR event on the line and automatically shut down, thus protecting its circuits.

In typical installations, the impedance of the antenna system is not well matched, and in fact, in many instances there are impedance matching devices that matches the radio to the coax and antenna system. The impedance is complex — it has both a resistive and reactive



components — and varies with frequency. This creates a peak voltage across the surge suppressor based on the RF frequency, the complex impedance, and transmitted power. The mismatched impedance creates standing waves on the transmission line that modifies the peak voltages present on the line and is characterized by the Standing Wave Ratio (SWR).

### Terminology

During researching this topic, I noted that manufacturers used their own terminology to describe their products. Some of these terms are listed in Table 1. I will try to be careful to use their terminology when describing this technology.

### Surge Suppressors and Vacuum Discharge Tubes

The Alpha Delta Model TT3G50 and the predecessor Transi-Trap model coaxial surge protectors use a replaceable vacuum discharge tube to provide protection across the transmission line. The discharge tubes are manufactured by several vendors, including EPCOS and Littelfuse. When the discharge tubes have outlived their service life, they should be removed and replaced with one of the same part number. After multiple strikes, the discharge tubes can become shorted and create a high SWR condition on the transmission line. A direct strike cannot

be protected as the tubes would likely be destroyed. My station encountered a near strike while using the Transi-Trap surge protector. It did protect the front end of the transceiver. Other equipment like light dimmers, stereos, and TV's did not do so well.

The EPCOS<sup>4</sup> and Littelfuse<sup>5</sup> discharge tubes can be delivered in a capsule or axial wire lead format. The axial leads must be carefully snipped leaving just the capsule for insertion into the Arc-Plug™ mechanical assembly. Insertion of the new tube and replacement of the screw cap must be done carefully, and hand tightened so as not to over-tightened the screw cap. Figure 2(a) shows an example of the axial lead device, and Figure 2(b) shows its schematic symbol.

Replacement vacuum discharge tubes can be obtained from electronic distributors on the internet such as Digi-Key<sup>6</sup> and Mouser Electronics<sup>7</sup> for a few dollars (\$US) each. This makes it very economical to provide replacements during maintenance, or to change the ratings of the RF surge protector assembly.

Table 2 lists the RF surge protector models from Alpha Delta, along with the vacuum discharge tube installed, based on my inspection of the part numbers and the specification of the vacuum discharge tube.

### Voltage Across an Impedance

In a 50 Ω impedance system, the rms voltage across the load is

$$V_{rms} = \sqrt{50 \times PWR}$$

where *PWR* is the RF power, W, and the characteristic impedance of the transmission line is 50 Ω. Multiply *V<sub>rms</sub>* by the square root of 2 to obtain the peak voltage, as given by Eq (1).

When including the *SWR* on the line, the peak voltage becomes<sup>8</sup>

$$V_{pk} = \sqrt{100 \times PWR \times SWR} \quad (2)$$

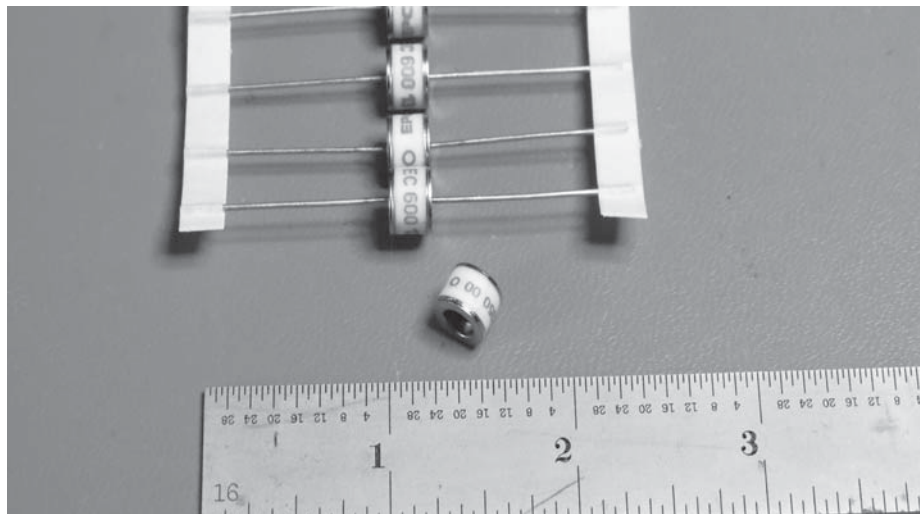
This peak voltage must not break down the discharge tube protecting the transmission line from surges.

**Table 1**  
Terminology used by different manufacturers and vendors.

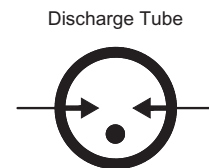
Company	Terminology	Product Guide
Alpha Delta	(1) Transi-Trap Surge Protector (2) Arc-Plug™ cartridge	See Note 1 See Note 1
EPCOS	Gas-filled surge arresters	See Note 4
Littelfuse	Gas Discharge Tube (GDT)	See Note 5

**Table 2**  
RF surge protectors and discharge tubes.

Manufacturer	Manufacturer Model No	Power Capability (Vendor Data)	P/N	DC Voltage Breakdown	Impulse Spark-over @1 kV/μS Typ.	Single Pulse Discharge Current
Alpha Delta	TT3G50	200 W	EPCOS, EC350-00 O	350 VDC	< 800 V	10 kA
Alpha Delta	TT3G50HP	2000 W	Littelfuse, CG2-1000	1000 VDC Typ.	< 1600 V	10 kA
—	—	500 W	EPCOS EC-600 B88069X0780S102	540 to 720 600 Vdc nom.	< 1100 V	10 kA



←Figure 2(a) — Axial lead format of EPCOS discharge tube.



QX1607-Hinkle02b

Figure 2(b) — Discharge tube schematic symbol.

## Using TLW Software

The Table 3 shows the peak voltage at various load impedance values and power levels. A very short length of RG-213 coaxial cable is assumed since anything longer would be more conservative if the surge protection device were mounted at the antenna. If surge protection device is mounted at the transmitter, the longer transmission line has the effect of reducing the actual SWR of the antenna due to the line loss at the operating frequency. The software program *TLW* is quite useful for calculating the SWR and impedance across the transmission lines. I used *TLW* to create the values in Table 3.

The *TLW* software program provides several screens, see Figure 3, that make it easy to input your antenna impedance, transmission line characteristics like type, impedance, and length, the RF power and the matching networks, see Figure 4.

The antenna impedance can be measured with a Vector Impedance Analyzer (VNA) — I used the Array Solutions AIM-4170C — but an RF noise bridge would also work. If these transmission parameters are not known, then use just the SWR. The value of using *TLW* is to understand the variation of the peak currents and peak voltages, see Figure 5, as you move along the transmission line, and to calculate other parameters such as additional loss due to SWR.

Other values of the peak voltage may be calculated directly using Eq (2). Note that the expression for peak voltage can also be rewritten so it expresses the power level and SWR that the discharge tube can withstand. Thus, the maximum power that can be safely applied, given the peak voltage rating of the discharge tube and SWR is

$$PWR_{max} = \frac{V_{pk}^2}{100 \times SWR} \quad (3)$$

Thus, for a discharge tube rated at 1000 V and with an SWR of 10, the maximum power that could be applied is 1000 W, and for a vacuum discharge tube rated at 350 V and with SWR of 10, the maximum power

would be 122 W.

I applied Eq (1) – (3) to the vendor data and listed my recommendations in Table 4.

## Summary and Lessons Learned

With the help of Eq (2) and (3), the Amateur Radio operator can select the correct rating of surge suppressors discharge tube to use with RF surge protection devices.

Applying the formulas to the commercially available Alpha Delta TT3G50 and TT3G50HP surge suppressors indicate a maximum power at 5:1 SWR of 245 W and 2000 W, respectively. Using an alternate vacuum discharge tube device shows that the breakdown power can be increased and therefore tailored to the RF power requirements of your transmitter system.

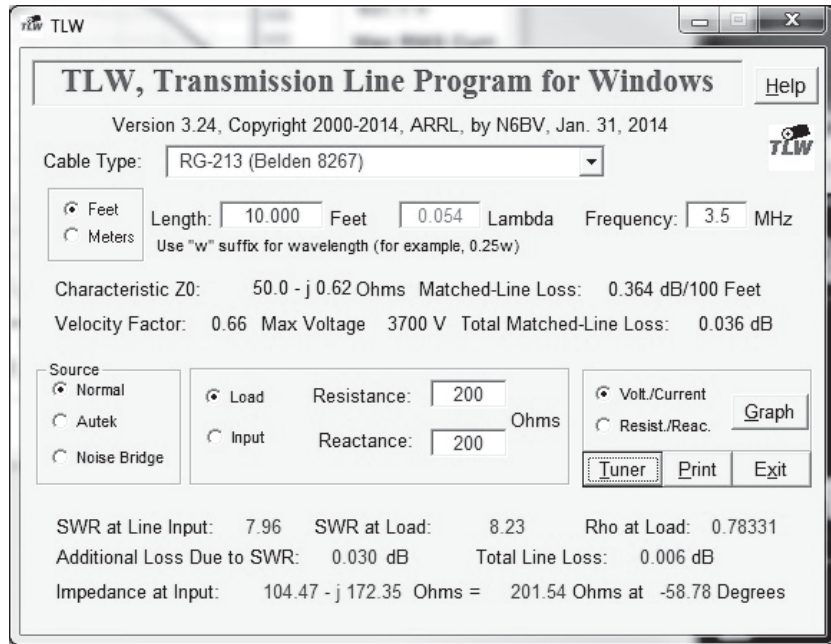


Figure 3 — Main screen of *TLW* software program Graphical User Interface (GUI).

**Table 3**  
Peak voltage across transmission line at various powers and load impedance values at 3.5 MHz.

Power, W	RG-213, ft.	R load, Ω	X load, Ω	Z  load, Ω	Load SWR	V <sub>pk</sub> (Eq 2)
1	10	50	0	50	1	10
10	10	50	0	50	1	32
100	10	50	0	50	1	100
500	10	50	0	50	1	224
1000	10	50	0	50	1	316
500	10	200	200	283	8.23	641
1000	10	200	200	283	8.23	907

**Table 4**  
Recommended RF surge protectors and vacuum discharge tubes.

Manufacturer	Model No.	Power Capability (Vendor Data)	Discharge Tube Manufacturer, P/N	Breakdown voltage, V	Working SWR	Max. Power
Alpha Delta	TT3G50	200 W	EPCOS, EC 350 00 O	350	2	613
				350	5	245
				350	10	123
Alpha Delta	TT3G50HP	2000 W	Littelfuse, CG2 1000	1000	2	5000
				1000	5	2000
				1000	10	1000
				540 to 720	2	1458
—	—	500 W	EPCOS EC 600 B88069X0780S102	540 to 720	5	583
				540 to 720	10	291
				540 to 720	10	291

Here is a summary of my lessons learned while studying RF surge suppressors with my transmission lines.

If the antenna system is matched to 50 Ω, such as a beam or dipole antenna used over a small bandwidth where the impedance does not vary considerably, the SWR will be low and stable across the band. Therefore, the surge protector at the transmitter would protect according to its rating.

If a wider multi-band antenna is being used such as a G5RV or Windom antenna,

you must give attention to the SWR at the point where the RF surge protector is located. If it is located on the antenna side of an RF matching network, or at the antenna, the SWR may be high, and the peak voltage needs to be calculated based on this SWR. Otherwise, the discharge tube protection device will breakdown during peak-power transmissions, creating a high SWR and may possibly trigger a shut down of the amplifier or transmitter.

Alternate discharge tubes can be

purchased, relatively inexpensively, that can replace the currently used tube. This discharge tube will protect against high voltage surges yet still allow transmissions to occur without breaking down.

It would be wise to have spare discharge tubes available to replace ones that fail during a high voltage surge event. These can be purchased directly from the manufacturer, vendor of the RF surge suppressor, or as a component from an electronic distributor.

*Gene Hinkle's, K5PA, father introduced his teenage son to amateur radio more than 50 years ago at the local MARS station on Randolph AFB near San Antonio, Texas. Gene began experimenting with the mysteries of radio, building transmitters, receivers and antennas that eventually led him to a solid career in RF engineering. He earned the MSEE from The University of Texas at Austin. He is an IEEE, Life Senior Member and a licensed (retired) Professional Engineer in Texas. Gene is a Life Member of the ARRL and serves as a Volunteer Examiner, assisting others to reach their goal of becoming Amateur Radio operators. He recently retired as a Systems Engineer from a radio communications technology company specializing in T/FDOA radio-geolocation.*

*His lovely wife, Carolyn, AD5HP, daughter, two sons-in-law, late father, sister, brother-in-law are also hams. His interests include working satellites, the International Space Station (ISS), low power digital modes, DX, State QSO Parties, ARRL Field Day, QRP to the field, and HF mobile. His favorite operating modes are Morse CW, low bandwidth digital modes and searching for DX. He and Carolyn enjoy participating in ARRL Field Day and the Texas QSO Party from Bed and Breakfast locations in the Texas Hill Country. Gene's web page is [www.k5pa.com](http://www.k5pa.com).*

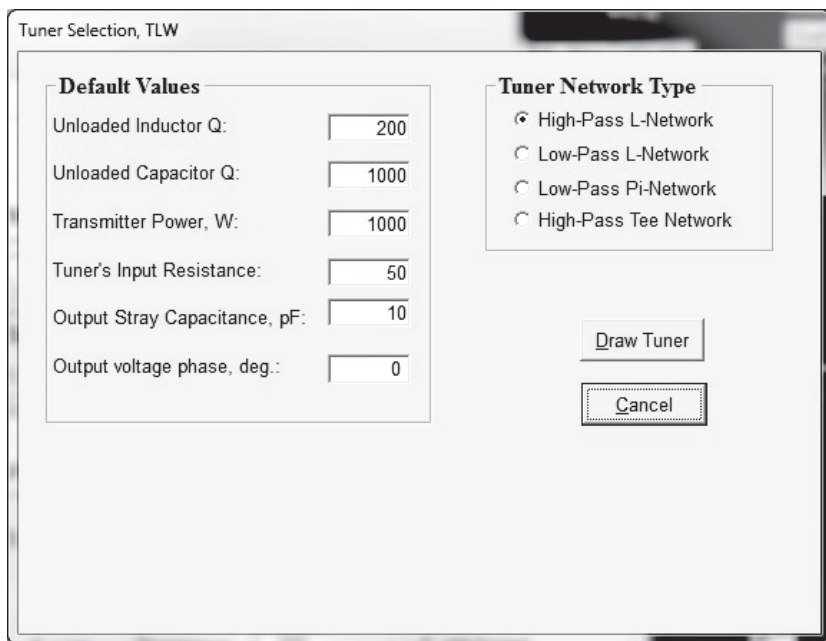


Figure 4 — Enter the transmitter power, 1000 W shown, on the Tuner selection TLW GUI.

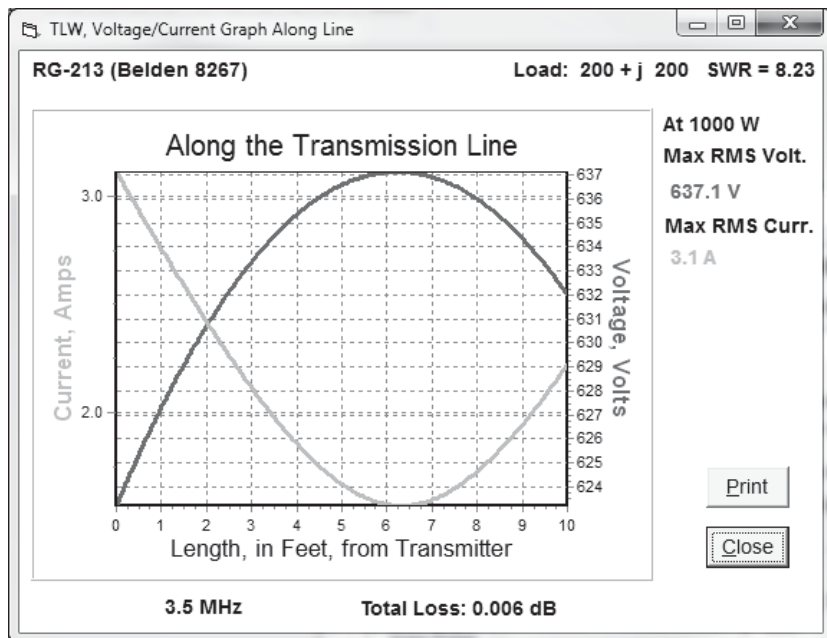


Figure 5 —The transmission line TLW GUI shows the rms voltage peak at 6.3 feet, and the rms current dips at 6.3 feet.

### Notes

<sup>1</sup>Alpha Delta, [https://www.alphadeltacom.com/pdf/TT3G50\\_instruction\\_sheets-6.pdf](https://www.alphadeltacom.com/pdf/TT3G50_instruction_sheets-6.pdf).

<sup>2</sup>TLW User Manual, [www.arrl.org/files/file/Product%20Notes/Antenna%20Book/tlw.pdf](http://www.arrl.org/files/file/Product%20Notes/Antenna%20Book/tlw.pdf)

<sup>3</sup>The ARRL Antenna Book, 23rd Edition. Available from your ARRL dealer or the ARRL Bookstore, ARRL item no. 0390 (hardcover), 0444 (soft cover). Telephone 860-594-0355, or toll-free in the US 888-277-5289; [www.arrl.org/shop](http://www.arrl.org/shop); [pubsales@arrl.org](mailto:pubsales@arrl.org).

<sup>4</sup>EPCO Technical Data, [en.tdk.eu/inf/100/ds/ec350x\\_x0810.pdf](http://en.tdk.eu/inf/100/ds/ec350x_x0810.pdf).

<sup>5</sup>Littelfuse Technical Data, [www.littelfuse.com/products/gas-discharge-tubes/medium-to-high-surge-gdt.aspx](http://www.littelfuse.com/products/gas-discharge-tubes/medium-to-high-surge-gdt.aspx).

<sup>6</sup>Mouser Electronics, [www.mouser.com](http://www.mouser.com).

<sup>7</sup>Digi-Key Electronics, [www.digikey.com](http://www.digikey.com).



# The Case of Declining Beverage-on-Ground Performance

*Detailed modeling and measurements that validate the use of NEC help explain why over the course of two winter seasons the performance of the Beverage on the Ground (BOG) antenna dropped off dramatically as the antenna slowly sank into the ground.*

In midsummer of 2013 I placed a 450 foot length of insulated wire in my pasture configured as a Beverage-on-the-Ground (BOG) receiving antenna. At the same time I erected a terminated loop receiving antenna — a triangle, 70 feet high by 30 feet on the base. I already had a 30 foot vertical working as a non-directional *E*-probe with an amplifier. Over the last 18 months I've been decoding WSPR transmissions — which provide S/N estimates — and comparing reports between the antennas in an attempt to quantify their relative performances.

Initially the BOG and the loop were clearly superior to the vertical, and throughout the 18 months the loop performance was very consistent. The BOG worked well at first. However, over time and especially during the two intervening winter wet seasons, I noticed the BOG signal amplitudes dropping off significantly (-15 dB) and the S/N improvement dropped to no better than the vertical. With the coming of the last summer's dry season the BOG improved somewhat but never really came back. This winter the BOG was not very useful. I checked the connections, feed lines and all associated hardware carefully but found no problems, so this rather radical decline in performance was a mystery!

Recently, I received an email from Al Christman, K3LC, relaying a question he received from Carl Luetzelschwab, K9LA, regarding the reliability of NEC modeling for wires close to, or on the surface, or buried in the soil. There has been some skepticism



Figure 1 — Test antenna #1.

regarding the validity of NEC modeling in these situations. Over the years I've often compared my modeling predictions with finished antennas and generally found very good correlation. However, while modeling *E*- and *H*-fields for verticals close to the soil-air interface I saw some anomalies in the *H*-field calculations when using NEC4.1, which uses the GN2 ground code.

These problems have long been recognized but recently Jerry Burke modified the NEC code to NEC4.2 upgrading to GN3, improving modeling of the ground interaction. I've had a chance to try GN3 (incorporated into NEC4.2) and it did not generate the anomalies I'd seen with GN2. This prompted me to ask, "does NEC4.2 model antennas with wires close to and/or



buried in soil well enough to explain why the performance of my BOG was declining so badly?" To answer that question I felt I had to validate NEC4.2 modeling to my satisfaction before I could confidently move on to my BOG problem.

I decided to perform a series of field experiments to see how well NEC predictions would correlate with actual antennas having wires parallel to the soil at low heights or buried in the soil. I also wanted to investigate an antenna that employed a ground rod. Since my interest is in antennas for 80 m and 160 m, I used test frequencies ranging from 1 to 4 MHz. By no means do my examples cover all possibilities but they are representative. Here is what I found.

### Modeling Software and Instrumentation

NEC solves for the currents on the wires. From these currents both the feed-point impedance and the radiation pattern are calculated. If the impedances from the NEC model agree with the values measured on the actual antenna over a wide range of frequencies you can be reasonably sure the modeling is reliable. In the case of my BOG it would also be helpful to see if NEC4.2 would predict the current distribution along the wire at a given frequency, for example 1.83 MHz.

For the modeling part of this experiment I used *EZNEC Pro4 v6*, courtesy of Roy Lewallen, W7EL.<sup>1</sup> That version of *EZNEC* uses NEC 4.2. I also used the latest version of *AutoEZ* from Dan Maguire, AC6LA.<sup>2</sup> *AutoEZ* is an Excel<sup>®</sup> spreadsheet with macros that automate a wide range of modeling tasks using *EZNEC* as the engine. For impedance measurements I used a vector network analyzer (VNA), either the VNA2180 from W5BIG or a homebrew N2PK VNA. I've made it a point to display the raw measurements without any "corrections" to the data points. That is why you can see noise present on the graphs of VNA measurements at frequencies associated with my local broadcast stations and, in one case, coupling to nearby verticals. The soil electrical characteristics were calculated at the same frequencies as the impedance measurements. This ground data was then inserted into the model. *AutoEZ* makes it easy to blend this kind of data into a model.

The following discussion addresses only NEC4.2, since NEC2 does not allow buried wires and does not do a very good job when the wires are close to ground. It is very possible that GN3 was not required for all the comparisons. NEC4.1 might very well have returned very similar results. I didn't repeat the modeling with NEC4.1 (GN2).

### Soil Surface

First let's clarify the nature of the ground surface. When modeling, we assume the air-ground interface is a distinct line with the properties of air above it and the soil below it. NEC in its present form cannot model a "transition" zone. It's important to recognize that with real antennas the soil-air interface is not smooth nor sharply defined. Unless carefully reworked, the soil surface will be lumpy with varying characteristics both vertically and horizontally. As we'll see later, the characteristics of an antenna close to, or buried in, the soil are very sensitive to soil electrical characteristics so this "lumpiness" in the surface makes it difficult to get good correlation when modeling wires that are between one inch above and one inch below the surface. In effect there is no distinct soil-

surface interface. What we do have in reality is a transition zone from air to soil, which we can model only approximately.

For example, in a pasture as you get closer to ground, first there is grass, then there is the body of grass plant, then there is the root system, and finally you reach actual soil. Even then you're still not home free. The moisture in the top few inches of soil varies quickly with rain and subsequent drying. If the antenna is installed in a forest, initially a surface wire will be lying on top of leaves or needles in various stages of decay, and other woody debris. In summer time this surface may be quite dry, so in effect the antenna is at a height of a few inches.

My experience, and that of others, as well as the modeling, show that this can provide a very good receiving antenna. However, with

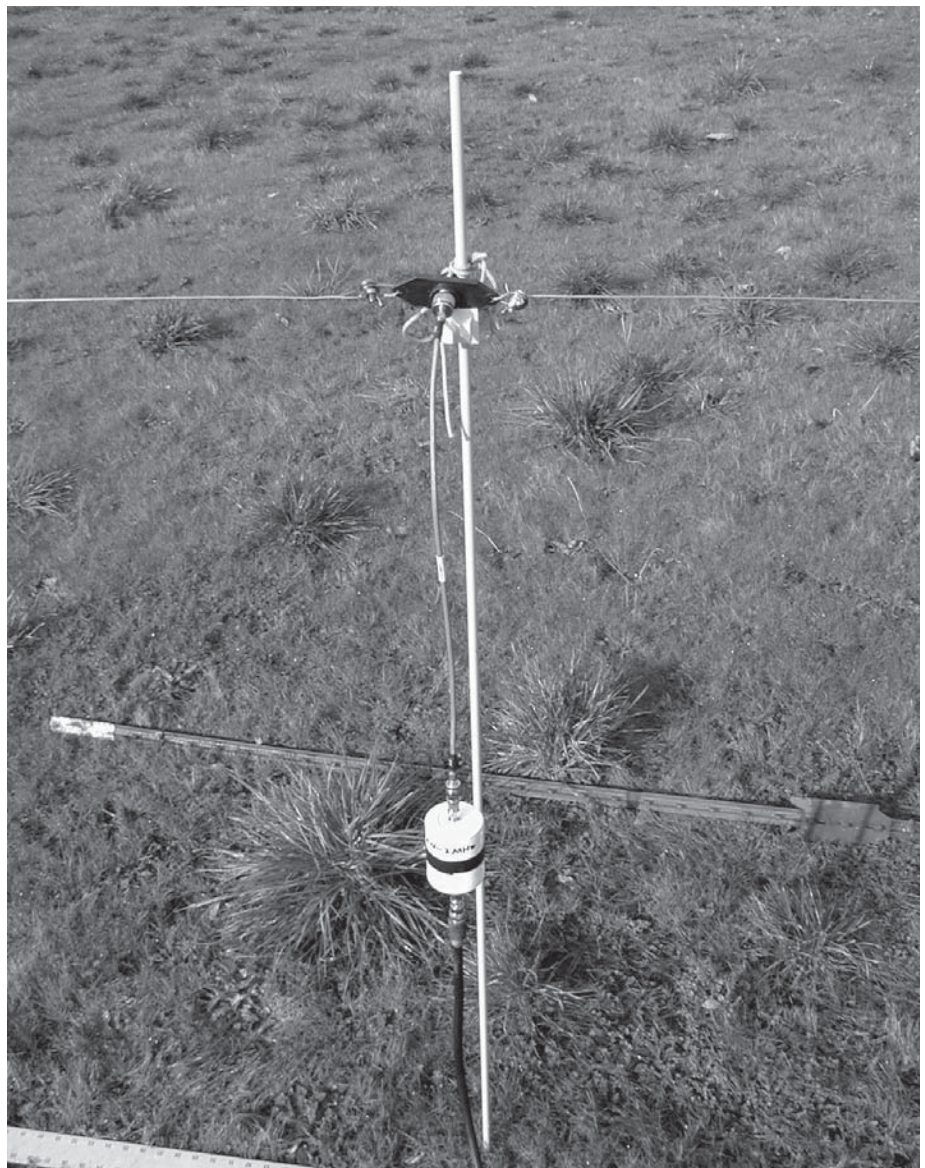


Figure 2 — Center connector, common mode choke and feed point support.



the arrival of fall, leaves and needles will drop down on the wire, burying it to some degree. Also it's likely that the forest floor will be quite wet or even frozen.

I had an interesting exchange with Don Johnson, N4DJ, about his work with BOG antennas in a forest. His results were very good, and he did not notice the severe degradation in performance that I had experienced. It appears that the degradation over time is highly variable and specific to a particular installation, so we want to be careful about drawing general conclusions. If you live in the desert you may be able to place a wire directly on the soil surface and have that remain relatively unchanged for an extended period of time.

I think it is important to reiterate that modeling a wire lying on the ground surface is a special problem. My test antennas #1, #2, and #3 were modeled with the assumption that the air-soil interface was distinct, not fuzzy, and that seems to have worked well. In my case, the BOG wire (test antenna #4) was placed on the surface of a pasture in the summer time when the grass had been mowed and was very dry. The soil also was very dry, so the wire was effectively 1 to 3 inches above the soil. But over the period of 18 months the wire was swallowed up by the weeds, and by this winter it was buried in wet sod and tall grass. There really is no way to model this transition layer between air and the actual soil. What I've done is to compare a BOG antenna one inch above the soil to a BOG antenna one inch below the soil. There was good agreement between modeling and experiment.

### Test antenna #1

The first test antenna was a centered dipole. I chose a length of 300 feet because that included both series (odd half-wave multiples) and parallel (even half-wave multiples) resonances within the test frequency range. This presented a wide range of impedance values at the feed point, from a few tens of ohms to several thousand ohms. I varied the height above ground from 48 inches down to 1 inch in the sequence 48, 24, 12, 6, 3 and 1 inch. A common mode choke was used for isolation. The feed-point impedance was measured with a VNA. The VNA calibration plane was directly at the antenna terminals. Soil electrical characteristics were measured concurrently. The details of the soil measurements are given in articles on soil electrical characterization.<sup>3</sup>

Figure 1 shows a view along the length of test antenna #1. The #17 AWG aluminum electric fence wire was supported on 5-foot fiberglass wands with plastic wire clips. The clips were moved up and down to adjust wire height. The wands were spaced 10 to 20 feet

apart and the wire was anchored at the ends to steel fence posts that were more than 6 feet away from the ends of the wire. Multiple support points and significant wire tension kept the droop to less than a quarter of an inch. I used high quality insulators and non-conducting Dacron line at the wire ends, and a Budwig center connector. Figure 2 shows the Budwig connector and common-mode

choke at the feed point.

Another view of the center connector is shown in Figure 3, which also shows a measurement of the shunt capacitance ( $C_p$ ) across the feed point introduced by the Budwig and the cable shield. The center wire of the cable connecting the fitting to the choke was open-circuited so only the capacitance of the fitting and the outside of



Figure 3 — Shunt capacitance measurement of the center fitting.

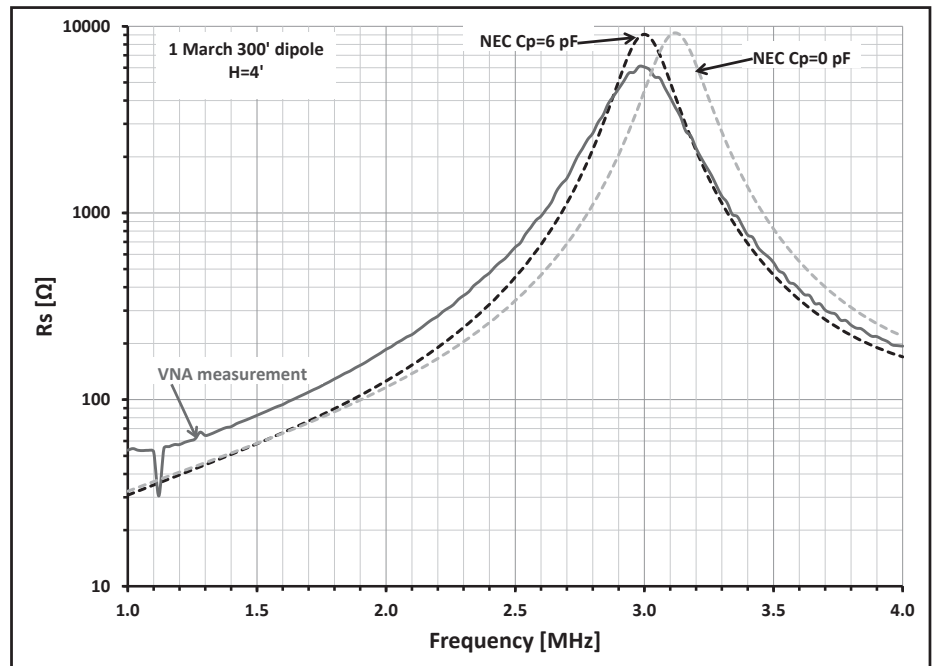


Figure 4 — Modeling with and without  $C_p$ .

the cable was included. Shunt capacitance  $C_p$  turned out to be about 6 pF, which was added to the model as a capacitive load in parallel with the source. In the 1 to 4 MHz range a shunt capacitance of 6 pF would not seem to matter but, as seen in Figure 4, when added to the model, significantly improved the correlation around the high impedance point.

Figure 5 shows the measured impedance of the common mode choke. While the choke impedance is more than 2 k $\Omega$ , at some frequencies the feed-point impedance was even higher. For this reason the graphs show some reduction in measured compared to predicted impedance at the high impedance points.

The measured and computed comparisons of test antenna #1 resistance and reactance are shown in Figures 6 through 17 for heights of 48, 24, 12, 6, 3 and 1 inch above the soil. Note that there are glitches in the VNA measured data around 1.2 to 1.6 MHz

on many of the figures. These correspond to local radio station transmissions. These spurious signals are obvious and can be ignored.

NEC4.2 based calculations appear to do a very good job of matching measurements down to 1 inch above ground. I didn't go lower because the soil surface had variations of more than a half inch, and despite weed-whacking closely, there were still grass lumps under the antenna. The zero reactance measurements of Figure 18 show how the resonant frequencies, both series (odd half wave multiple) and parallel (even half wave multiple), vary with height.

Figure 18 illustrates the important point that the resonant frequency goes down in frequency as the antenna comes closer to ground, and that the change is relatively slow until you get to very low heights (less than 3 inches) at which point the change is rapid.

### Test antenna #2

The second test antenna was a 40 foot dipole using #26 AWG insulated wire buried 1 inch below ground surface. I wanted to have both series and parallel resonances like I had with the 300 foot dipole but that wasn't possible over the 1 to 4 MHz range so I settled for a 40 foot length that was resonant at about 2.5 MHz. The length of test antenna #2 is 1/9 the length test antenna #1 but we still have a series resonance frequency comparable to the 300 foot above-ground dipole. This observation reinforces the message in Figure 18, that placing the antenna close to or in the soil drastically and rapidly decreases the resonant frequency. As shown in Figure 19, I cut a slot in the soil with a lawn edger. I then inserted the antenna and backfilled the slot with compacted dirt.

After inserting the wire into the slot but before backfilling it, I measured the

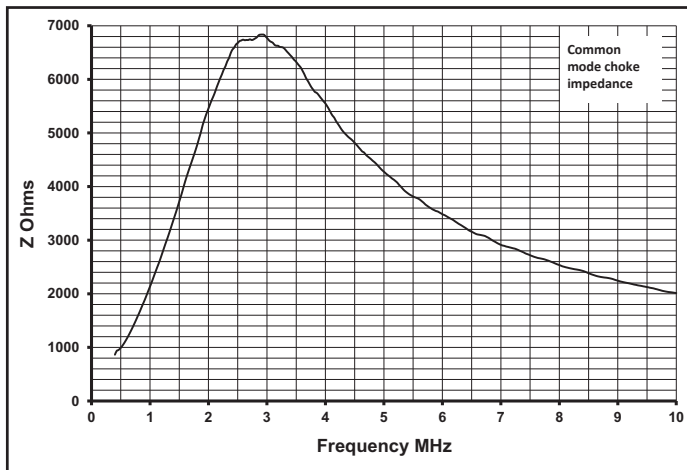


Figure 5 — Measured impedance of the common mode choke.

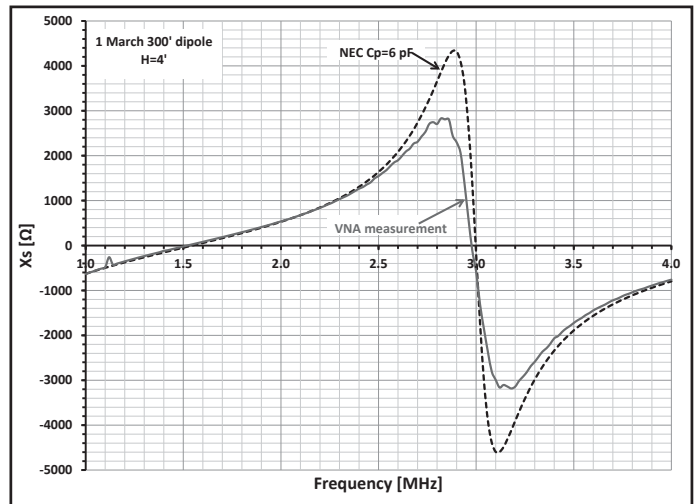


Figure 7 — Reactance measurement at antenna height of 48 inches.

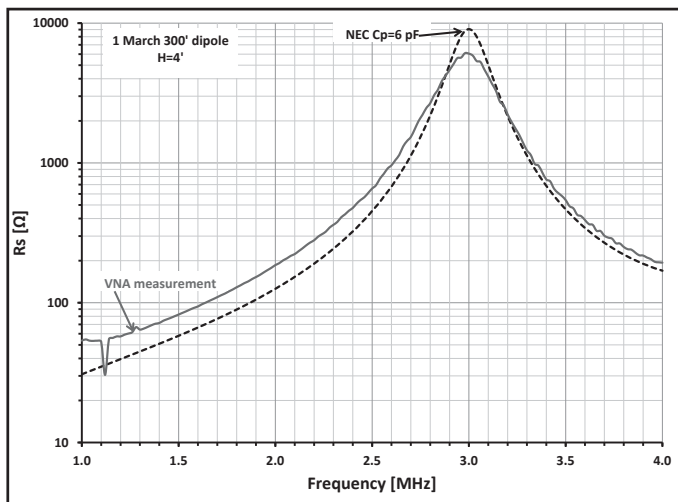


Figure 6 — Resistance measurement at antenna height of 48 inches.

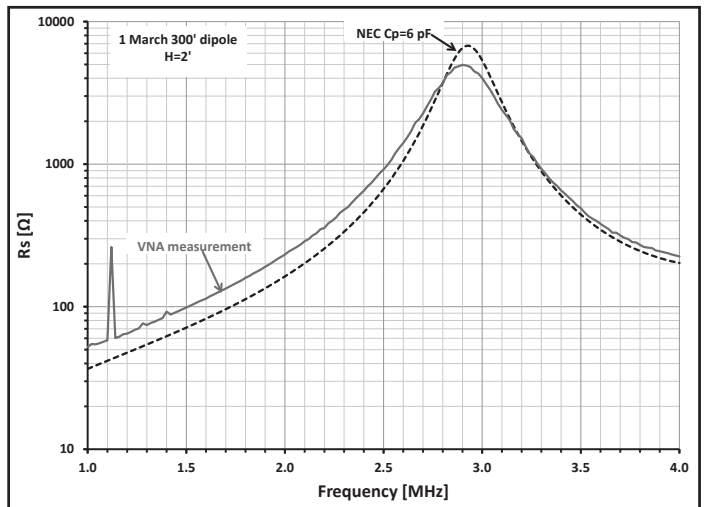


Figure 8 — Resistance measurement at antenna height of 24 inches.



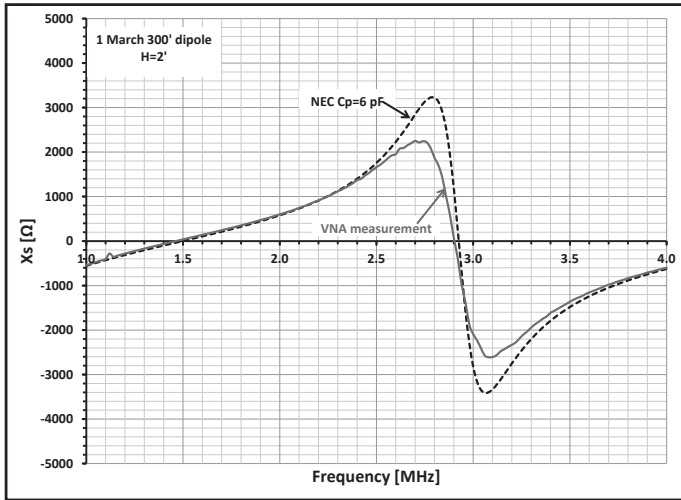


Figure 9 — Reactance measurement at antenna height of 24 inches.

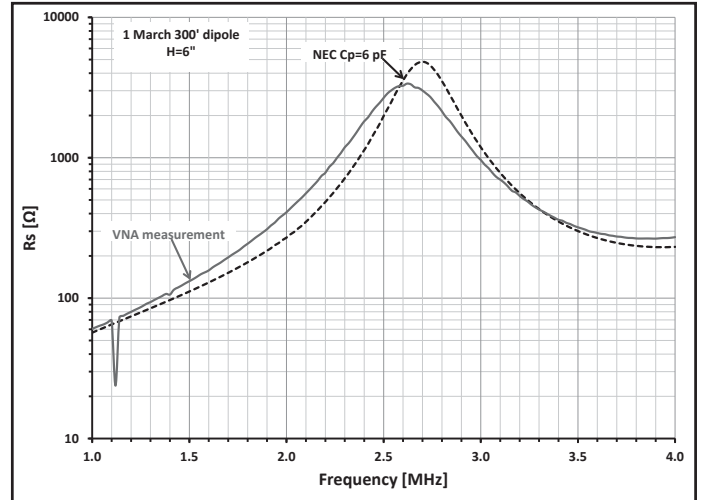


Figure 12 — Resistance measurement at antenna height of 6 inches.

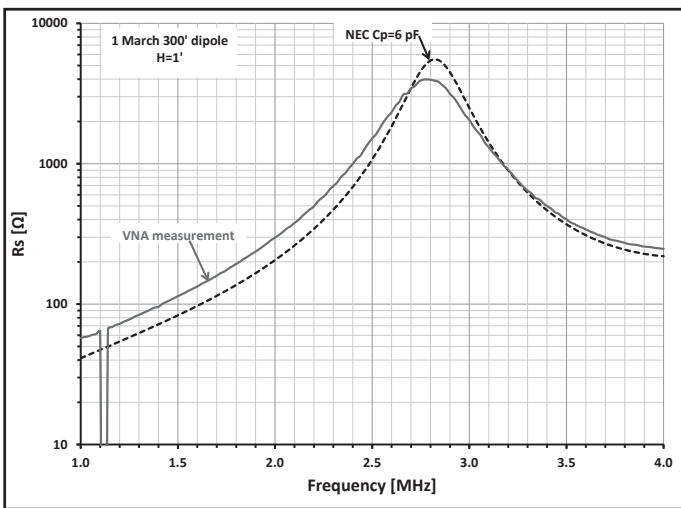


Figure 10 — Resistance measurement at antenna height of 12 inches.

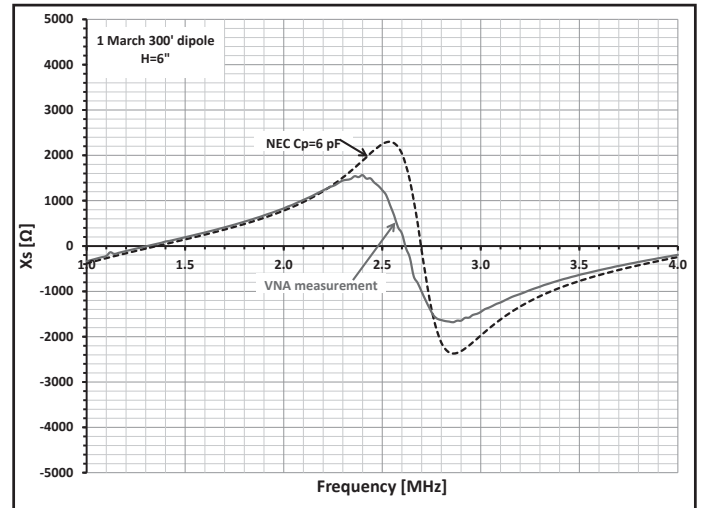


Figure 13 — Reactance measurement at antenna height of 6 inches.

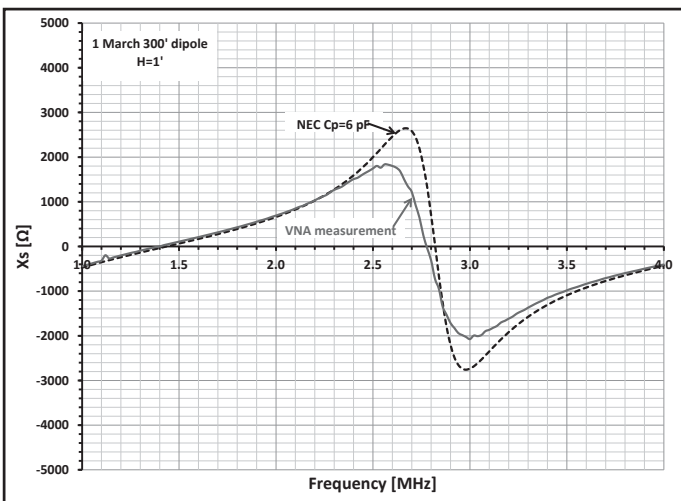


Figure 11 — Reactance measurement at antenna height of 12 inches.

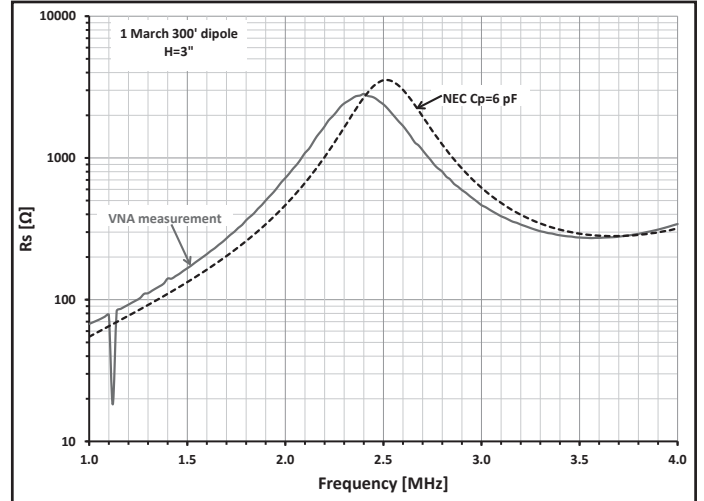


Figure 14 — Resistance measurement at antenna height of 3 inches.

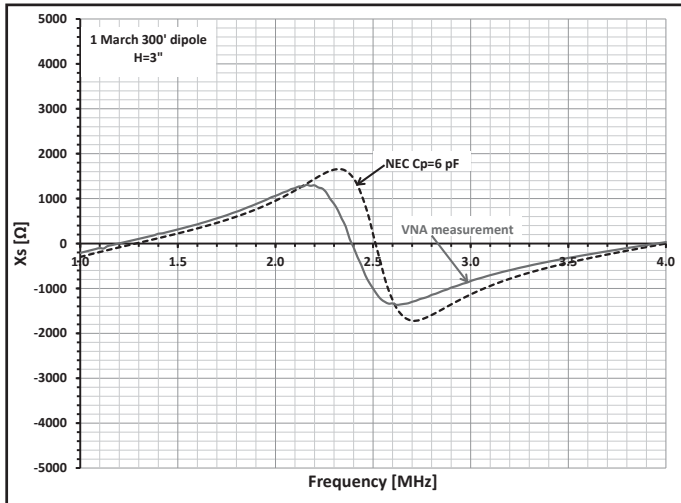


Figure 15 — Reactance measurement at antenna height of 3 inches.

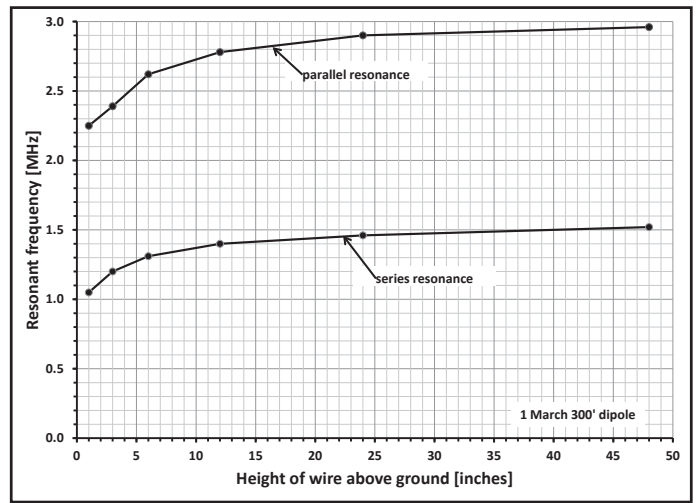


Figure 18 — Resonance variation with height for the 300 foot dipole.

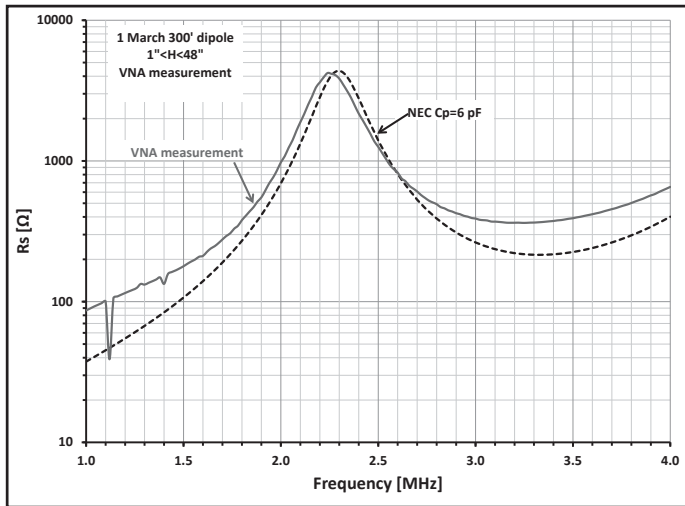


Figure 16 — Resistance measurement at antenna height of 1 inches.

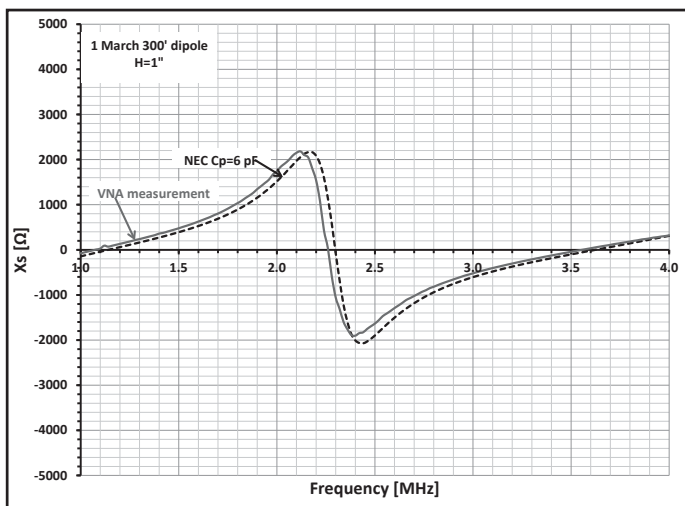


Figure 17 — Reactance measurement at antenna height of 1 inches.

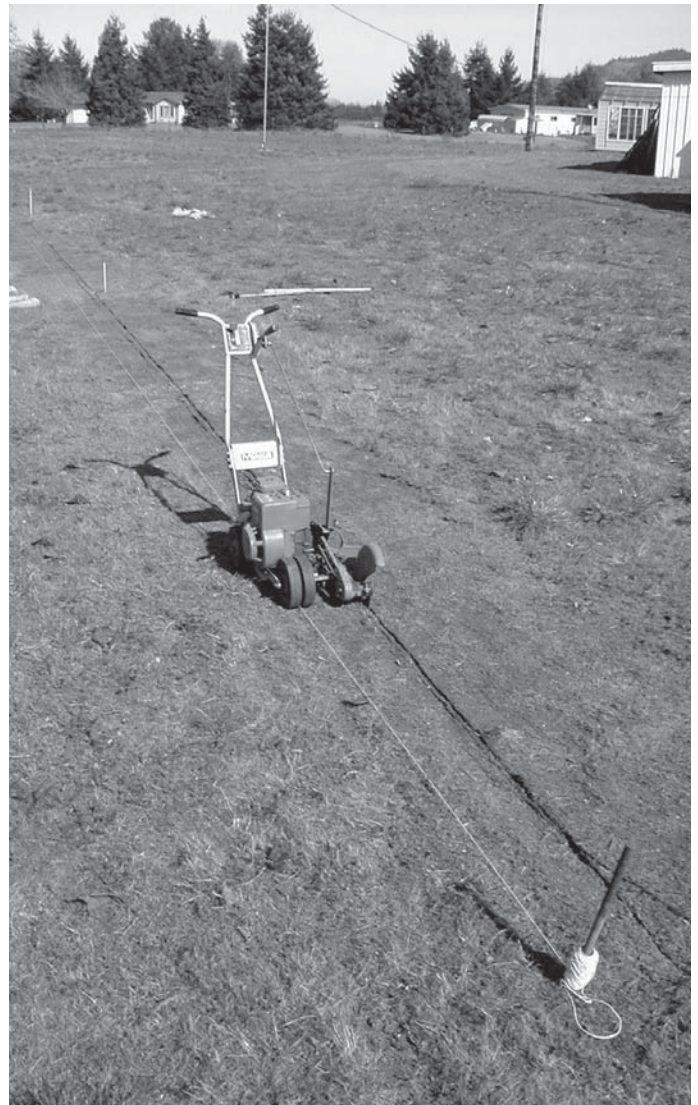


Figure 19 — Cutting a slot in the soil for the 40 foot buried dipole.



impedance. The result was very different from the NEC-based calculation for a buried antenna, and instead behaved as though the antenna were lying on the surface. However, as soon as I backfilled the soil slot and re-measured the impedance, I obtained the results shown in Figures 20 and 21. The good agreement in Figures 20 and 21 between measurements and calculations indicates the NEC model provides reasonable predictions.

I tried both a 19-inch monopole probe and a 12-inch open wire line probe (OWL) to measure the soil characteristics.<sup>3,4,5</sup> The monopole probe gives a good estimate of the average soil characteristics from the surface down to three feet or so. The OWL probe, on the other hand, measures a cylinder of soil just 12 inches from the surface. Figures 22 and 23 illustrate the differences in measurements between the two probes in the same soil.

I felt the OWL data was more appropriate for a wire buried only 1 inch deep. OWL measured values yielded better correlation with modeled values.

Because soil measurements are not perfect, I wondered just how sensitive the model was to variations in the soil characteristics. I reran the VNA measurement of the buried dipole nine days later after it had rained. A comparison between the two measurements is shown in Figures 24 and 25. After the rain, soil moisture was higher, which increased significantly in both conductivity and permittivity, and lowered the resonant frequency from 2.4 to 2.2 MHz.

We can get a feeling for the sensitivity of the modeling to variations in soil electrical characteristics by taking a soil measurement and varying the values  $\pm 10\%$  as shown in Figure 26. This example illustrates why good soil measurements are needed to get reasonable correlation, at least for antennas with wires close to or buried in soil.

The sensitivity of modeled resistance calculations is shown in Figure 27 for variations of the insulation relative dielectric constant, and in Figure 28 for insulation thickness. The choices for insulation thicknesses in Figure 28 were not random. The wire used for the antenna had an insulation thickness of 0.008 inches marked on the reel label, however my actual measurements, using a micrometer, of the total outer diameter minus the wire diameter revealed that the actual thickness was 0.009 inches. Using the measured value in the model improved the correlation as shown in Figure 28. Figures 24 through 28 illustrate the sensitivity of resistance and reactance of buried wires to different variables, such as the effect of rain, ground constants, insulation permittivity and insulation thickness.

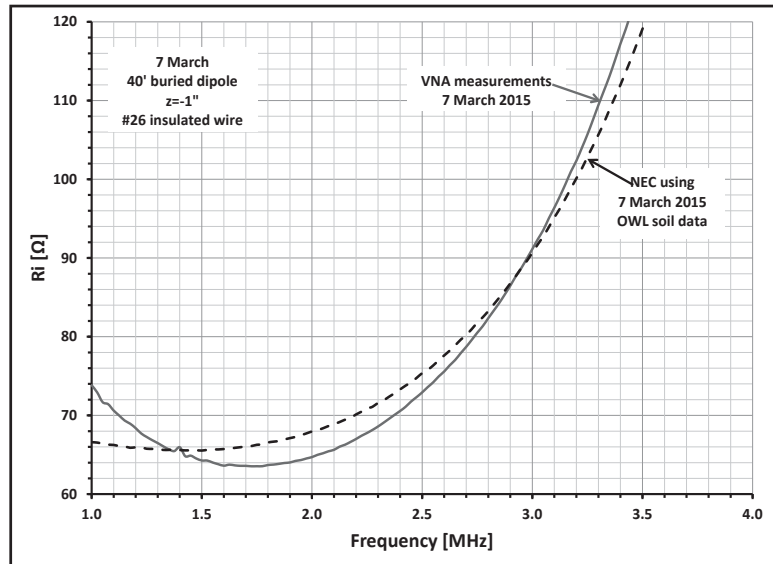


Figure 20 — Resistance measurement of the 40 foot dipole buried 1 inch.

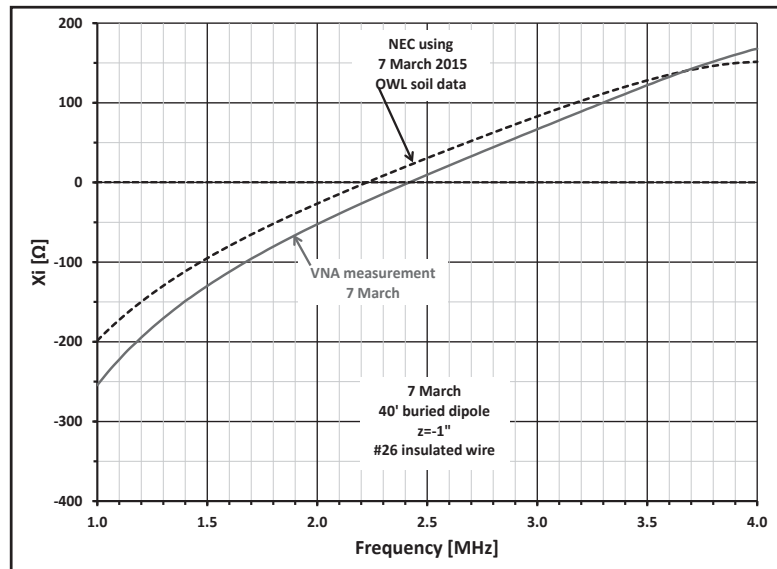


Figure 21 — Reactance measurement of the 40 foot dipole buried 1 inch.

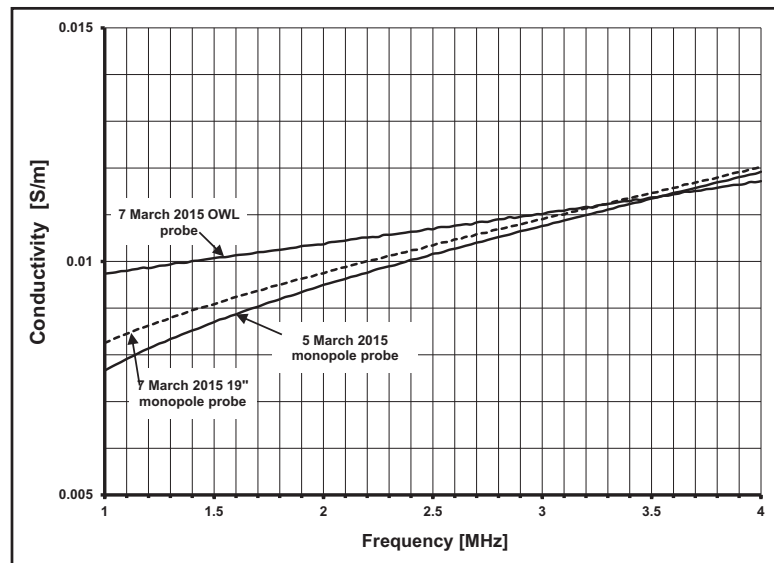


Figure 22 — Soil conductivity measurements.

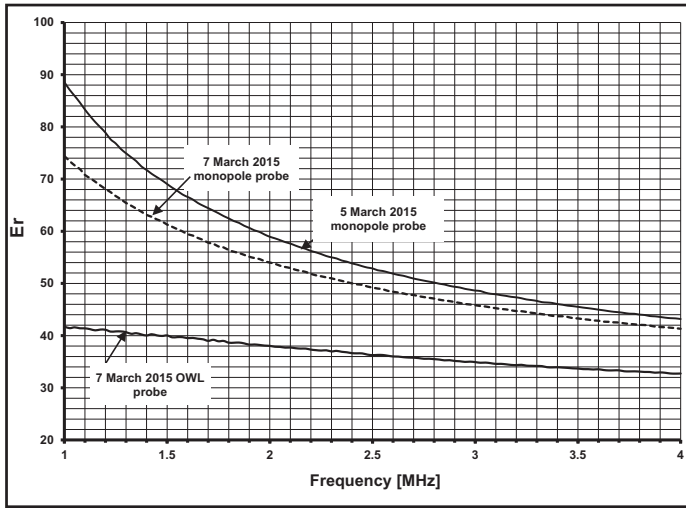


Figure 23 — Soil relative permittivity measurements.

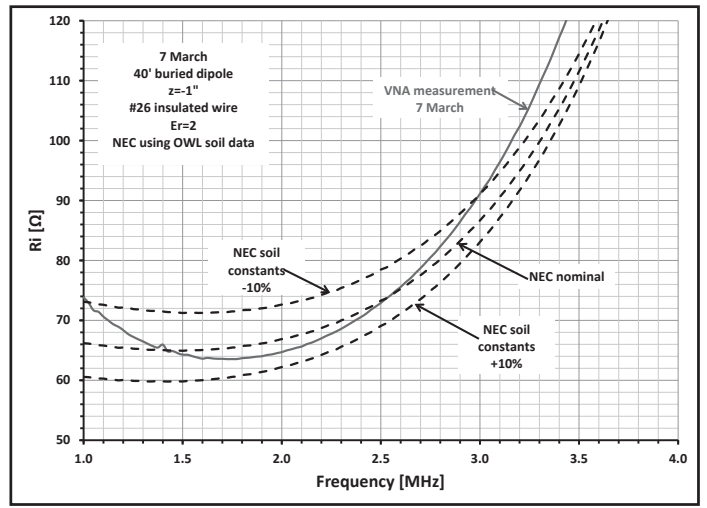


Figure 26 — Variations in modeled resistance for different ground constants.

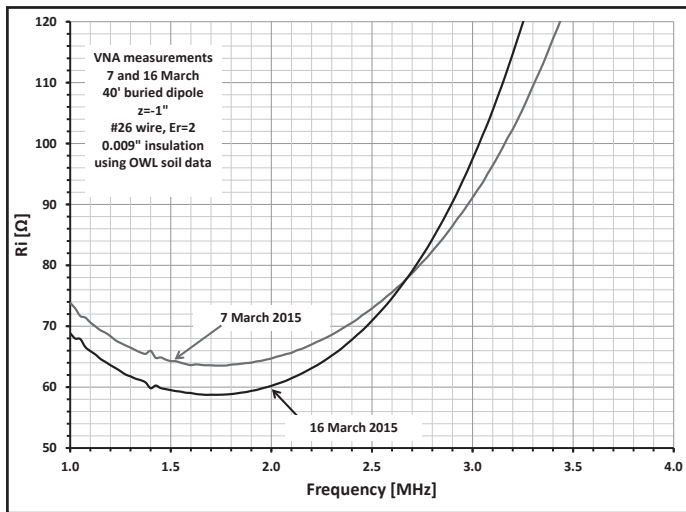


Figure 24 — Resistance measurement of the buried 40 foot dipole on March 7, and on March 16 following rain.

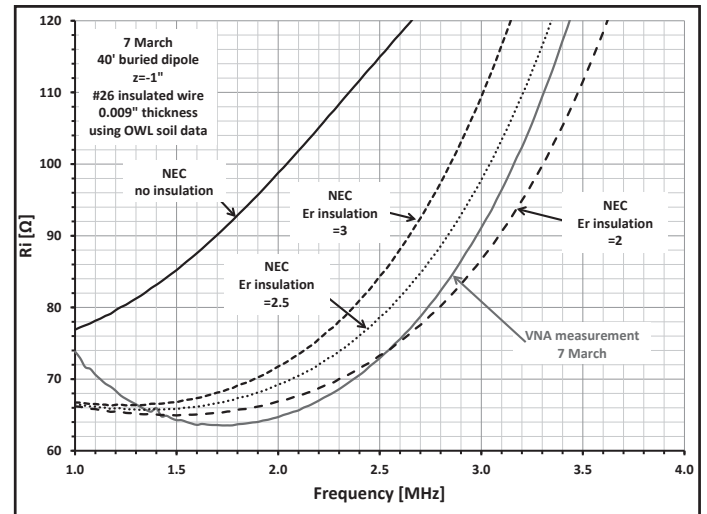


Figure 27 — Effect of wire insulation relative dielectric constant.

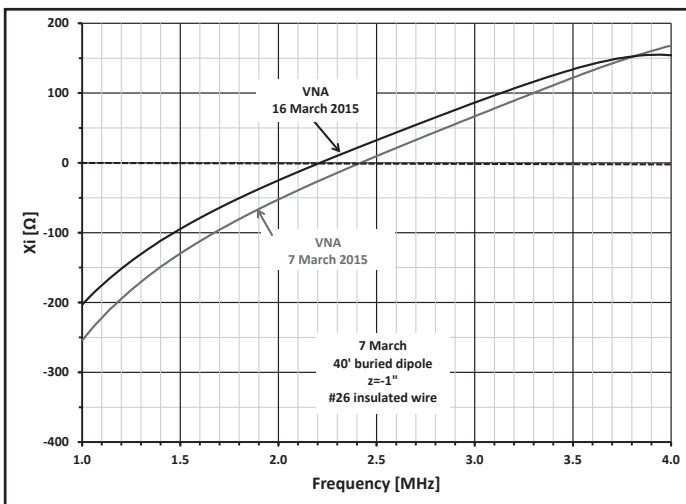


Figure 25 — Reactance measurement of the buried 40 foot dipole on March 7, and on March 16 following rain.

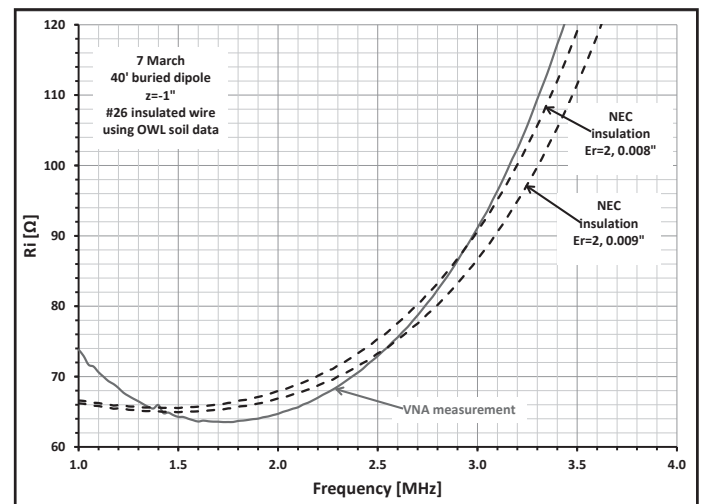


Figure 28 — Effect of insulation thickness.



### Test antenna #3

I wanted to test an antenna that incorporated a ground rod, and one that would have a radiation resistance comparable to the loss resistance associated with a rod to get a feeling of how well ground rods are modeled. I have a pair of tall support poles so I simply suspended a 77 foot length of #26 AWG insulated wire from the midpoint of a Dacron line stretched between the poles directly over the ground stake shown in Figure 29. One of the rules for NEC modeling is that a source cannot be on a segment directly adjacent to a wire-size discontinuity. In this case that would be the ground stake to the #26 AWG wire connection. In the model, the source must be in the center of three consecutive segments of the same length and wire diameter. To meet those requirements I used 3-inch segments in the model and placed the

source at the center of the second segment (at 4.5 inches), which matched the actual feed point configuration of the test antenna. Using concurrent soil measurements, I got the results shown in Figures 30 for the resistance, and Figure 31 for the reactance.

The overall agreement between measurements and calculations is good, and the resonant frequency is particularly close. The noise introduced into the VNA from local AM broadcast stations picked up by the tall vertical is also obvious. There were other antennas and a metal building within 150 feet of the test vertical, which also introduced some spurious resonances. Unfortunately there's not much I can do about the local AM signals. Their bandwidths are all narrow so I fit a 3rd order polynomial trendline ( $R^2=0.987$ ) into the VNA data, which pretty well filtered out the noise. The NEC calculation is a good fit to the trend line.

### Test antenna #4

This entire exercise had been prompted by a mystery concerning the declining performance of a BOG, and by questions regarding the validity of NEC modeling of BOGs so, appropriately, my final test antenna was a BOG.

Using the 450' BOG already in place I measured the feed point impedance from 400 kHz to 4.4 MHz. I also measured the current amplitude and phase along the wire at 1.83 MHz. I added the current measurements as a further confirmation of the NEC modeling predictions, that is, the rapid exponential decrease in current with distance along the wire. Figure 32 shows the BOG in relation to a measuring tape alongside the wire to locate the sampling points. Figure 33 shows the instrumentation position. Figure 34 shows the probe for



Figure 29 — Feed point and ground rod of test antenna #3.

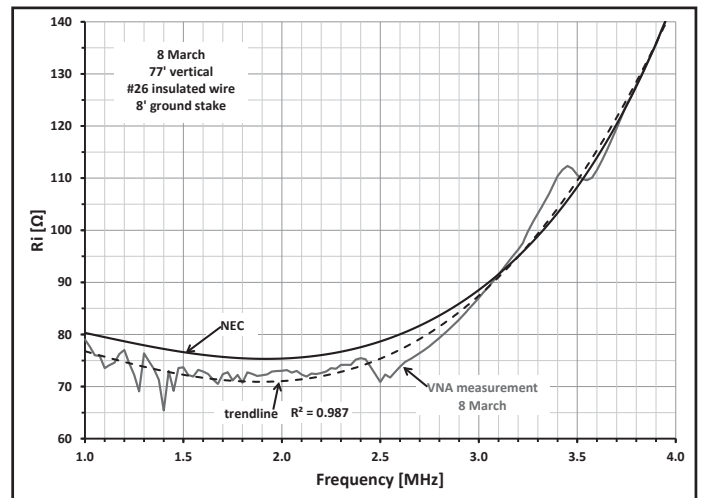


Figure 30 — Measured and computed resistance of the 77 foot vertical with a single ground stake.

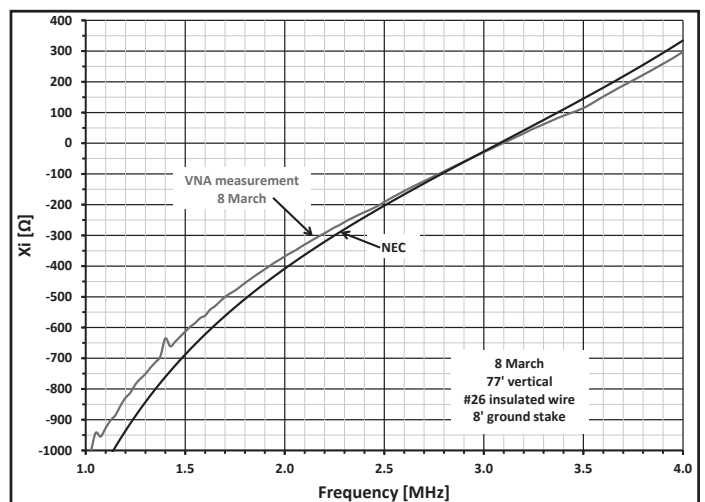


Figure 31 — Measured and computed reactance of the 77 foot vertical with a single ground stake.





Figure 32 — View of the BOG with measuring tape.

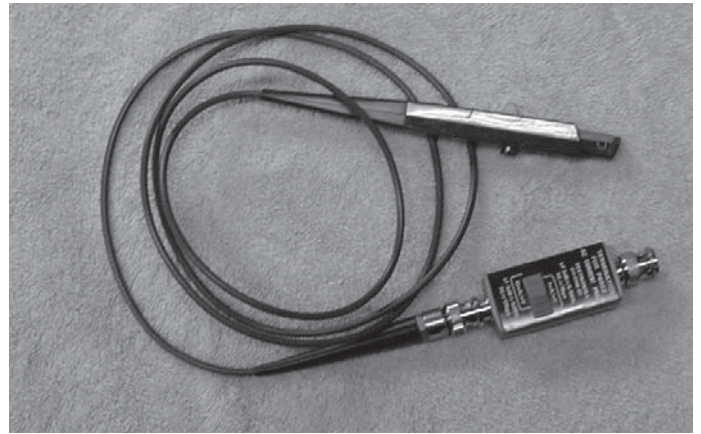


Figure 34 — Scope probe used for current pickup.



Figure 35 — Base excitation and current sampling example.



Figure 33 — Instrumentation position.

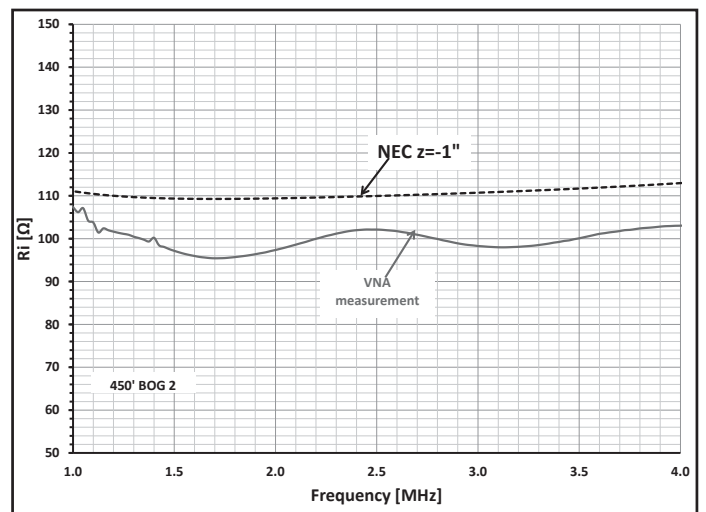


Figure 36 — Measured and computed BOG resistance.



picking up the antenna currents. Figure 35 shows the excitation point at the base, and a current sampling example. For the current measurements, the VNA was in the transmission mode where the antenna was excited at the feed point and the transmission gain (S21) was sampled at several points along the wire using the oscilloscope current probe shown in Figure 34. S21 is a surrogate for the current.

The antenna was modeled one inch below the soil. Modeling results and comparisons to the VNA measurements are shown in Figure 36 (resistance), Figure 37 (reactance) and Figure 38 (current amplitude). The impedance and current distribution graphs show good correlation between NEC and the real antenna despite the uncertainties in the ground surface transition zone.

The rapid exponential decay of the antenna current was a surprise, but the field measurements confirmed it. This goes a long

way towards explaining why the antenna performance was so poor. Functionally it behaves more like a short radial than an antenna! Disconnecting the ground rod at the far end had no effect on either the current distribution or feed point impedance, which was no surprise since there was very little current at the far end of the antenna.

Next, I modeled the BOG with the antenna wire one inch above and one inch below the soil to approximately represent the changes from the time it was first installed to the present. The radiation patterns are compared in Figure 39.

I think antenna patterns of Figure 39 solves the initial mystery! The larger pattern with receive directivity factor (RDF) of 12 dB and peak gain  $G_p$  of -21.47 dB represents the initial condition of the antenna. The smaller pattern with an RDF of 6 dB and  $G_p$  of -37.4 dB is the present condition of the BOG. These patterns make it clear just how severely the

performance was declining as the BOG gradually sank into the sod and soil through two winters. At the time of the measurements spring had arrived and the grass was growing rapidly. The pattern differences shown in Figure 39 agree well with S/N comparisons made over the past 18 months.

### Insulated wire

One of the small mysteries was the observation that placing the dipole loosely in the ground slot — which was quite narrow — without packing it with soil had much less affect on the antenna impedances than when the soil was packed around it. One way to explore this is to model a buried dipole as if it were inside a hollow pipe. We can do this with NEC by setting the insulation parameters  $\sigma=0$  and  $\epsilon_r=1$ , that is, air insulation. We can then vary the radius of the insulation from 0.001 to 3 inches as shown in Figure 40.

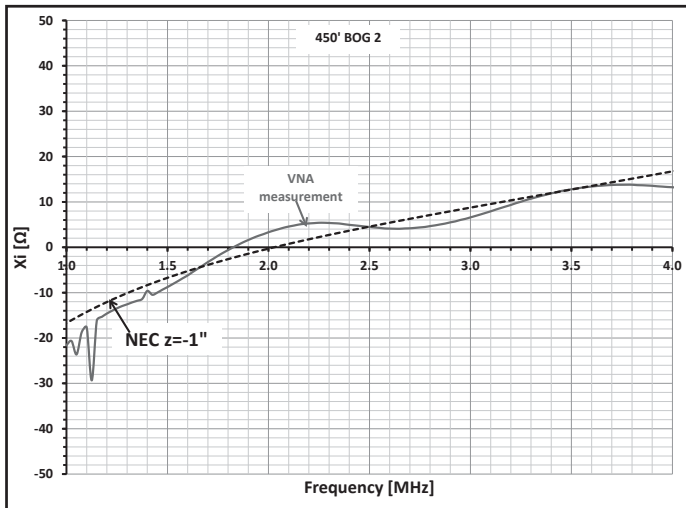


Figure 37 — Measured and computed BOG reactance.

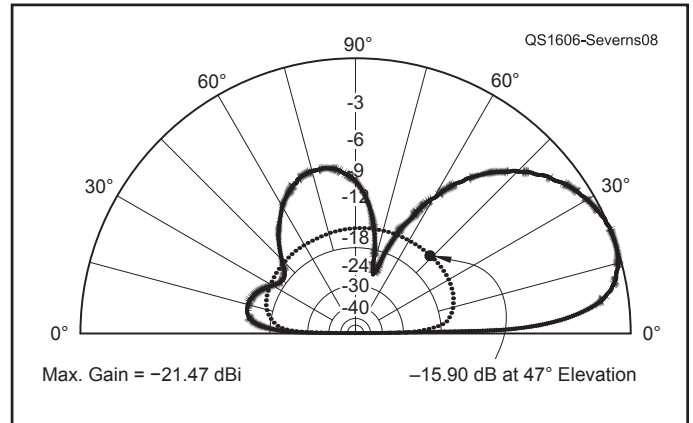


Figure 39 — Computed elevation antenna patterns for the BOG one inch above and one inch below ground.

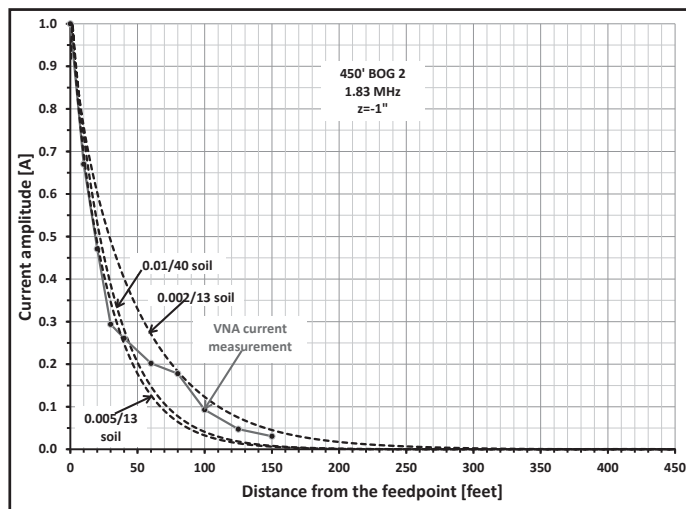


Figure 38 — Measured and computed BOG current amplitude.

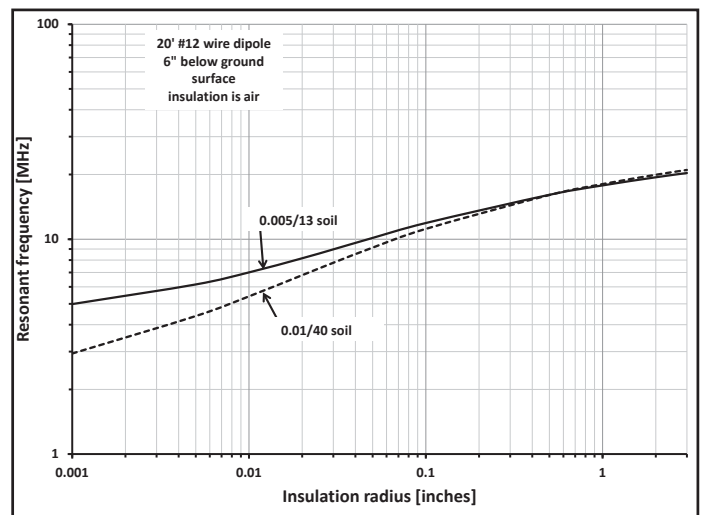


Figure 40 — Resonance frequency in two different soils for different air insulation thickness.

What we see is that even a very thin layer of air around the wire will rapidly increase the resonant frequency. In effect, laying test antenna #2 directly into the soil slot resulted in a layer of air around the wire except at a few points where it was resting on the soil. This also affects test antenna #4, the BOG. The vegetation had grown up gradually around the wire so that it was embedded in the weeds and sod with very little air gap. The same wire BOG centered within a small diameter plastic pipe would behave quite differently. Buried Beverages in plastic pipes?

## Conclusions

In the four examples, correlation between measurement and modeling was excellent. These do not by any means represent all the possibilities but the antennas chosen cover a range of practical examples using very low or buried wires.

Based on this work I believe that if we use NEC4.2, and follow the NEC modeling guidelines closely, make sure the model is dimensionally as close as possible to the actual antenna, and make careful soil measurements, then NEC modeling will give reliable results. The practical

limitations of NEC4.2 modeling are not due to computational shortcomings in the NEC code. What limits us is our knowledge of the details of the actual antennas and the associated soil characteristics and our ability to replicate these in a model.

As a practical matter we can never be perfect, but modeling should get us close. I think we can use NEC to compare elevated radials and buried radials, both insulated and non-insulated, with reliable results.

There are many other questions we can ask, like what happens when interlaced elevated radials are used in vertical arrays. I think that NEC should give reliable results. The results for Beverage antennas, both elevated and buried with resistor and ground rod terminations should also be reliable.

In the case of the BOG the news is bit ambiguous. NEC modeling demonstrates that the BOG antenna can work very well, and from my experience I agree. However, your results may vary. High conductivity soil, for example, may result in very low signal levels. If the BOG is slowly being covered by whatever grows around it or falls from the sky, you may experience significant degradation in performance over time. As always, buyer beware!

## Acknowledgements

I express my sincere appreciation to both Roy, W7EL, and Dan, AC6LA, for the use of their latest software. Without these tools the study would have been impractical. My thanks to Don, N4DJ; Greg, W8WWV, and Carl, K9LA, for reading and helpful comments on draft versions of this article.

*Photos courtesy of the author.*

*Rudy Severns, N6LF, was first licensed as WN7AWG in 1954. He is a retired electrical engineer, an IEEE Fellow and ARRL Life Member.*

## Notes

<sup>1</sup>Several versions of EZNEC antenna modeling software are available from developer Roy Lewallen, W7EL, at [www.eznect.com](http://www.eznect.com).

<sup>2</sup>AutoEZ automates use of EZNEC, see [www.ac6la.com](http://www.ac6la.com).

<sup>3</sup>Rudy Severns, N6LF, "Experimental Determination of Ground System Performance for HF Verticals", QEX, in seven parts, Jan/Feb 2009 pp 21-25 and pp 48-52, Mar/Apr 2009 pp 29-32, May/June 2009 pp 38-42, Jul/Aug 2009 pp 1-3, Nov/Dec 2009 pp 19-24, Jan/Feb 2010 pp 18-19.

<sup>4</sup>Rudy Severns, N6LF, "An Experimental Look at Ground Systems for HF Verticals", QST Mar 2010 pp 30-33.

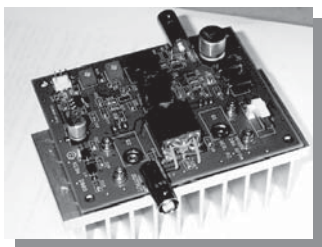
<sup>5</sup>Rudy Severns, N6LF, "A Closer Look at Vertical Antennas With Elevated Ground Systems", QEX, Part 1 Mar/Apr 2012 pp 32-44, Part 2 May/June 2012 pp 24-33.



**HPSDR** is an open source hardware and software project intended to be a "next generation" Software Defined Radio (SDR). It is being designed and developed by a group of enthusiasts with representation from interested experimenters worldwide. The group hosts a web page, e-mail reflector, and a comprehensive Wiki. Visit [www.openhpsdr.org](http://www.openhpsdr.org) for more information.

**TAPR** is a non-profit amateur radio organization that develops new communications technology, provides useful/affordable hardware, and promotes the advancement of the amateur art through publications, meetings, and standards. Membership includes an e-subscription to the *TAPR Packet Status Register* quarterly newsletter, which provides up-to-date news and user/technical information. Annual membership costs \$25 worldwide. Visit [www.tapr.org](http://www.tapr.org) for more information.

**NEW!**



**PENNYWHISTLE**  
20W HF/6M POWER AMPLIFIER KIT

**TAPR is proud to support the HPSDR project.** TAPR offers five HPSDR kits and three fully assembled HPSDR boards. The assembled boards use SMT and are manufactured in quantity by machine. They are individually tested by TAPR volunteers to keep costs as low as possible. A completely assembled and tested board from TAPR costs about the same as what a kit of parts and a bare board would cost in single unit quantities.

- **ATLAS** Backplane kit
- **LPU** Power supply kit
- **MAGISTER** USB 2.0 interface
- **JANUS** A/D - D/A converter
- **MERCURY** Direct sampling receiver
- **PENNYWHISTLE** 20W HF/6M PA kit
- **EXCALIBUR** Frequency reference kit
- **PANDORA** HPSDR enclosure

**HPSDR Kits  
and Boards**



**TAPR**

PO BOX 852754 • Richardson, Texas • 75085-2754

Office: (972) 671-8277 • e-mail: [taproffice@tapr.org](mailto:taproffice@tapr.org)

Internet: [www.tapr.org](http://www.tapr.org) • Non-Profit Research and Development Corporation





8:30 am to midnight ET, Monday-Friday  
1230 to 0400 UTC March-October

8:30 am to 5 pm ET, Weekends  
1230 to 2100 UTC March-October

International/Tech: 330-572-3200  
8:30 am to 7 pm ET, Monday-Friday  
9:00 am to 2 pm ET, Saturday  
Country Code: +1 Sale Code: 1608QEX

**800-777-0703 | DXEngineering.com**



## New Products Added Every Day at DX Engineering!

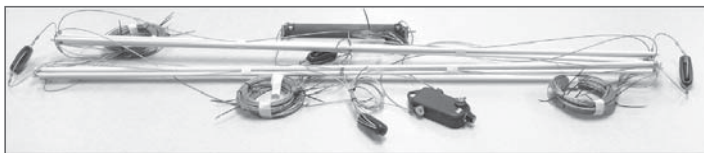
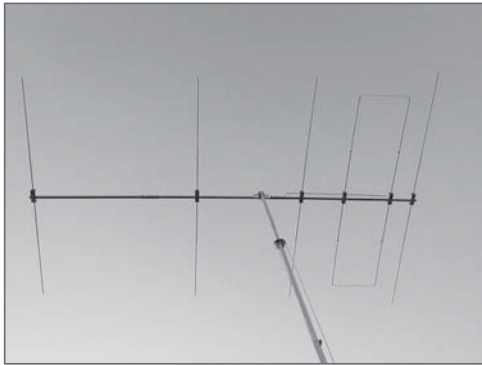


### HF and VHF Yagis

Contesters have been clamoring for rugged, high performance antennas that won't break the bank. EAntenna's Yagi and dipole antenna designs deliver on all fronts. Here's a pair of the most popular models. They are available now at DXEngineering.com.

For HF operating, the DY-MINI3B is a 20/15/10 meter tri-bander that gives you impressive gain on each of the three bands—all with a boom only 12.5 feet long.

And for VHF, the 144LFA16 designed by G0KSC is a 16-element Yagi for the 2 meter band. It can handle full-legal power, and offers excellent gain characteristics and front-to-back performance.



### HF Antenna Systems

Bushcomm gear is ideally suited for emergency and portable duty, so it performs very well in mobile, base station, and marine applications too.

Bushcomm's BBA100DXE is a DX Engineering exclusive, delivering 80-10M coverage at a VSWR under 2:1. The HF broadband three-wire antenna handles 130 watts CW and 250 watts PEP. The wire length is roughly 90 feet.

For mobile operation, Bushcomm offers its Highlander 8. It's an 80-6M whip that can handle up to 250 watts PEP. Carefully coiled antenna wire keeps the fiberglass mast's height under six feet. Want to change bands? Simply plug into a different tap.



### DX ENGINEERING

#### NCC-2 Receive Antenna Variable Phasing Controller

The NCC-2 now combines the NCC-1 Phase Controller and our RTR-1A Receive Antenna Interface technologies into one box. It also has enhanced balance functionality, increasing its ability to phase between two different types of antennas. This is a handy feature if you've got space constraints on your property. We've also made it easier (and more economical) to expand the NCC-2's versatility by providing slots for plug-in modules, like the new plug-in versions of our Receiver Guard 5000 and RPA series preamplifier.



### DX ENGINEERING

#### Automatic Band-Pass Filter

Select from an assortment of band-pass filters with the simple push of a front-panel button. Introducing DX Engineering's new Automatic Band-Pass Filter. A band-pass filter is a smart way to remove unwanted signals and hear only the band you've selected. Having multiple filters in one box means you can quickly switch bands without the hassle of changing components in your signal path. The unit comes preloaded with filters for the 160, 80, 40, 20, 15 and 10 meter bands.



### DX ENGINEERING

DX Engineering supports the CY9C St. Paul Island DXpedition.

**CY9C 2016**  
St. Paul Island



Email Support 24/7/365 at [DXEngineering@DXEngineering.com](mailto:DXEngineering@DXEngineering.com)

Stay connected:

# A PLL Based Stand Alone Signal Generator with I and Q Outputs

*This general purpose signal generator produces precise quadrature signals, and can support SDR projects from 160m to 6m.*

I started this project because I needed a general purpose stand alone I/Q signal generator that would cover all Amateur Radio bands through 6 m, and generate precise quadrature outputs in addition to single tones. Crystal stability and “re-setability” were definite requirements. An Internet search revealed PIC / AVR microcontrollers that drove direct digital synthesizer (DDS) chips, and plenty of circuits, but none met my requirements.

One of my main applications would use the signal generator as the local oscillator for RF down converters. These converters supply signals to computer sound card *Software Defined Radio* programs, and most require quadrature local oscillators. I discovered the AD9850 DDS boards that needed appropriate inputs from a PC or microcontroller to operate. They provide a single signal output below 35 MHz or so. Their on-board 125 MHz clock circuits are sometimes inaccurate, and zero beating is hit or miss with software controllers.

I decided that the clock issue, frequency range and I/Q generation would best be solved with PLL technology.

## Playing the Numbers Game with PLLs

Phase Locked Loops (PLLs) serve two basic functions. They translate signals at one frequency to another, and they reduce or attenuate the jitter of the signals. There are a lot of numbers to crunch to set the internal register values. Manufacturers often offer free PC-based straightforward software that makes this problem easier to solve. That was the case for the devices I chose. Just let the software compute the PLL register values and plug them into the CPU I2C handler for upload to the PLL.

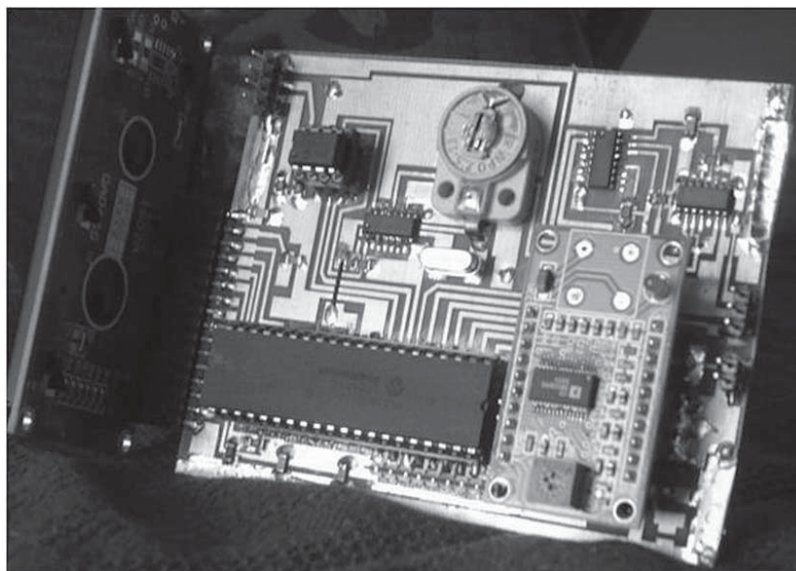


Figure 1 — The signal generator hardware.

After inspecting several available PLL integrated circuits, I chose the FS7140 and the FS6377 integrated circuits. They are relatively inexpensive, and the FS7140 has symmetrical true/complement CMOS outputs. This will drive a flip-flop quadrature generator circuit with out having to resort to divide-by-four circuits as is often done. A simple divide-by-two operation is all that is needed. That eases the upper frequency requirement for the PLL translator circuits. Register calculation software is available free from the manufacturers for both devices.

The upper frequency limit of the FS7140 is 340 MHz, so 2 m operation might be possible. The input reference lower frequency is not specified, but the maximum is 80 MHz. The specifications appear adequate for my application. The major components retailers

offer these integrated circuits (ICs) for a few dollars each; EBay offered a package of fifty FS7140 ICs for \$22 with free shipping. I used EBay ([www.ebay.com](http://www.ebay.com)) and Digikey ([www.digikey.com](http://www.digikey.com)) as sources for most of the components in this project. The devices are available in 16-pin SOIC packages with .05 inch pin spacing, so soldering is not too difficult. The FS7140 is also available in the smaller SSOP package, so be careful when ordering the part.

I chose the FS6377 PLL to generate the processor clock and the 125 MHz clock for the DDS board. The advantage of this is that the generator board needs just a single crystal, which can be trimmed with a small capacitor to zero beat the generator outputs. This application uses only two of the three programmable outputs available from the



FS6377 PLL. The FS6377 operates from a 5 V supply. The FS7140 and 74ALVC74 are 3.3 V devices and require a separate 3.3 V regulator.

### The Basic Topology

I decided to use the 16F877A PIC as a controller. It has ample I/O ports and adequate programming space and supports a 2 by 16 LCD display. One with back lighting is best. My finished circuit boards are pictured in Figure 1, and the LCD display is seen in Figure 2.

The Direct Digital Synthesizer (DDS) is a AD9850 board available from EBay. You must carefully remove the on-board 125 MHz clock module. Both the FS7140 PLL and FS6377 PLL ICs are available from Digikey. I added a 12F629 PIC to handle an inexpensive rotary encoder, and initial setup for the FS6377 master oscillator. I wanted a “knob” to rotate up and down the bands. A 74ALVC74 D-flip flop provides symmetrical quadrature outputs. This flip-flop has a typical toggle frequency of 250 Mz, so over-clocking to 296 MHz for 2 meter capability might be possible. Add a few surface mount resistors and capacitors, along with a 16 MHz crystal, and you are almost done.

### The Circuit Board

I designed a 3 by 4 inch PC board using the free PCB layout CAD Program from Cadsoft (Eagle Light), and I used a laser print transfer to copper process.<sup>1</sup> My heat source is a laminator, where I use foil for a second pass to “crisp up” the trace image before I etch with a solution of peroxide and muriatic acid. I also use a yellow colored transfer paper available from several EBay sources.

This process is quick and easy. My board has all the circuit traces on the upper side and a solid copper ground plane on the back side. I make circuit connections to ground by drilling a few small holes and soldering “thru-hole via wires” to the solid conductor back plane. All other construction involves SMD components and surface mounted sockets.

Just two jumper wires are required. One from the FS6377 output to the 20 MHz PIC 16F877A clock input, and another for the 125 MHz input to the DDS module. Remember, the original DDS module clock chip was removed so the external clock can be used.

The controller is powered with a separate 5 V regulator board operating from a 12 V “wall wart” supply. The 3.3 V regulator, see Figure 3, is on the main generator board. My prototype board draws approximately 150 mA.

The Eagle Light PCB file is available

on the *QEXfiles* web page.<sup>2</sup> The board file shows all the parts placement and component values.

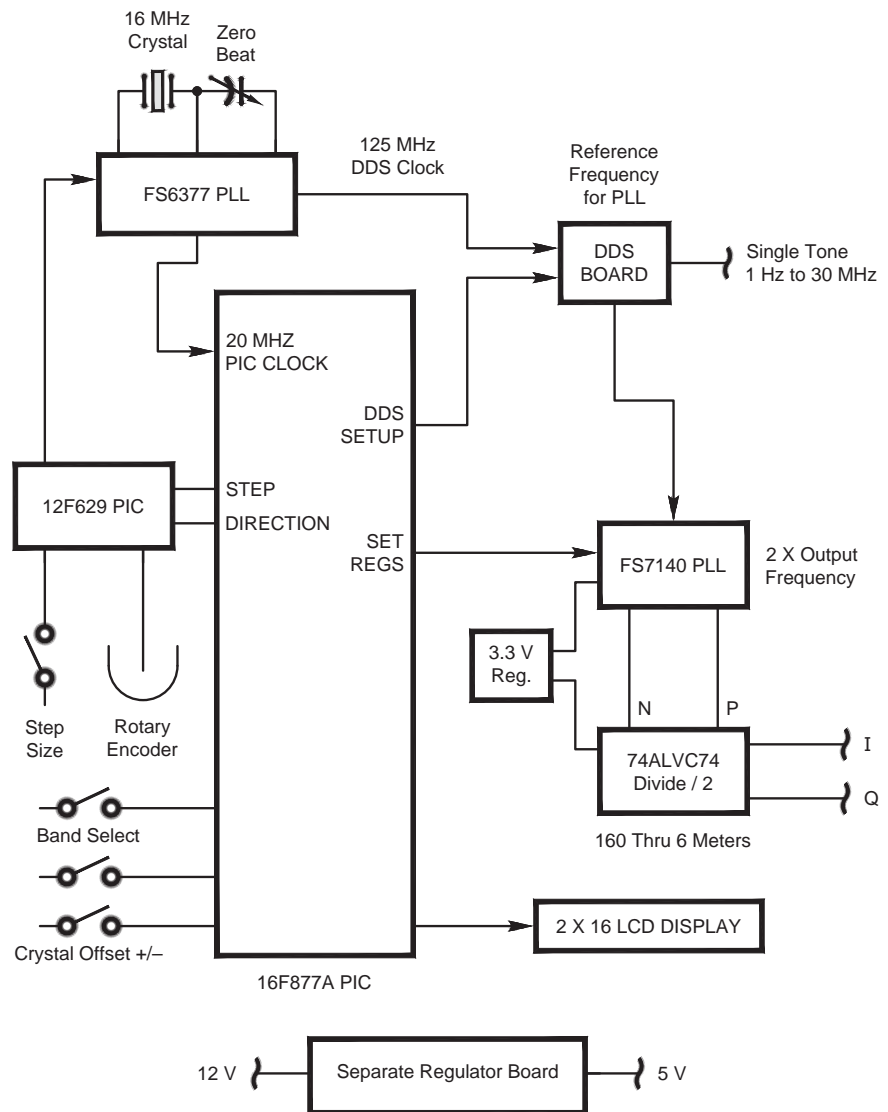
### Operation

Operation is very intuitive. A pushbutton switch on the rotary encoder changes the frequency step size from 1 Hz to 1 MHz in a ring-times-ten mode. Another band

select pushbutton selects the desired band 160 through 6 meters. The processor will remember the last frequency/band displayed at power-off and restore it at power-on. There are also two additional band selections that enable the I/Q outputs for general coverage operation. The first band spans 1.4 to 35MHz, while the second band spans 35 to 125 MHz. The actual frequency can be seen on the LCD.



Figure 2 — The LCD shows the PLL reference frequency and the target output frequency.



QX1605-Templeman03

Figure 3 — Block diagram of the PLL-based I/Q signal generator.

Frequencies on most bands are usually within 10 to 100 Hz. At 50 MHz errors can be as much as 150 Hz. This means that 5 and 10 kHz channels settings are possible. Adjust the 16 MHz master crystal oscillator by zero-beating against a stable reference. The crystal can be warped as much as 10 kHz up or down by the trimmer capacitor. Additionally, jumpers signal the PIC processor what factors to use when calculating the DDS programming values. The DDS module has an adjustment potentiometer for adjusting square wave outputs. Set it to produce a symmetrical output.

### Theory of Operation

Please refer to the block diagram of Figure 3. The 12F629 PIC is programmed to initialize the FS6377 PLL master clock generator on initial power-up. This PLL generates the 20 MHz clock for the PIC processor as well as the 125 MHz clock for the DDS module. Additionally, the 12F629 constantly polls the rotary encoder to determine step size and direction of changes. It passes this information to the main 16F877A PIC CPU.

The 16F877A PIC processor manages the correct programming values for the AD9850 DDS module and the FS7140 PLL. The FS7140 PLL must be updated for each individual band change. The step and direction signals control the AD9850 DDS frequency output, which becomes the reference clock for the FS7140 PLL. The band pushbutton selects and displays a midpoint frequency for each of the ham bands. For example, 160 meters becomes 1.9 Mz and 40 meters becomes 7.125 MHz and so on.

### The Math

All of the band-frequency calculations require that the FS7140 PLL be programmed to two times the low frequency edge of each

**Table 1.**  
**Factors for computing DDS frequency.**

Band, m	BANDSTART	FACTOR
2	144 MHz	×14.4
6	50 MHz	÷5.0
10	28 MHz	÷2.8
12	24 MHz	÷2.4
15	21 MHz	÷2.1
17	18 MHz	÷1.8
20	14 MHz	÷1.4
30	10 MHz	×1
40	7 MHz	÷0.7
60	5 MHz	×2.0
80	3.5 MHz	÷0.35
160	1.8 MHz	÷0.18

band, as shown in Table 1. For example, 40 meters would require the FS7140 PLL to be set to 14 MHz. Remember, we divide by two later. The DDS output is set as the PLL zero reference, which I have chosen as 10 MHz. That sets the I/Q outputs to 7 MHz.

### Setting PLL/DDS Factors

The PLL/DDS factors are derived by accumulating the net result of the various dividers in the FS7140 PLL for each band and depicted as a single number.

(1) Find the *difference* between the band start and desired I/Q frequency output.

(2) Multiple or divide (as per Table 1) the *difference* by each band factor, and add 10 MHz.

This is the DDS set frequency for that I/Q output frequency.

### Example: Setting a 40 meter Frequency

The algorithm for setting frequency begins with the difference between the band start frequency and the desired I/Q output frequency, for example, 7.125 MHz.

(1) Find the *difference*: 7.125 – 7.000 MHz = 125000 Hz.

(2) Divide 125000 by 0.7, and add 10 MHz to get 10,178,571 Hz. Note that 0.7

is the 40 meter band factor from Table 1.

(3) Set the DDS to 10,178,571, and the output of the PLL will be 7.125 MHz.

You must compute new FS7140 PLL values for each band according to Table 1. In the case of the single tone output, the DDS sine wave output is taken directly from the AD9850 IC. This sine wave (single tone) is limited to 30 MHz or so because of DDS limitations. Square wave outputs are always available through 6 meters by using one, or the other, or both of the I/Q outputs.

### Manufacturer's Software

Calculate the PLL values using PC software packages supplied by the manufacturers. For the FS6377 software package, enter 16 MHz as the reference frequency and then choose 20 MHz as the 'A' output and 125 MHz for the 'B' output.

For the FS7140 software package, enter 10 MHz as the reference frequency. Check the reference source boxes 'Ref pin' and 'CMOS'. Enter the band lower edge frequency from Table 1 for the band of interest. Do this for each band. The reference pin is the input from the DDS and its use is fundamental for correct operation.

### Conclusion

The intent of this article is to highlight the use of Phase Lock Loop technology to improve on some limitations of simple DDS or analog VFO frequency signal generators. There is nothing mysterious about a PLL. A PLL offers an easy way to extend the frequency coverage of lower frequency RF sources.

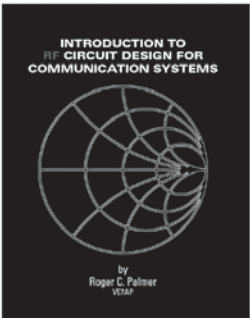
To help you duplicate this project, the Eagle Light PCB file and HEX programming files for the 12F629 and 16F877A are available on the *QEXfiles* web page.

*ARRL member Charles Templeman, W2EHE, holds the Amateur Extra class license. He was first licensed as a Novice in the early 50s as WNØHOU and advanced to General Class within a year. Charles set Amateur Radio aside for a number of years for education, raising a family and pursuing a technical career with IBM. He assisted in the development of many products, including Systems 1400/360/370 in the IBM Glendale Lab, Endicott, NY, as well as RISC processors at IBM Austin, TX. Charles retired from IBM as a Senior Engineer in 1991 and renewed his Amateur Radio interests. He upgraded to Amateur Extra class and began to assemble a station with primary interests in design and construction projects, circuit and antenna simulation programs.*

### Notes

<sup>1</sup>[www.cadsoftusa.com/download-eagle/freeware/](http://www.cadsoftusa.com/download-eagle/freeware/).

<sup>2</sup>[www.arrl.org/QEXfiles](http://www.arrl.org/QEXfiles).



**INTRODUCTION TO RF CIRCUIT DESIGN FOR COMMUNICATION SYSTEMS**

New, practical, easy-to-read text book written for technicians and amateurs who want to learn more about RF Circuit Design techniques.

By Roger C. Palmer, VE7AP

[www.paltec.ca](http://www.paltec.ca)

Now available from Amazon.com    208 pages, \$29



# Zolotarev Low-Pass Filter Design

*G3TMG explains the filter approximation problem relating to the synthesis of Zolotarev low-pass functions with finite zeros.*

This article develops a relatively simple method of using the known even-order mapping function to transform a pseudo-elliptic Chebyshev polynomial of odd order into a similarly pseudo-elliptic Zolotarev polynomial that can be used for a more efficient, realizable, low-pass, lumped element filter. “All working is shown in the method of polynomial construction for firstly, a Chebyshev response and secondly, the superior Zolotarev response, both possessing 7 poles and a single conjugate pair complexity.”

## Introduction

Using a stock Chebyshev low-pass filter design, providing a well matched pass-band from dc to a pre-defined cut-off frequency  $\omega_c$ , is not efficient, since more than half of the low-pass bandwidth is of no practical value. The required signal frequency to be filtered must lie above  $\omega_c/2$  so as to provide any harmonic attenuation from the filters transition edge. Pseudo-elliptic filters, which use just a single conjugate pair of transmission zeros, can significantly improve harmonic rejection for the same chosen order of low-pass filtering function. This is usually achieved by adding just one more electrical component to the conventional ladder network. A much more efficient filter design can be obtained by combining the concepts that the bottom half of the passband need not to be well matched, together with the pseudo-elliptic single conjugate zeros approach.

In the 1970's, Zolotarev functions were rediscovered and found to be more useful than the ubiquitous Chebyshev low-pass characteristic, in the context of an efficient filtering function.<sup>1</sup> However, the generation of the odd-ordered Zolotarev functions —

the most appropriate for low-pass filters — is very complicated and is a task that can only be described as torturous. Interestingly, even-ordered functions are more easily obtained since they have an extremely simple closed-form solution to the mapping of existing Chebyshev reflection zeros. Although not perfect, here we describe a somewhat simpler approach to odd-ordered functions using the even-ordered solution with the addition of a simple fractional bandwidth transformation, which corrects a significant scaling error that would otherwise be introduced.

## Some Basics

The transfer function for the general low-pass prototype 2-port filter is usually given in terms of the transmission scattering parameter as

$$|S_{21}(\omega)|^2 = \frac{1}{1 + \varepsilon^2 F_N^2(\omega)} \quad (1)$$

where  $F_N$  is known as the filter characteristic function of order  $N$ , and  $\varepsilon$  is a constant related to the pass-band ripple amplitude or reflection return loss  $R$ , and is defined by

$$\varepsilon = \frac{1}{\sqrt{10^{R/10} - 1}} \quad (2)$$

For the creation of a *Generalized Chebyshev* characteristic — also known as pseudo-elliptic and defined by a specified equi-ripple pass-band with arbitrarily placed stop-band transmission zeros — the filter function needs to be a rational polynomial described by

$$F_N(\omega) = \frac{P_N(\omega)}{D_N(\omega)} \quad (3)$$

It has been shown<sup>2</sup> that, in general, the denominator is given by the product of all the necessary transmission zeros such that

$$D_N(\omega) = \prod_{k=1}^N \left( 1 - \frac{\omega}{\omega z_k} \right) \quad (4)$$

It should be noted here that if all the necessary zeros lie at  $\omega z_k = \infty$ ,  $D_N(\omega)=1$  and the response degenerates to the standard Chebyshev characteristic also known as an all-pole function.

There are many ways of generating the  $P_N$  polynomial,<sup>3,4</sup> the simplest and most efficient being a recursion technique developed from the expansion of the Chebyshev function as shown by Amari.<sup>5</sup> Therefore, having identified a preferred pass-band ripple amplitude and any required finite frequency transmission zeros,  $D_N$  and  $P_N$  can be generated and the transmission frequency response evaluated using Eq (1). Also, using energy conservation, the reflection function can also be determined because under lossless conditions

$$|S_{21}(\omega)|^2 + |S_{11}(\omega)|^2 = 1$$

so that

$$|S_{11}(\omega)|^2 = 1 - |S_{21}(\omega)|^2 \quad (5)$$

Since these response expressions are power equations they do not fully characterize the synthesized response, since phase information cannot be extracted directly, and there is no apparent means of evaluating loss or delay information. To do this we must consider the equivalent of expressing the transmission and reflection parameters in terms of voltage and/or current. Phase

information is required, of course, to form the necessary relationship between the desired responses and the electrical network that would be able to realize the target function.

This is usually achieved in the  $s$ -plane by using the complex frequency variable  $s = \sigma + j\omega$  where  $\sigma$  represents the damping factor associated with voltage and/or current in lossy circuits and  $\omega$  is the usual real frequency variable. Therefore, in synthesis we let  $\sigma = 0$  so that energy conservation is obeyed and the synthesized response is ideal, or perfect. For analysis however, we can allow  $\sigma > 0$ . which is inversely proportional to the intended component  $Q$ 's, and represents real circuit losses. Therefore, the generated responses are imperfect and a close approximation to that which would be achieved in reality — an invaluable asset when making a determination of acceptability.

To begin then we expand Eq (1) as

$$S_{21}(s) \cdot \overline{S_{21}(s)} = \frac{1}{(1 + j\varepsilon \cdot F_N(s)) \cdot (1 - j\varepsilon \cdot F_N(s))} \quad (6)$$

Here, we can solve either or both of the denominator factors as they both contain the transmission function roots, albeit for low-pass functions in conjugate pairs. By choosing just one of the denominator factors, the phase information can be obtained directly as long as the factor is strictly *Hurwitz*, meaning that all of its roots lie in the left half of the  $s$ -plane.

We then write

$$S_{21}(s) = \frac{1}{1 + j\varepsilon \cdot F_N(s)}$$

where  $s = \sigma + j\omega$

and

$$F_N(s) = \frac{P_N(s)}{D_N(s)} \quad (7)$$

then we have

$$S_{21}(s) = \frac{D_N(s)}{D_N(s) + j\varepsilon \cdot P_N(s)} \quad (8)$$

It also follows from Eq (5) that

$$S_{11}(s) = \frac{\varepsilon \cdot P_N(s)}{D_N(s) + j\varepsilon \cdot P_N(s)} \quad (9)$$

### Example Generation of Generalized Chebyshev Filter Function

As an example, suppose we wish to synthesize a 7<sup>th</sup> order Chebyshev low-pass

function with a single finite frequency conjugate pair of transmission zeros at  $s = \pm j 1.75$ . With the five remaining zeros at infinity, Eq (4) gives the polynomial  $D_7(s)$  as

$$D_7(s) = \begin{pmatrix} 1 \\ 0 \\ 0.3265 \end{pmatrix} \cdot s^r$$

From here on, the polynomial coefficients are in zero-based vector format with the  $r^{\text{th}}$  row entry from the top representing the coefficient of  $s^r$ , so, the first or top entry is the coefficient of  $s^0$ , which is always a constant. Now, setting the pass-band return-loss to 20 dB — equivalent to a ripple of 0.044 dB — Eq (2) gives  $\varepsilon = 0.1005$ . Using Amari's recursive algorithm we get

$$P_7(s) = \begin{pmatrix} 0 \\ j6.641 \\ 0 \\ j49.704 \\ 0 \\ j95.426 \\ 0 \\ j53.036 \end{pmatrix} \cdot s^r$$

From Eq (9) it should be clear that the roots of  $P_7(s)$  are the zeros of the reflection function  $S_{11}(s)$ , and is a list of frequencies written in vector form where, from Eq (5), the response gain is unity. These frequencies are

$$S_{11 \text{ zeros}} = \begin{pmatrix} -j0.9777 \\ -j0.7988 \\ -j0.4531 \\ 0 \\ +j0.4531 \\ +j0.7988 \\ +j0.9777 \end{pmatrix} \quad (10)$$

The common denominator polynomial is therefore constructed as

$$D_7(s) + j\varepsilon P_7(s) = \begin{pmatrix} 1 \\ -0.6675 \\ 0.3265 \\ -4.995 \\ 0 \\ -9.591 \\ 0 \\ -5.330 \end{pmatrix} \cdot s^r \quad (11)$$

From Eq (8) it should also be clear that the roots of the denominator are the poles of the transmission function  $S_{21}(s)$ . These singularities are

$$S_{21}(\text{poles1}) = \begin{pmatrix} -0.0845 - j1.0591 \\ +0.2583 - j0.8786 \\ -0.4082 - j0.5060 \\ 0.4689 \\ -0.4082 + j0.5060 \\ +0.2583 + j0.8786 \\ -0.0845 + j1.0591 \end{pmatrix}$$

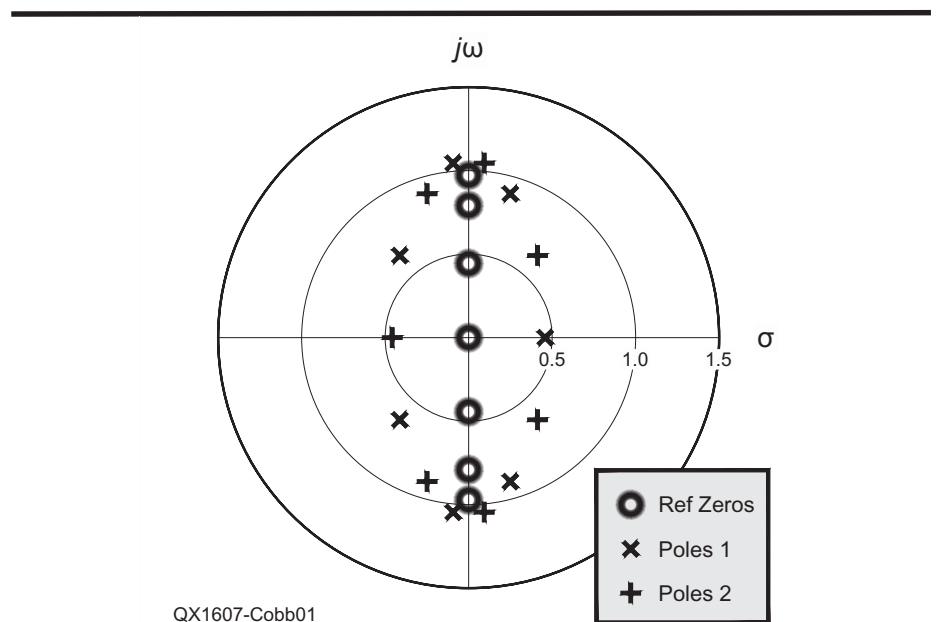


Figure 1 — The  $s$ -plane view of transmission poles and reflection zeros.



From the values shown, this polynomial is clearly not *Hurwitz* since some roots are in the left half-plane while others are in the right. However, if we had chosen the alternative denominator factor of Eq (6), the pole singularities would be the complementary ones,

$$S_{21}(poles2) = \begin{pmatrix} +0.0845 - j1.0591 \\ -0.2583 - j0.8786 \\ +0.4082 - j0.5060 \\ -0.4689 \\ +0.4082 + j0.5060 \\ -0.2583 + j0.8786 \\ +0.0845 + j1.0591 \end{pmatrix}$$

If we plot both sets of roots in the *s*-plane, we see in Figure 1 that the roots alternate from left to right about the *jω* axis.

By just reversing the positive sign of the real part of the denominator roots, the polynomial factor will be the strictly *Hurwitz* one needed. However, after multiplying out, it will be found that the new

$$(D_N(s) + j\varepsilon \cdot P_N(s))'$$

polynomial will always be monic. It is important to note that this will affect the unity gain condition defined at each reflection zero. The new pole positions are

$$S_{21}(poles) = \begin{pmatrix} -0.0845 - j1.0591 \\ -0.2583 - j0.8786 \\ -0.4082 - j0.5060 \\ -0.4689 \\ -0.4082 + j0.5060 \\ -0.2583 + j0.8786 \\ -0.0845 + j1.0591 \end{pmatrix}$$

and are plotted in Figure 2.

Multiplying out creates the new denominator polynomial as

$$(D_7(s) + j\varepsilon \cdot P_7(s))' = \begin{pmatrix} 0.1867 \\ 0.9061 \\ 2.2076 \\ 3.6690 \\ 4.1159 \\ 3.7413 \\ 1.9708 \\ 1 \end{pmatrix} \cdot s^7$$

Because the new denominator polynomial was expected, and clearly is monic, the gain

error can be found simply by evaluating  $S_{21}$  using Eq (8) at any of the known  $S_{11}$  singularities in Eq (10) as

$$G = \left| \frac{\sum_{r=1}^7 D_r \cdot (S_{11zero})^r}{\sum_{r=1}^7 (D_r + j\varepsilon \cdot P_r) \cdot (S_{11zero})^r} \right| = 5.3303$$

$G$  now acts as a scaling factor for all response calculations so that Eq (8) and (9) are rewritten as

$$S_{21}(s) = \frac{1}{G} \cdot \frac{D_7(s)}{(D_7(s) + j\varepsilon \cdot P_7(s))'} \quad (12)$$

and

$$S_{11}(s) = \frac{j}{G} \cdot \frac{\varepsilon \cdot P_7(s)}{(D_7(s) + j\varepsilon \cdot P_7(s))'} \quad (13)$$

Because of the unitary condition required by the scattering matrix,  $S_{21}$  and  $S_{11}$  must be, as indicated, orthogonal functions. The expression for  $S_{22}$  would be the same as Eq (13) except the  $j$  term would be  $-j$ .

With the polynomials thus far generated, Eq (12) and (13) produce the expected symmetrical response with the correct unity gain and phase that matches the targeted example specification. Figures 3(a) shows the overall amplitude response, Figure 3(b) shows the passband ripple, and Figure 3(c) shows phase response for 7-2 Chebyshev function.

### Zolotarev Approximation

Zolotarev functions are similar to Chebyshev functions in that they have an equi-ripple in-band amplitude characteristic, except that with an extra design parameter  $x$ , the ripple peaks nearest to the origin are allowed to exceed the unit passband ripple amplitude. The ripple characteristics for the Zolotarev even (8<sup>th</sup> order) function are shown in Figure 4(a), and for the odd (9<sup>th</sup> order) functions in Figure 4(b), where the intervals ( $x < \omega < 1$ ) and  $-(1 < \omega < x)$  are the desired equi-ripple passbands. The Chebyshev function of the same order is also shown for comparison.

There are restrictions associated with the use of Zolotarev functions for lumped element passive circuit realizations. For example, it's not immediately obvious that even orders of Zolotarev polynomials are of little value for use in low pass filters due to the fact that the ratio of source to load resistances is usually required to be large because little of the available source power needs to be developed in the load at  $\omega = 0$ , or dc. They are however useful in generating dual band-pass filters where the prototype network is ultimately transformed into the real frequency band-pass domain – recently a popular area of study.

Odd ordered functions, on the other hand, do not have this problem as they always require that the source to load resistance ratio be unity. They also offer superior stop-band rejection and better component values with less abrupt changes throughout the circuit when compared to similar Chebyshev pseudo-elliptic response realizations.

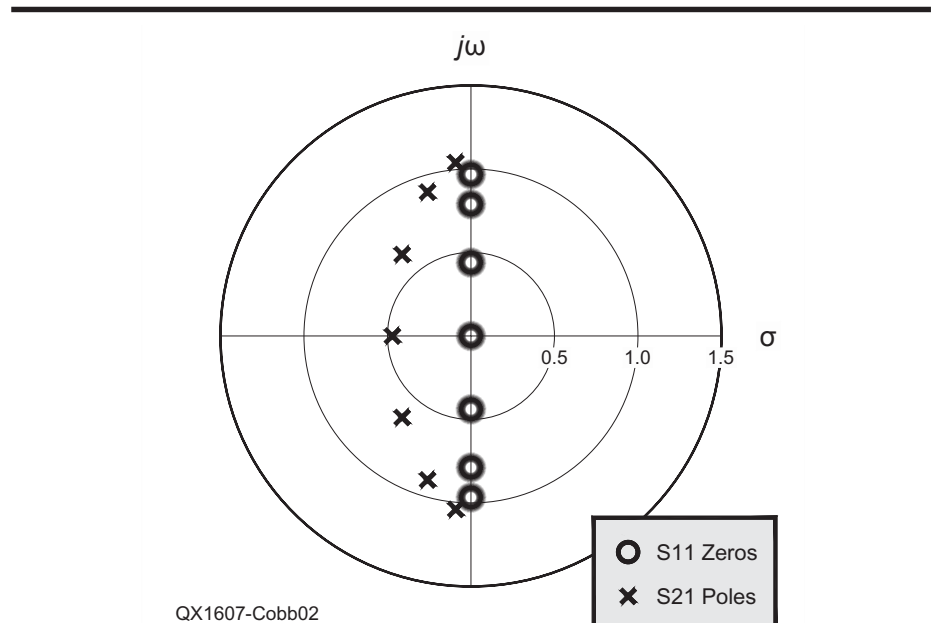
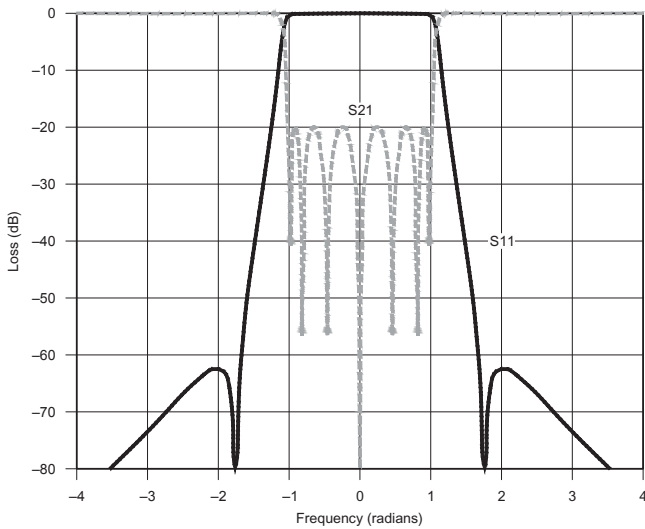
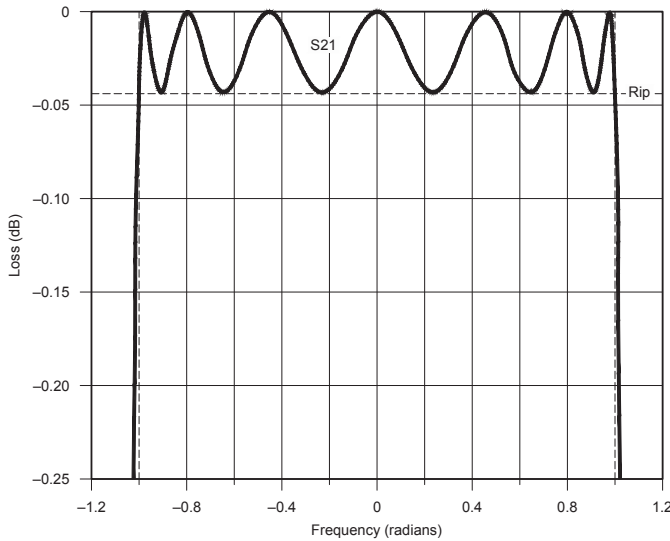


Figure 2 — The *s*-plane view of new transmission poles and reflection zeros.



**Figure 3(a) — Overall amplitude response for 7-2 Chebyshev function.**

QX1607-Cobb03a



**Figure 3(b) — Pass-band ripple response for 7-2 Chebyshev function.**

QX1607-Cobb03b

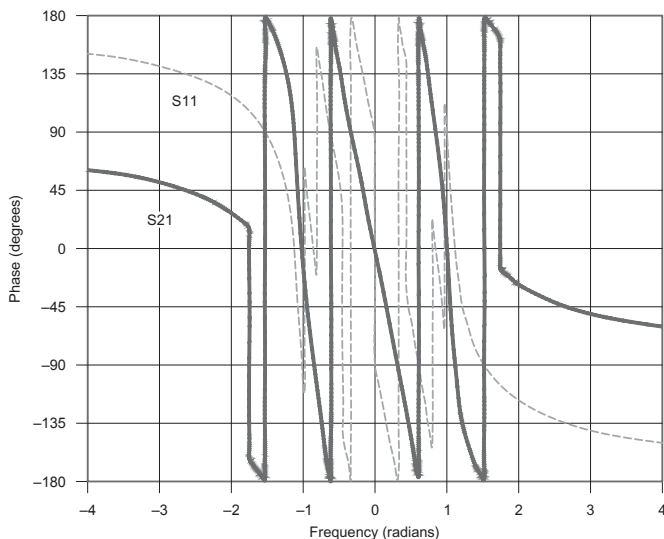


**Figure 3(c) — Complete phase response for 7-2 Chebyshev function.**

QX1607-Cobb03c

### Synthesis of Zolotarev Functions

Even ordered functions can easily be synthesized by transforming existing Chebyshev reflection zeros  $s_k$  into new positions  $s'_k$  using the mapping

$$s'_k = \pm \sqrt{s_k^2(1-x^2) - x^2} \quad (14)$$

where  $x$  is the real frequency value at which the equi-ripple behavior begins such that  $0 < x < 1$ . Note here that the equi-ripple fractional bandwidth ( $F_{bw}$ ) of the new response is  $(1-x)$  and when  $x=0$ ,  $F_{bw} = 1$  and the original zeros are unchanged.

Unfortunately, this expression is exact only for even-ordered functions and the work of Levy and Horton<sup>6,7</sup> has shown that the generation of an odd-ordered Zolotarev function that is exact is not a trivial undertaking. However, it is here shown by example, that the use of Eq (14) for odd ordered functions can yield acceptably near-Zolotarev characteristics with just one additional mapping of the  $x$  parameter so as to achieve the correct fractional bandwidth. The degree of nearness can already be seen in Figure 4(b), where the first equi-ripple turning point adjacent to, and to the right of, the positive  $x$  boundary, is slightly larger (more negative) than the -1 ideal value. Since the overall pass-band has complementary symmetry, the same deviation exists on the other side of the zero frequency axis where the first equi-ripple turning point, adjacent to, and to the left of the negative  $x$  boundary, is slightly larger (more positive) than the +1 ideal value.

Given that the highlighted pass-band amplitude errors are acceptable, it is found that the correlation between the fractional bandwidth scaling parameter  $x$  and achieved response bandwidth is the most significant issue. I decided to correct this scaling error by transforming  $x$  to a new parameter  $x'$  that equates correctly to the specified fractional bandwidth.

Consequently, I carried out a curve fitting exercise, concluding that the error characteristics are nearly linear with a small parabolic curvature. Therefore, a simple 2<sup>nd</sup> degree polynomial mapping provides correction to within 0.2% for a range of odd-ordered Zolotarev functions from 5 to 19 — a large enough range to be able to cope with most requirements. It is worth noting that filter functions below order 4 are in fact irrelevant because orders 2 and 3 are merely degenerate Chebyshev functions with parametrically scaled ripple factors.

The correction polynomial coefficients are conveniently written in matrix form such that the  $x$  to  $x'$  mapping is simply



$$x' = \begin{pmatrix} -0.5015 & 1.7150 & -0.2174 \\ -0.3164 & 1.5217 & -0.2121 \\ -0.2216 & 1.3988 & -0.1853 \\ -0.1653 & 1.3134 & -0.1555 \\ -0.1299 & 1.2566 & -0.1341 \\ -0.1062 & 1.2192 & -0.1202 \\ -0.0884 & 1.1878 & -0.1059 \\ -0.0713 & 1.1507 & -0.0838 \end{pmatrix} \cdot \begin{pmatrix} 1 \\ x \\ x^2 \end{pmatrix} \quad (15)$$

where the zero based row index is determined from  $(N - 5)/2$  and  $N$  is odd from 5 to 19.

### Example Generation of Generalized Zolotarev Filter Function

Suppose, for example, we wish to synthesize a 7<sup>th</sup> order Zolotarev low-pass function with a single finite frequency conjugate pair of transmission zeros at  $s = \pm j 1.75$  exactly as in the previous Chebyshev case. Here, however, we wish to compress the matched region to 35% of the unit bandwidth ( $F_{bw} = 0.35$ ) but again with the same specified ripple value.

So, the initial bandwidth scaling factor  $x$  is

$$x = 1 - F_{bw} = 0.65$$

which is corrected using Eq (15) to give

$$x' = 0.583$$

Next, the reflection zeros from Eq (10) are transformed using the mapping of Eq (14) and the new parameter  $x'$  giving

$$S_{11zeros} = \begin{pmatrix} -j0.9777 \\ -j0.7988 \\ -j0.4531 \\ 0 \\ +j0.4531 \\ +j0.7988 \\ +j0.9777 \end{pmatrix}$$

$$\text{maps to } \rightarrow \begin{pmatrix} -j0.9853 \\ -j0.8724 \\ -j0.6896 \\ 0 \\ +j0.6896 \\ +j0.8724 \\ +j0.9853 \end{pmatrix} = ZS_{11zeros}$$

(16)

Multiplying out now gives the new  $P$  monic polynomial  $ZP_7(s)$  as

$$ZP_7(s) = \begin{pmatrix} 0 \\ 0.35138 \\ 0 \\ 1.56253 \\ 0 \\ 2.20750 \\ 0 \\ 1 \end{pmatrix} \cdot s^7$$

Since we require the transmission zeros to be the same as in the previous Chebyshev case, the  $D_7$  polynomial does not need altering and Eq (7) can be used to establish that  $\lambda \cdot ZP_7(s) = P_7(s)$ .

In the typical Zolotarev case, the reflection zero frequencies of either side of this expression clearly do not correspond. So, the only point where the two sides are guaranteed to be equal is at the cut-off frequency  $s = \pm j$ . So, evaluating at  $s = j$  provides the scaling factor  $\lambda = j 184.47$  so that  $ZP_7$  is correctly specified as

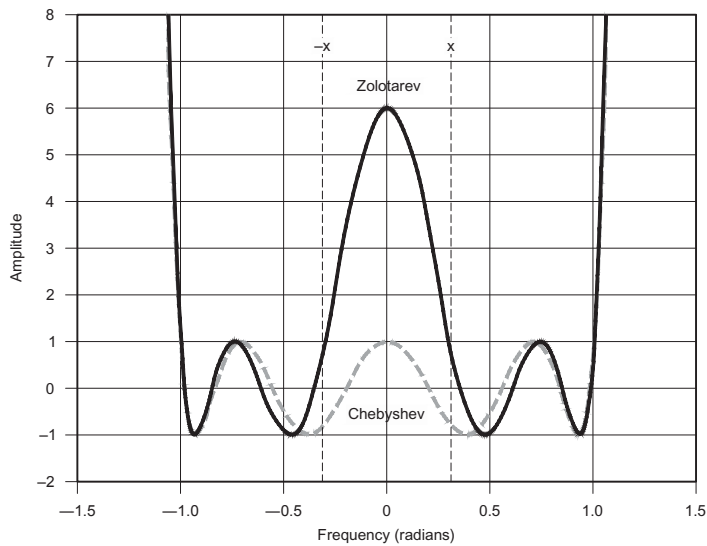


Figure 4(a)  
— Pass-band amplitude of 8<sup>th</sup> order Zolotarev function.

QX1607-Cobb04a

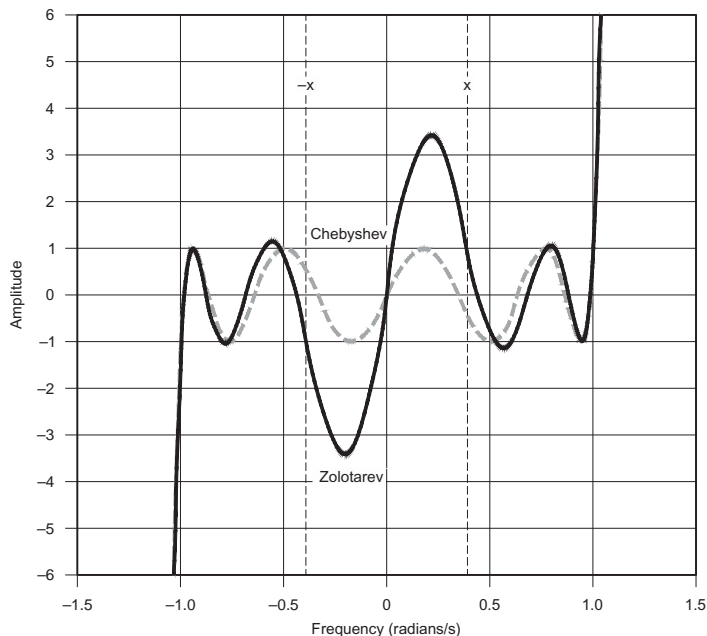


Figure 4(b)  
— Pass-band amplitude of 9<sup>th</sup> order Zolotarev function.

QX1607-Cobb04b

$$ZP(s) = \begin{pmatrix} 64.82 \\ 288.25 \\ 407.23 \\ 184.47 \end{pmatrix} \cdot s$$

$$ZS_{21}(\text{poles}) = \begin{pmatrix} -0.05982 - j1.03886 \\ -0.16426 - j0.89974 \\ -0.17522 - j0.62451 \\ -0.14154 \\ -0.17522 + j0.62451 \\ -0.16426 + j0.89974 \\ -0.05982 + j1.03886 \end{pmatrix}$$

As in Eq (11) before, the common denominator is constructed as

$$D_7(s) + j\epsilon ZP_7(s) = \begin{pmatrix} 1 \\ -6.515 \\ 0.3265 \\ -28.97 \\ 0 \\ -40.93 \\ 0 \\ -18.54 \end{pmatrix} \cdot s^r$$

$$(D_7(s) + j\epsilon \cdot ZP_7(s))' = \begin{pmatrix} 0.05394 \\ 0.45315 \\ 0.77662 \\ 2.07789 \\ 1.68971 \\ 2.64942 \\ 0.94013 \\ 1 \end{pmatrix} \cdot s^r$$

Similarly, it will be found that the roots of this polynomial are not *Hurwitz* so the singularities are determined (they are the poles of  $S_{21}$ ), and the alternating poles technique is used to reconstruct the denominator whose roots lie in the left half-plane, see Figure 5.

Multiplying out creates the new denominator polynomial

As before, this new denominator polynomial is monic and the gain error needs to be found by evaluating  $S_{21}$  using Eq (8) at any of the known  $ZS_{11}$  singularities from Eq (16).

$$GZ = \frac{\sum_{r=1}^7 D_r \cdot (ZS_{11zero})^r}{\sum_{r=1}^7 (D_r + j\epsilon \cdot PZ_r)' \cdot (ZS_{11zero})^r} = 18.540$$

With the new

$$(D_7(s) + j\epsilon \cdot P_7(s))'$$

polynomial and  $GZ$ , Eq (12) and (13) are used to produce the expected symmetrical response with the correct unity gain and phase that matches the desired example specification. Figures 6(a) shows the overall amplitude response, Figure 6(b) shows the pass-band ripple and Figure 6(c) shows the complete phase response for 7-2 Zolotarev function. Here, only the positive real frequencies are shown for relevance to a real low-pass frequency response demonstrating the near Zolotarev behavior in terms of both the pass-band ripple amplitude and superior rejection, when compared to the equivalent Chebyshev response, which is also shown. Finally, observe that using the new transformation Eq (15), the equi-ripple fraction bandwidth achieved is precisely 0.35 of the unit bandwidth, as was intended.

### Concluding Remarks

A technique used to create the necessary transmission and reflection polynomials approximating the superior Zolotarev low-pass filter function of odd order has been shown. A transformation Eq (15) has also been shown to be effective in correcting the scaling parameter  $x$  so that the simple reflection zero position mapping function Eq (14) can be systematically applied in a predetermined synthesis procedure.

The only disadvantage of using such a simple procedure is the slight distortion that occurs in the target equi-ripple behavior for the first ripple most adjacent to, and on the right side of, the low frequency cut-off point of the required passband. However, it can be shown that after component extraction, the degree of observed distortion is comparable with the SVC (standard value component) design tolerance issue. If an optimization technique is adopted, as demonstrated by Gary Appel<sup>8</sup>, it is suggested that using the synthesis procedure shown here provides a better and more stable starting point yielding the least number of iterations to achieve precise results. In practice, the response can easily be corrected by hand in the circuit simulation tuning environment for responses up to the maximum order of 19 proposed here, well beyond typical design requirements.

To demonstrate the practical use of this synthesis procedure, a second article will follow, which shows several examples of real filters constructed using two different inductor techniques. These are air-cored shielded solenoid and ferrite toroidal inductors appropriate for VHF and HF designs respectively.

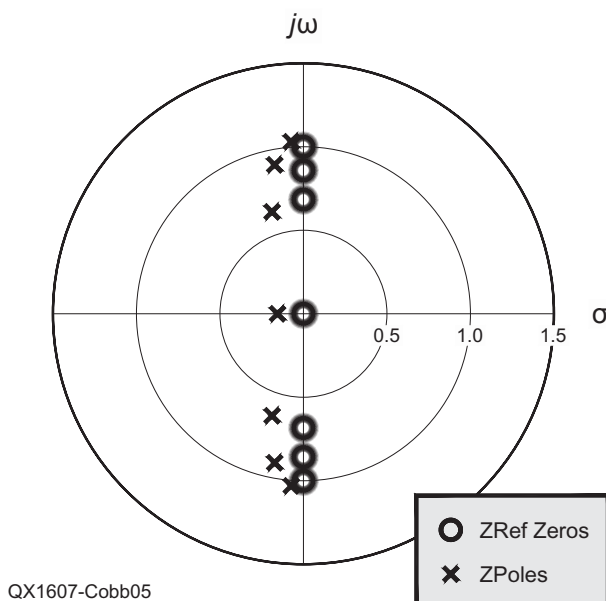
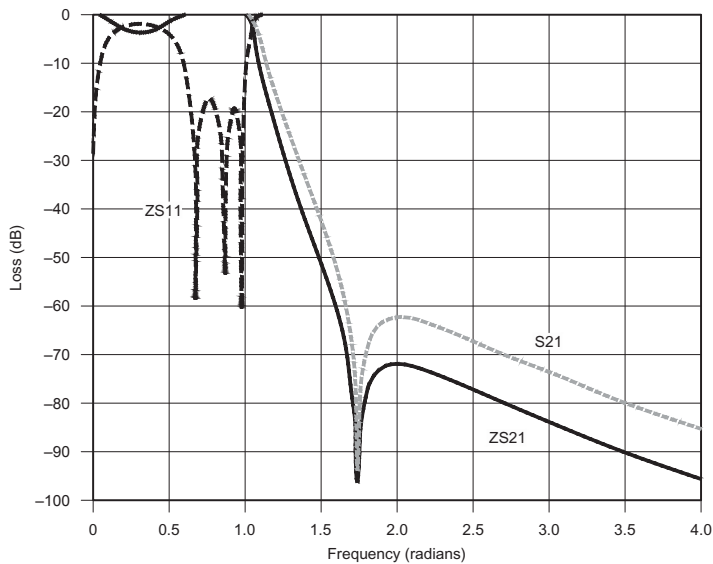


Figure 5 — The  $s$ -plane view of Zolotarev transmission poles and reflection zeros.





**Figure 6(a)**  
— Overall  
amplitude  
response for  
7-2 Zolotarev  
function.

QX1607-Cobb06a

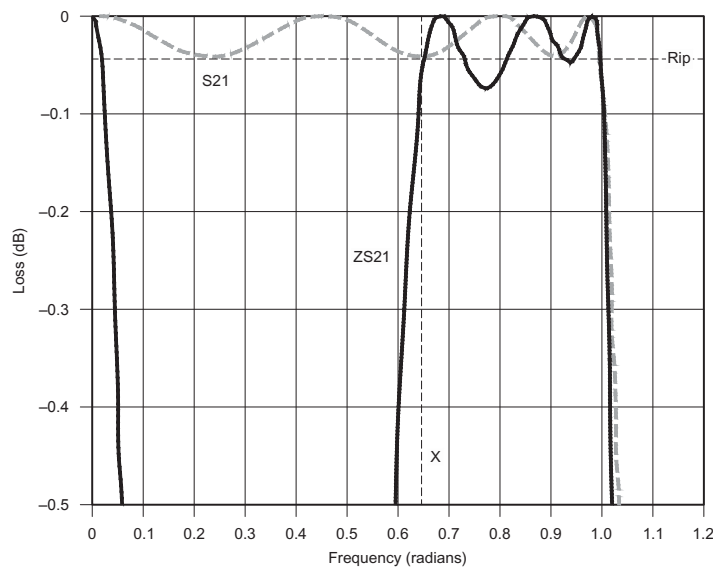


**Figure 6(b)**  
— Pass-band  
ripple response  
for 7-2 Zolotarev  
function.

QX1607-Cobb06b

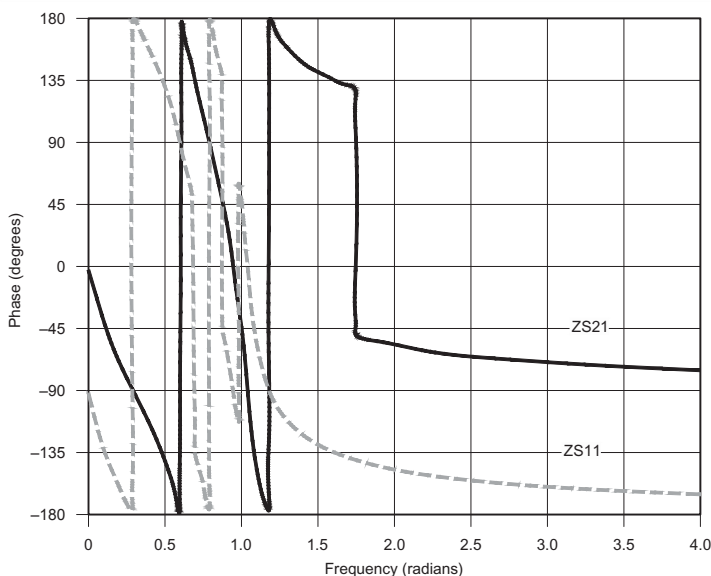


**Figure 6(c)**  
— Complete  
phase  
response for  
7-2 Zolotarev  
function.

QX1607-Cobb06c

Gary Cobb, G3TMG, has held the same call sign since he was first licensed in 1964. He holds a BA in Mathematics, an MSc in Microwave Physics, and is a Life Member of the IEEE. His early professional career development took place in the defense industry where he designed high resolution microwave antenna interferometry systems. His later, research activities moved toward the realization of adaptive arrays for ship-borne radio communications in a Navy environment. Gary spent the last 20 years in military and commercial satellite payload engineering, developing output multiplexers, multi-port amplifiers and filter techniques appropriate for high-power geostationary systems. Now retired, Gary operates CW and SSB on HF and VHF amateur bands with a special interest in sporadic-E during the summer months.

## Notes

- <sup>1</sup>R. Levy, "Generalized Rational Function Approximation in Finite Intervals Using Zolotarev Functions", *IEEE Trans, MTT*, Vol 18, December, 1970, pp 1051-1064.
- <sup>2</sup>R.J. Cameron "Fast generation of Chebyshev filter prototypes with asymmetrically-prescribed transmission zeros", *ESA Journal*, Vol 6, 1982, pp 83-95.
- <sup>3</sup>R.J. Cameron et al, *Microwave Filters for Communications Systems*, John Wiley & Sons Inc, 2007, Chapter 6.3.
- <sup>4</sup>J.D. Rhodes and S.A. Alseyab, "The generalized Chebyshev low-pass prototype filter", *Circuit Theory Application*, Vol 8, 1980, pp 113-125.
- <sup>5</sup>S. Amari, "Synthesis of Cross-Coupled Resonator Filters Using an Analytical Gradient-Based Optimization Technique", *IEEE MTT*, Vol 48, Sep, 2000, pp 1559-1564.
- <sup>6</sup>M.C. Horton, "Quasi-Lowpass, Quasi-Elliptic Symmetric Filter", *IEEE Trans, MTT-S Digest*, 1987, pp 129-132.
- <sup>7</sup>See Note 1.
- <sup>8</sup>Gary Appel, "Filter Synthesis using Equal Ripple Optimization", *QEX*, Jul/Aug, 2011, pp 22-30.

# Hands-On-SDR

*The author explains using the FPGA with SDR designs.*

In this installment we will continue onwards and upwards into more inner workings of the Field Programmable Gate Array or FPGA used in many of our SDR designs. This column relies heavily on what I covered in my Mar/Apr 2015 and Jan/Feb 2016 columns.<sup>1,2</sup> If you have not read at least the most recent one, please take a minute and do a quick review. It has been a while since we covered some of this material, so we will start with a quick review here.

In the Mar/Apr 2015 column, we covered getting the free tools set up and showed you how to compile and run an example design. In the Jan/Feb 2016 issue, we covered porting of open-source FPGA code to run on Arrow's BeMicroCVA9 FPGA development board used in the Hermes-Lite and IQ2 Software Defined Radios.

Many revisions have been made to the Hermes software that we used as a starting point in my last column. As a review, I will quickly cover the steps necessary to port the newest version of the Hermes FPGA code to the BeMicroCVA9. Please refer to my last column for more detail or if you need a refresher.

Once again, I want to thank Phil Harman, VK6PH, for his work in updating this FPGA code. It is truly a Herculean task!

## What Do We Need to Get Started?

As with each of these columns, I always try to define what you need in the way of

knowledge and equipment to get the most out of the "Hands On SDR experience". You will need a basic working knowledge of the Verilog hardware description language. Once again, my assumption is that the existing code is working, and we will try not to introduce any new bugs as we port to the new device. As we did last time, we are *targeting* a new device, not *designing code* from scratch.

For hardware, you will need a BeMicroCVA9 development kit.<sup>3</sup> To actually run the code that we are going to compile in this column, you will also need an HF2 board (to receive), or both HF2 and TX2 boards (to transceive).<sup>4,5</sup> As a lower-performance (and less expensive) alternative, you can use an HF1 or Hermes-Lite, but you will need to make other modifications to the code if you go that route.<sup>6,7</sup> I believe that the Hermes-Lite group has ported their firmware to the BeMicroCVA9. After wading through this column, you should be expert enough to compile their source and run it on the BeMicroCVA9. Even if you do not have the hardware, you can still follow along with the text and learn about porting FPGA code to new devices.

For tools, we will still need *two* versions of Altera's Quartus FPGA design software to complete the porting work. The first version is Quartus II version 13.1, which is the version that was used to create the code that we are going to port. The second version is the latest (and newly released as of this writing),

version 16.0. It is now called Quartus Prime Lite, and requires a 64-bit operating system. You will need 64-bit Windows XP, Windows 7 or later or 64-bit Linux in order to run this new version. All of the information from my Mar/Apr column applies to both Quartus versions. Before you continue, you will need to download and install both of the free web versions (Quartus II version 13.1 and Quartus Prime Lite 16.0) from the Altera web site.<sup>8</sup> To save some download time, you only need to download Cyclone III and Cyclone V device support for Quartus II version 13.1, and only Cyclone V device support for Quartus Prime Lite version 16.0.

## Why Two Quartus Versions?

The conditions that required us to use two versions of the design software still exist, even with the release of the new Quartus Prime Lite 16.0. I explained this in my last column, but it is important enough to bear repetition here. The explanation is tied to the capabilities of each Quartus version and the FPGA part that we are migrating *from* as well as the part we are migrating *to*. The Hermes code targets the Cyclone III EP3C25Q240C8 (our *from* part number), while the BeMicroCVA9 uses a Cyclone V 5CEFA9F23C8 (our *to* part number). Quartus II version 13.1 supports all Cyclone III parts and some of the Cyclone V parts, but unfortunately not our *to* part number. Quartus Prime Lite version 16.0 supports

**Table 1.**  
Clock name changes in the Hermes.sdc file.

Line(s)	original name in <i>Hermes.sdc</i> file
19, 154	PHY_CLK125
33, 143	PLL_IF_inst altpll_component auto_generated pll1 clk[0]
34, 144, 184	PLL_IF_inst altpll_component auto_generated pll1 clk[1]
35, 145, 184	PLL_IF_inst altpll_component auto_generated pll1 clk[2]
37, 157	network_inst rgmii_send_inst tx_pll_inst altpll_component auto_generated pll1 clk[2]
39, 158, 171	network_inst rgmii_send_inst tx_pll_inst altpll_component auto_generated pll1 clk[4]
48, 156	network_inst rgmii_send_inst tx_pll_inst altpll_component auto_generated pll1 clk[1]
155, 169, 171, 193	network_inst rgmii_send_inst tx_pll_inst altpll_component auto_generated pll1 clk[0]
161	OSC_10MHZ PLL2_inst altpll_component auto_generated pll1 clk[0]



all Cyclone V parts (including our *to* part number), but no Cyclone III parts at all! The easiest way to migrate to the new part and new Quartus version is to change part families first and then upgrade to the latest version of Quartus as a separate operation. Here is the flow of part numbers and Quartus versions that we will use: 3C25 with v13.1 → 5CEFA7 with v13.1 → 5CEFA7 with v16.0 → 5CEFA9 with v16.0.

Notice that Quartus II version 13.1 does not support our 5CEFA9F23C8 part, so we pick a dummy part (5CEFA7F23C8) that it does support just to get us into the Cyclone V family. After we migrate to Quartus Prime Lite version 16.0, we will pick our final, correct 5CEFA9F23C8 target. Also notice that in the flow above, we only change *one* item in each step: either the part number or the Quartus version, but never both.

---

## FPGA Code Porting Tasks

We covered these steps last time, but here they are again:

- Open design in original Quartus version
- Update wizard-generated modules
- Add code to hook in new signals and remove unused old signals
  - Add new location properties
  - Update SDC timing constraints file with new signals and remove old signals
  - Compile-debug-repeat.

I explained the first four steps in detail last time, so I will focus on the last two this time around. That doesn't mean that I will leave you completely on your own, just don't expect as much detail as last time. We want save room to do some *new* things! Unfortunately, we have some *old* things to get out of the way before we can move on to the new.

---

## Open and Compile the Design

To get a copy of the FPGA source code, download a copy of the Quartus archive from the SDRstick SVN webserver.<sup>9</sup> Open the archive in Quartus II version 13.1 and fire off a trial compile right off the bat. This will tell you if you have everything set up correctly.

You should get a bunch of warnings from Quartus (I got 400!), but no errors. As usual, if Quartus reports errors, you must fix them before you can continue.

The cleanup step that we had to perform last time has already been done as part of the many upgrades that have been done since we last looked at the code.

---

## Update Wizard-generated Modules

The Hermes design uses four PLLs, seven FIFO memories, four ROM memories, one RAM memory, one multiplier and three other functions for a total of 20 Wizard generated modules. Check the IP Components tab of the Project Navigator to see a list of IP components and version numbers. Each of these modules must be updated first to the Cyclone V family under Quartus II version 13.1 before we can open them in Quartus Prime Lite version 16.0.

Move the design to the Cyclone V family and remove all location assignments. We will add the new (and different) location assignments for the new FPGA part number later. Select the **5CEFA7F23C8** part. Note that this is not the final part, but an intermediate one that we must pick due to the vagaries of the Quartus software. And we are still using Quartus II version 13.1. We will fix both of these problems after we finish updating the wizard-generated modules.

Update the 20 wizard-generated modules, taking care with the PLLs and the **firromH** module. Remember that Cyclone V PLLs are different from Cyclone III PLLs, so you must create new ones and replace the old ones with the new ones. Close Quartus and re-open the project in Quartus Prime Lite version 16.0. The new version of Quartus will ask you if it should overwrite the database with the new format. You can safely answer **Yes**. Change the part number to 5CEFA9F23C8 and run a compile to see if we broke anything. Now we are using version 16.0 with the correct FPGA part number. We are almost done!

---

## Add and Remove Code and Signals

The next step in our 6-step program is to match up the old design (Hermes)

signals with the new design (CVA9) signals. Remember to account for every one of the Hermes signals, as well as every one of the new design pins (CVA9) by either ignoring it, adding code to support it or just connecting it to its counterpart from the old design. I have created a file for you containing a table of all of the signal names in the design to help make the changes. This **Hermes\_1\_May\_to\_IQ2\_pins** table will tell us which pins map directly onto new pins and which do not.<sup>10</sup> I will not revisit the changes covered in my last column; please refer back to it to make the changes (see Note 2).

---

## Add New Location Properties

Now it is time to add the new location properties back in to replace the old ones that we deleted when we changed part numbers. Again, I have created a file for you to save you the effort of typing all those lines into the script file. You can download it from the SDRstick SVN webserver.<sup>11</sup>

To run the script, place the file in your top directory (that is, the directory that contains your **Hermes.qsf** file and all of your Verilog source files). Now add it to your project using **<Project> <Add/Remove Files in Project...>**. Under **<Tools> <Tcl Scripts...>**, select the file and click **Run**. All of your pin locations from the script file have now been added. If you want to check your new assignments (you should believe me by now) you can open the Assignment Editor from (where else) the **<Assignments> <Assignment Editor>** menu. You should see all of your new **Location** assignments listed. Run a compile to make sure things are as they should be.

Wow, all that work just to get to the same point that we were at the end of the last column! Well, not quite... This time we started with FPGA code that is many revisions better than the version that we started with last time, and we are now using the latest and greatest version of the Altera tools (Quartus Prime Lite 16.0). And best of all, we have proven that we have learned enough to do it over and over again. Next time, no peeking at the previous column!

---

*new name in Hermes.sdc file*

```
DDR3_CLK_50MHZ
PLL_IF_inst|pll_if_new_inst|altera_pll_i|cyclonev_pll|counter[0].output_counter|divclk
PLL_IF_inst|pll_if_new_inst|altera_pll_i|cyclonev_pll|counter[1].output_counter|divclk
PLL_IF_inst|pll_if_new_inst|altera_pll_i|cyclonev_pll|counter[3].output_counter|divclk
network_inst|rgmii_send_inst|tx_pll_inst|tx_pll_new_inst|altera_pll_i|cyclonev_pll|counter[2].output_counter|divclk
network_inst|rgmii_send_inst|tx_pll_inst|tx_pll_new_inst|altera_pll_i|cyclonev_pll|counter[3].output_counter|divclk
network_inst|rgmii_send_inst|tx_pll_inst|tx_pll_new_inst|altera_pll_i|cyclonev_pll|counter[1].output_counter|divclk
network_inst|rgmii_send_inst|tx_pll_inst|tx_pll_new_inst|altera_pll_i|cyclonev_pll|counter[0].output_counter|divclk
PLL2_inst|c10_pll_new_inst|altera_pll_i|cyclonev_pll|counter[1].output_counter|divclk
```

## Update SDC Timing Constraints

Now we will update the **Hermes.sdc** timing constraints file line by line to remove constraints for signals that we have removed, add (or expand existing) constraints for new signals and update constraints for anything that we changed. This is where we left off last time, so it is time to do it now.

Most of the changes to the **Hermes.sdc** file are due to the changes that we made to the PLLs. The SDC file refers to the PLL pins by name, and remember that we changed some of them. We have to fix the names in the SDC file so that the timing analyzer can match them up with the design files. I have listed the changed names in Table 1. The first entry is not a PLL change, but a clock pin name change. Remember that there is no **PHY\_CLK125** clock from the Ethernet PHY chip on the BeMicroCVA9. We changed that to a 50 MHz clock (from an external oscillator). The only place that this 125 MHz clock was used was as a reference clock input to the **tx\_pll**. When we created **tx\_pll\_new**, we simply changed the PLL programming a bit so that it uses a 50MHz reference rather than the original 125MHz reference. On line 19 of the **Hermes.sdc** file, change **PHY\_CLK125** to **DDR3\_CLK\_50MHZ** in both places it appears, then change the **8.000**

after -“period” to **20.000**. Why? Because this number represents the clock period in ns; 8ns period is 125 MHz and 20 ns period is 50 MHz. Make the name changes shown on each line in Table 1. Note that some lines require multiple changes.

Next, we want to remove references to any signal that we removed. Rather than remove a line, comment it out by placing an octothorpe (# symbol) in the first column of the line<sup>12</sup>. Affected lines (and signal names) are 88 (SO), 94 (ADCMISO), 120 (MOSI, nCS), 123 (CMODE only), 126 (J15\_5, J15\_6, SPI\_SDO), 129 (CS, SCK, SI), 132 (ADCMOSI, nADCCS), 196 (SSCK, ADCCLK, SPI\_SCK only), 205 (USEROUT\* only), 208 (ANT\_TUNE, IO4-IO8 only). Note that the lines that I have marked “only” cannot be commented out, since we are only removing the reference to the listed signals. Other signals listed on the same line must remain, so just delete the signal(s) that I have indicated above and leave the rest alone. Since we removed all of the pins associated with the EEPROM (since the CVA9 does not have one), we can comment out line 211. Since we commented out lines 94, 126 and 132, **data\_clk2** is no longer used; we can comment out line 54 and remove line 147. (Leave just the “\n”

line 147 to preserve the line numbering.) The last thing we will do is comment out lines 70 and 104 to eliminate unnecessary timing constraints on the ASMI block, which we upgraded to a Cyclone V version.

This should result in a **Hermes.sdc** file that generates no warnings. To check to see if we missed anything, open TimeQuest by clicking on **<TimeQuest Timing Analyzer>** under the **<Tools>** menu. Once TimeQuest opens, double click on **Update Timing Netlist** in the Tasks pane on the left side of the screen. This will cause all three tasks listed under Netlist Setup to run: **Create Timing Netlist**, **Read SDC File** and **Update Timing Netlist**. All three of these lines should turn green, and a check mark should appear next to each of them (see Figure 1). Most importantly, though, is that any warnings will appear in the Console pane across the bottom of the screen. If you see any warnings, then TimeQuest is not happy with your **Hermes.sdc** file and you should make corrections before proceeding. If you want to see what a warning looks like, go back to the **Hermes.sdc** file and undo one of the fixes that you just put in. (As an example, un-comment out line 70.) Save the SDC file, return to the TimeQuest screen (or re-open TimeQuest) and this time click on **Reset Design** before you click on **Update Timing Netlist**. Doing this tells TimeQuest to re-run the three Netlist Setup tasks from scratch, so you get a fresh read-in of the SDC file. Note that you do not need to recompile the design to do this. The design hasn’t changed; we are merely checking the design against different timing constraints to see if it meets them. If you actually changed a timing parameter (such as a clock period or an input delay), you would have to recompile your design so that Quartus could optimize the routing to try and meet your new constraint.

## Compile-Debug-Repeat

The last thing we will do this month is to wade through some of the warnings that Quartus generates to get a feel for which ones can be safely ignored and which ones you should fix. My last compile generated 0 errors and 140 warnings. Your numbers may be slightly different, but not *too* different. This seems like an awful lot of warnings, doesn’t it? After we review some (or most) of these warnings and their causes, you will see that, in fact, it really isn’t that many. Quartus “warns” you about many things that you either can’t do anything about because they are generated by internal code that you cannot edit or are simply unimportant, such as a size mismatch in an assignment statement. Quartus also warns you about things that really are problems, just not fatal ones. For example, suppose we forgot to

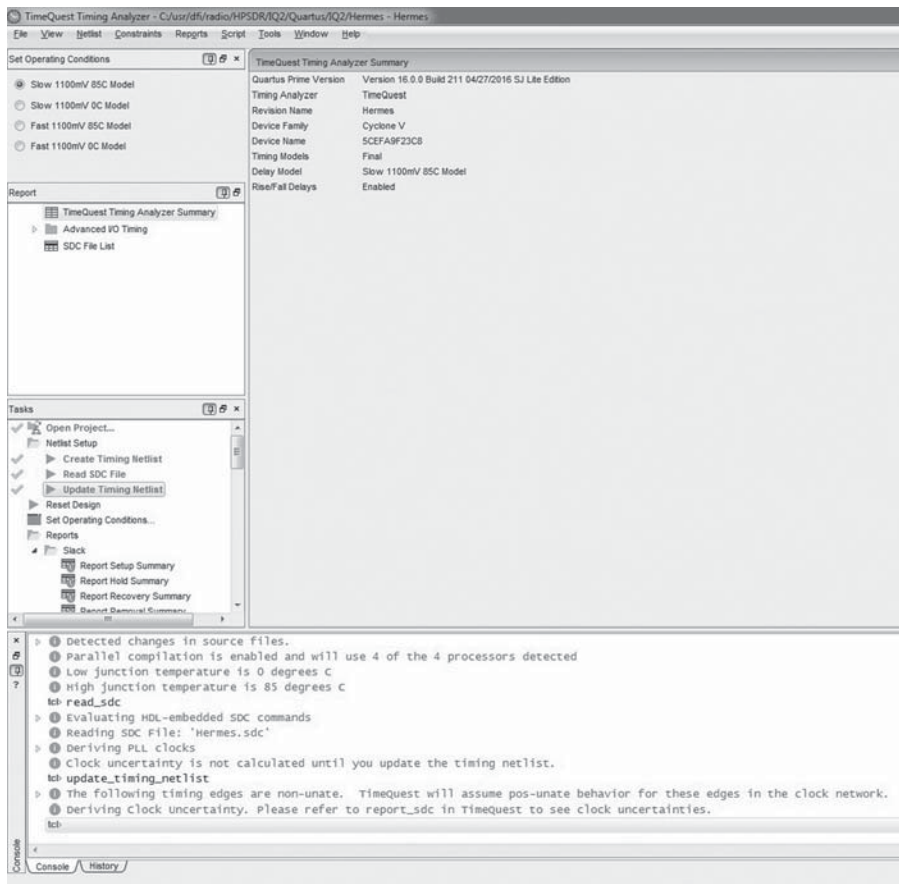


Figure 1 — TimeQuest timing analyzer.



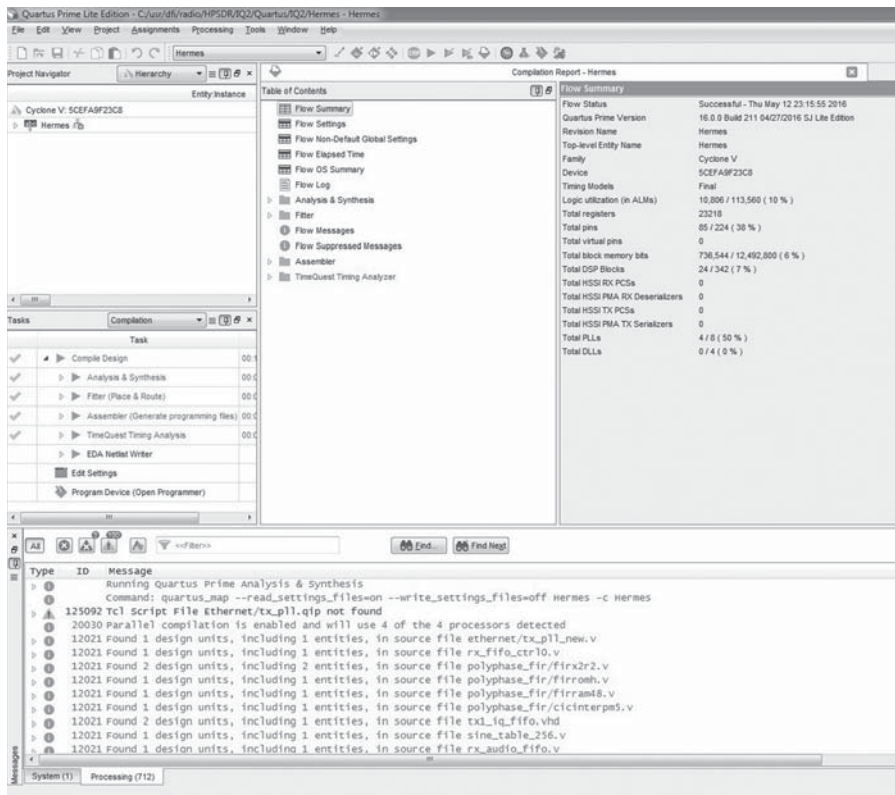


Figure 2 — Quartus Prime Lite 16.0 screen showing a warning in the message pane.

connect a signal to an I/O pin on the part. Quartus will remove all of the unused logic that connects to that signal. Maybe that is OK if you did it intentionally. If it was an oversight (we won't say *error*), you will be grateful that Quartus warns you that it removed logic and why it did so. The bottom line is that you must look at every warning to determine if it is important enough for you to investigate its cause. Since there are typically many warnings, you must be able to quickly assess the importance of each one. This takes skill, and skill comes through experience. So let's get some experience now.

Start a new compile and let it run to completion. After it finishes, scroll up in the messages window (the full width pane across the bottom of the Quartus window) to the first line that appears in blue. Warning messages are in blue and information messages are in green. Error messages are in red and will generally stop the compilation prematurely (you should not see any of these). You may or may not get the same messages that I get or in the same order that I get them. It will depend on the changes that you made versus the ones that I made, and in what order you made them as well as any mistakes that I made that you did not (or vice-versa). It will also depend to some extent on what options you have set in your project. Most warning messages will take you to the source of the warning if you double-click on the warning text, but not all of them will do this. Finding the source of the warning is the first step.

Correcting it is the second, unless you decide that it is unimportant and can remain.

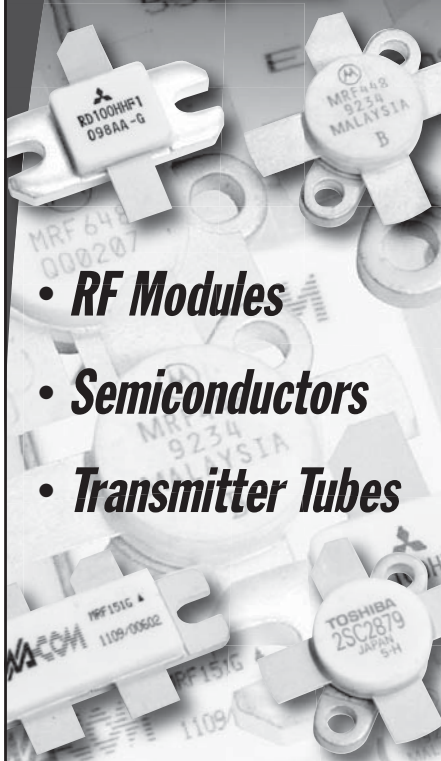
The first blue line that I encounter is (see Figure 2): **125092 Tcl Script File Ethernet/tx\_pll.qip not found**

This is interesting, since it refers to an old PLL that I removed from the project, tx\_pll. Click the triangle in column 1 to expand the warning and get more information. Unfortunately, this is one of those warnings that you cannot click on, so we have to figure it out for ourselves. The second line says: **125063 set\_global\_assignment -name QIP\_FILE Ethernet/tx\_pll.qip**

This is an assignment present in the Hermes.qsf file. How do I know this? From experience. How can you come to know this? Google! Paste **set\_global\_assignment** into Google search and the first hit explains more than you ever wanted to know. Go ahead, try it. The Quartus help page that Google points you to explains what the command does, its syntax, and so on. But all we need to know is *where it is located*, so we can remove it. It is in the project's Quartus Settings File, or **Hermes.qsf**. We must be especially careful when modifying the qsf file; it is kind of like editing your Windows registry. You can damage your project beyond repair if you edit this file with wild abandon. So here are three rules to follow to keep you project safe.

1. **NEVER** edit the qsf file while Quartus is open.
2. Always make a backup before opening

From **MILLIWATTS**  
To **KILOWATTS**<sup>SM</sup>  
*More Watts per Dollar*<sup>SM</sup>  
**In Stock Now!**  
**Semiconductors**  
**for Manufacturing**  
**and Servicing**  
**Communications**  
**Equipment**



Se Habla Español • We Export  
Phone: **760-744-0700**  
Toll-Free: **800-737-2787**  
(Orders only) **800-RF PARTS**  
Website: **www.rfparts.com**  
Fax: **760-744-1943**  
**888-744-1943**  
Email: **rfp@rfparts.com**



**RF PARTS**<sup>TM</sup>  
COMPANY  
From Milliwatts to Kilowatts<sup>SM</sup>



the file in a text editor

3. Use a *text editor* (like notepad) not a *word processor* to make changes

Notice that in #1, the word never is in bold, underlined italics. Quartus reads this file in, modifies this internal copy and then writes it out upon exit. If you change it while Quartus has it open, you are wasting your time, and just asking for trouble. So, after all that, exit Quartus, open **Hermes.qsf** in your favorite text editor, find the offending line and delete it. Save the qsf file (remember: text-only format) and exit your text editor. Re-open the project in Quartus (hint: use <Recent Projects> on the <File> menu). But wait, all of my messages are gone! Don't panic, they were saved just for you. Under the <Processing> menu, click <Compilation Report>, or just type <ctrl>R if you are lazy like me. When the report window opens, look in the left pane for **Flow Messages** and click on it. Like magic, all of your messages are back, although in a different window. (You sure are being picky!) On to the next warning! **10858 Verilog HDL warning at Hermes.v(1068): object frequency\_change used but never assigned**

This is one that you can double-click, so go ahead and do it. Quartus automatically opens the **Hermes.v** file and highlights the offending line. Search through the file (use <ctrl>F) to see where the variable **frequency\_change** is used. Note that it is passed to the CC\_encoder module using the same name, so open **CC\_encoder.v** and search for it there. Note that it is an input to CC\_Encoder and used on line 108, but it is never set to a value anywhere. This is what Quartus is complaining about: shouldn't you set a variable to a value before you use it? Well, yes, but... If you choose to ignore this warning, you will get whatever the default value for the variable **frequency\_change** is. Go back to your Flow Messages window, and it tells you what value it will use. Darn clever, this compiler. This is not fatal, so we will opt to come back and fix it later. Next! **10034 Output port "outclk\_2" at PLL\_IF\_new\_0002.v(17) has no driver**

When you double-click on this one, Quartus takes you to the **PLL\_IF\_new\_002.v** file and highlights line 17. But wait, we didn't create this file, the Wizard did. This is one of those cases where we just leave it alone and live with the warning. There are lots of these "has no driver" warnings, and they all point to Wizard-generated files. We can ignore all of them. Next! **10230 Verilog HDL assignment warning at sdr\_send.v(118): truncated value with size 32 to match size of target (8)**

This kind of warning is very common. It occurs whenever we try to assign a value represented in a certain bit width to a variable of a different width. Double click on the warning to see line 118 in **sdr\_send.v**. The

parameter **NR** has a width of 32 bits, while the variable **number\_RX** is only 8 bits wide. Quartus tells us exactly what it is going to do: truncate (i.e., discard) the 24 upper bits of **NR** and use just the bottom 8 to set **number\_RX**. Since I would have to figure out how to define an 8-bit parameter, and the result is what I wanted anyway, I don't have to fix this one either. On to the next. **12030 Port "extclk" on the entity instantiation of "cyclonev\_pll" is connected to a signal of width 1. The formal width of the signal in the module is 2. The extra bits will be left dangling without any fan-out logic.**

If you double click on this one, you see that it is a Wizard generated warning, so we can't really fix it. **12020 Port "ordered port 0" on the entity instantiation of "fir3" is connected to a signal of width 32. The formal width of the signal in the module is 1. The extra bits will be ignored.**

This looks like the last one, but it points to **receiver2.v**, which is one of our files. This is like the truncated value warning. On line 144 of **receiver2.v**, the first value inside the parentheses is a zero. If you look at the file **firx2r2.v**, you will see that this corresponds to this input signal **reset**. The variable is one bit wide, but the default width of a number is 32 bits wide. Now since the number is zero in this case, it doesn't much matter. A better way would be to define the zero as a 1-bit constant (instead of 32-bits) like this: **1'b0**.

There are many more warnings than I have space to cover, but there is one more important one: **171167 Found invalid Fitter assignments. See the Ignored Assignments panel in the Fitter Compilation Report for more information.**

This usually means there are invalid fitter assignments in the qsf file that should be fixed or removed. To get to the Fitter Compilation Report, in the left pane of the compilation report click on the triangle next to **Fitter** to expand it, and then click on **Ignored Assignments**. Now you see a table (containing only one line) that shows you the name of the signal (**PHY\_CLK125** in this case) and where it is located (the qsf file in this case). You already know how to do this: close Quartus, backup **Hermes.qsf**, open **Hermes.qsf** and remove the offending line, save the file, reopen the project in Quartus.

Hopefully this exercise has given you a better feel for Quartus and what its capabilities are along with the confidence to jump in and get your feet wet. The final step, of course, is to recompile the project, see *fewer* warnings than before, then load the compiled programming file into the BeMicroCVA9 and test it to make sure that it works. I will cover how to load and run the code on real hardware in my next column.

An updated Quartus archive containing all of the changes that we have made is available on the SDRstick SVN webserver.<sup>13</sup>

## What's Next?

Remember that the openHPSDR project is open source, and the Apache Labs Anan series of transceivers are all powered by open-source FPGA firmware. Each openHPSDR board has an on-board FPGA and Verilog code to match. All of it is available from the openHPSDR repository<sup>14</sup>. Try your hand at some FPGA coding, now that you see how easy it is! The tools that you have used today are the very same tools that the developers use when they write or update the code.

Source code and reference files for this article are on the [www.arrrl.org/QEXfiles](http://www.arrrl.org/QEXfiles) web page.

As always, please drop me an e-mail if you have any suggestions for topics you would like to see covered in future Hands-On-SDR columns or even just to let me know whether or not you found this discussion useful.

## Notes

<sup>1</sup>Scotty Cowling, WA2DFI, "Hands On SDR", QEX, Mar/Apr 2015, pp 9-19.

<sup>2</sup>Scotty Cowling, WA2DFI, "Hands On SDR", QEX, Jan/Feb 2016, pp 28-34.

<sup>3</sup>BeMicroCVA9 from Arrow Electronics: [arrow.com/en/products/bemicrocva9/arrow-development-tools](http://arrow.com/en/products/bemicrocva9/arrow-development-tools)

<sup>4</sup>UDPSDR-HF2 from Arrow Electronics: [arrow.com/en/products/udpsdr-hf2/arrow-development-tools](http://arrow.com/en/products/udpsdr-hf2/arrow-development-tools)

<sup>5</sup>UDPSDR-TX2 from Arrow Electronics: [arrow.com/en/products/udpsdr-tx2/arrow-development-tools](http://arrow.com/en/products/udpsdr-tx2/arrow-development-tools)

<sup>6</sup>UDPSDR-HF1 from Arrow Electronics: [arrow.com/en/products/udpsdr-hf1/arrow-development-tools](http://arrow.com/en/products/udpsdr-hf1/arrow-development-tools)

<sup>7</sup>Hermes-Lite wiki: [github.com/softerhardware/Hermes-Lite/wiki](https://github.com/softerhardware/Hermes-Lite/wiki)

<sup>8</sup>Free Altera Web Edition software: [dl.altera.com/?edition=web](http://dl.altera.com/?edition=web)

<sup>9</sup>The source code is available from the SDRstick SVN at [svn.sdrstick.com](http://svn.sdrstick.com) under the <sdrstick-release/BeMicroCV-A9/Hermes-HF2-Port/firmware/source> directory. The file name is <Hermes\_1\_May.qar>

<sup>10</sup>The cross reference of Hermes to IQ2 pins is available from the SDRstick SVN in the same directory as above. The file name is <Hermes\_1\_May\_to\_IQ2\_pins.pdf>

<sup>11</sup>The pin location Tcl script file is available from the SDRstick SVN in the same directory as above. The file name is <Hermes\_1\_May\_map\_pins.tcl>

<sup>12</sup>Yes, a # symbol, commonly known as a pound sign is called an octothorpe. See [en.wiktionary.org/wiki/octothorpe](http://en.wiktionary.org/wiki/octothorpe)

<sup>13</sup>Source code containing all of the changes outlined in this column is available from the SDRstick SVN at [svn.sdrstick.com](http://svn.sdrstick.com) under the <sdrstick-release/BeMicroCV-A9/Hermes-HF2-Port/firmware/source> directory. The file name is <Hermes\_1\_May\_ported.qar>

<sup>14</sup>For HPSDR firmware, look in the TAPR repository [svn.taprr.org](http://svn.taprr.org) in <main/trunk>

# Letters to the Editor

## Introducing AACTOR: A New Digital Mode (Jan/Feb 2016)

Gentlemen,

The article, "Introducing AACTOR: A New Digital Mode", by Joseph Roby Jr, KØJJR, is very interesting, but so technically flawed that it actually caused me to laugh and to think this article might better be published for the April Fool's day issue.

Mr. Roby goes seriously astray in his attempt to describe binary notation as he delves into a description of using binary notation of fractional numbers by encoding their value in binary to the right of the decimal point. After all, it is "binary", a numbering system entirely based on two whole integer numbers, zero and 1, also described as "base 2". The decimal point by definition only applies to decimal, or base 10, notation. Although this approach has occasionally been used as a teaching method by academia, it is sadly inaccurate and confusing. Its use in converting decimal fractions to binary notation is a laborious process, and also is inaccurate in that it will produce binary numbers of infinite length.

The entire concept of a binary number using a decimal point in its representation is invalid, a detail that Mr. Roby himself asserts by stating, "By using binary notation, and by disregarding the 0 to the left of the decimal point as well as the decimal point itself, *f* simply becomes a stream of binary ones and zeros."

How true. This entire process is not applicable for use in software based algorithms.

For over fifty years, the common practice for representation of fractional numbers in binary has been floating point notation. Not only is its use common, it is the standard notation used by all computer platforms for fractional arithmetic operations. Throughout this time, computer scientists, programmers, engineers and academicians have understood and used floating point notation with absolute accuracy and confidence.

I'm sorry, I do appreciate Mr. Roby's attempt to present us with a fascinating method of improving the speed of RTTY mode communications, but his article is difficult to take seriously. — *Regards, Dave Phillips, KB7JS 3818 W. Sandra Terrace, Phoenix, AZ 85053, utahdog@msn.com.*

[Careful readers like you keep us all on our toes. You are right, of course, the "decimal point" refers to the radix character only in decimal or base-ten notation, not in binary notation.

I found nothing wrong in the way Joe, KØJJR, expresses the full gamut of binary numbers, as having an integer part and a fractional part separated by the radix character. This is the same as in decimal notation, and for that matter, in any radix (base) notation. Thus, the text surrounding his

Equation (3) looks robust. I don't think that he contradicts himself in your quotation of his work. He has simply found an efficient way of encoding characters. This leads me to ask you important questions. What are the specific errors that you have found in Joe's article that need correction? Is there an error in the algorithm? — *Ed.*]

### [Dear Editor,]

To be more specific, I do not intend to be critical of Mr. Roby's expertise, especially his compression algorithm, as it is a very intelligent and well thought work. However, the algorithm is successful for only its intended application because it is artificially limited by severe constraints placed on the input data. Compressing true random binary data is a much more challenging task.

Granted, the intent here is the exchange of human readable textual strings, nothing more. But even within that constraint, I believe other communications protocols in use today are far more useful, especially since the transmission medium is so inherently unreliable due to signal fading and noise. — *Regards, Dave Phillips, KB7JS 3818 W. Sandra Terrace, Phoenix, AZ 85053, utahdog@msn.com.*

### [The author responds]

Thank you for the opportunity to respond to KB7JS's letter, which has two questions. First, the letter questions my description of binary notation. Keeping in mind that the QEX mission "strive[s] to maintain a balance between theoretical and practical content." Keeping in mind that most QEX readers are not computer systems engineers, my description of binary notation was sufficiently accurate for purposes of the article. Indeed, the letter concedes that the article's description "has occasionally been used as a teaching method by academia." Also, as stated in the article, adaptive arithmetic coding (AAC) produces fixed-length strings of ones and zeros, not "binary numbers of infinite length" as stated in the letter. Were it otherwise, AAC would be useless for lossless data compression in any application.

Second, the letter states, correctly, that floating point notation is common practice in computer science. The letter then questions why the article did not utilize that notation. Perhaps there is a technique for utilizing floating point notation to convert a text message to a compressed string of ones and zeros, but the article employed a different technique. The article employed AAC and binary notation to create a string of one and zeros significantly shorter than the string of ones and zeros created by RTTY for the same message. The C++ code for doing so

From **MILLIWATTS**  
To **KILOWATTS**

*More Watts per Dollar*



**Transmitting & Audio Tubes**



**COMMUNICATIONS  
BROADCAST  
INDUSTRY  
AMATEUR**

*Immediate Shipment from Stock*

3CPX800A7	4CX1000A	810
3CPX1500A7	4CX1500B	811A
3CX400A7	4CX3500A	812A
3CX800A7	4CX5000A	833A
3CX1200A7	4CX7500A	833C
3CX1200D7	4CX10000A	845
3CX1200Z7	4CX15000A	6146B
3CX1500A7	4CX20000B	3-500ZG
3CX3000A7	4CX20000C	3-1000Z
3CX6000A7	4CX20000D	4-400A
3CX10000A7	4X150A	4-1000A
3CX15000A7	572B	4PR400A
3CX20000A7	805	4PR1000A
4CX250B	807	...and more!

*Se Habla Español • We Export*

Phone: **760-744-0700**

Toll-Free: **800-737-2787**

(Orders only) **RF PARTS**

Website: **www.rfparts.com**

Fax: **760-744-1943**

**888-744-1943**

Email: **rfp@rfparts.com**





**We Design And Manufacture  
To Meet Your Requirements**

**\*Prototype or Production Quantities**

**800-522-2253**

**This Number May Not  
Save Your Life...**

**But it could make it a lot easier!  
Especially when it comes to  
ordering non-standard connectors.**

**RF/MICROWAVE CONNECTORS,  
CABLES AND ASSEMBLIES**

- Specials our specialty. Virtually any SMA, N, TNC, HN, LC, RP, BNC, SMB, or SMC delivered in 2-4 weeks.
- Cross reference library to all major manufacturers.
- Experts in supplying "hard to get" RF connectors.
- Our adapters can satisfy virtually any combination of requirements between series.
- Extensive inventory of passive RF/Microwave components including attenuators, terminations and dividers.
- No minimum order.



**NEMAL ELECTRONICS INTERNATIONAL, INC.**

12240 N.E. 14TH AVENUE

NORTH MIAMI, FL 33161

TEL: 305-899-0900 • FAX: 305-895-8178

E-MAIL: INFO@NEMAL.COM

BRASIL: (011) 5535-2368

**URL: WWW.NEMAL.COM**

**Down East Microwave Inc.**

We are your #1 source for 50MHz to 10GHz components, kits and assemblies for all your amateur radio and Satellite projects.

Transverters & Down Converters, Linear power amplifiers, Low Noise preamps, coaxial components, hybrid power modules, relays, GaAsFET, PHEMT's, & FET's, MMIC's, mixers, chip components, and other hard to find items for small signal and low noise applications.

**We can interface our transverters  
with most radios.**

Please call, write or  
see our web site

**www.downeastmicrowave.com**  
for our Catalog, detailed Product  
descriptions and  
interfacing details.

Down East Microwave Inc.  
19519 78th Terrace  
Live Oak, FL 32060 USA  
Tel. (386) 364-5529

is posted on the [www.arrl.org/qexfiles](http://www.arrl.org/qexfiles) web page. It works, seriously. — 73 and thank you, Joseph J. Roby, Jr., KØJJR.

**[Errata]**

Author Roby, KØJJR, reports that in Equation (5) on page 14, the text above the summation symbol should be  $j=i$ , not  $j=1$ .

**Calculation of FM and AM Noise  
Signals of Colpitts Oscillators in  
the Time Domain (Mar/Apr 2016)**

**[Errata]**

Equations (1) and (2) show partial differentials of  $E_B$  and  $E_H$  with respect to themselves. What's the exact meaning? Also should the  $w$  in Equations (119) – (122) be  $\omega$ ? — 73, Ward Silver, NØAX, [hwardsil@gmail.com](mailto:hwardsil@gmail.com).

**[Errata]**

Victor Battaglia, KA2AGG, points out that on pages 33 – 34 equations 101 and 102 are the identical.

**[Reply from Dr. Ajay K. Poddar and  
author Dr. Ulrich Rohde, N1UL]**

The corrected Equations (1) and (2) are,

$$\left[ \frac{\partial E_H}{\partial X_H} \right]_s \partial X_H = J_H(\omega) \quad (1)$$

$$\left[ \frac{\partial E_B}{\partial X_B} \right]_s \partial X_B = J_B(\omega) \quad (2)$$

Yes, equations 101 and 102 on pages 33 – 34 are the same, it is a duplication error. The  $w$  in Equations (119) – (122) should be  $\omega$ . — Regards, Ajay Poddar, [akpoddar@synergymwave.com](mailto:akpoddar@synergymwave.com) .and Dr. Ulrich Rohde, N1UL.

**Perspectives (May/June 2016)**

**Hi Fellows,**

As a long time reader and contributor to both *QST* and *QEX*, I am somewhat perplexed with what looks like a major shift in the content of *QEX*. While *QEX* was born of a need to address the more technical aspects of the Amateur Radio hobby, I think the recent change in editorship has taken the technical side a bit too far. There are topics that *QEX* should address from a purely theoretical stance, but they should be coupled to the hobby and Amateur Radio service in some way. Granted, the hobby is changing and technology is pushing those changes, but let's not forget that it is a hobby for a broad spectrum of participants of whom very few are ready to deal with articles more fit for publication in the IEEE proceedings than in a ham radio publication.

And finally I found Kai's remarks on "Constants and Standards" to be pedantic,

if not condescending, comments that seem to be reflected in the slant of and contents of current *QEX* issues. — 73, Bob Miller, KE6F, 9239 Knights Lane, Wilton, CA 95693, [millerke6f@aol.com](mailto:millerke6f@aol.com).

**Hello Bob,**

[I very much appreciate your feedback and comments on the recent issues of *QEX*, and especially about *Perspectives*. Yes, we value your opinions about what you would like to read in *QEX*. The best way to express that opinion is by authoring articles. If you don't write it, we can't publish it for others to enjoy. — Ed.]

**Dear Editor,**

A comment about SI. The reason Myanmar (Burma) still uses the Imperial System is because it was heavily influenced by the British back when the UK was using the Imperial System. And of course Liberia was set up by the freed slaves from the US who went back to Africa, and what they knew was the Imperial System. I lived in Singapore for four years and understand that Myanmar now has a plan to switch to SI.

I too am a stickler about using standards, so much so that I have been accused of being anal. For instance the correct pronunciation of kilometer is KILO-METER, not KIL-UM-MET-TER, as you are to announce the prefix. And the correct pronunciation of gigahertz is JIG-AH-HERTZ, not GIG-AH-HERTZ. My areas of expertise are SI and schematic diagram reference designations. I am a volunteer member of the ASME Y14.44 subcommittee.

Welcome aboard as the new *QEX* Editor. — 73, Larry Joy, 9V1MI/WN8P, ARRL LM and MI Section TS.

**Dear Editor,**

Whatever you're doing to get these high-quality articles keep it up! I read every article of the Mar/Apr and May/June issues in detail. In particular, the coding article by Franke and Taylor (May/June) is a beautiful example of where amateurs are making meaningful contributions to the state of the art. We may not be inventing new semiconductors – at least not as amateurs – but in the protocol/coding area, it's great to see real innovation on a regular basis from MF through the microwave spectrum. — 73, Ward Silver, NØAX.

[The credit for high-quality articles belongs to the authors. Expect a few microwaves articles in September, while the November issue will feature propagation articles. — Ed.]

**Dear Editor,**

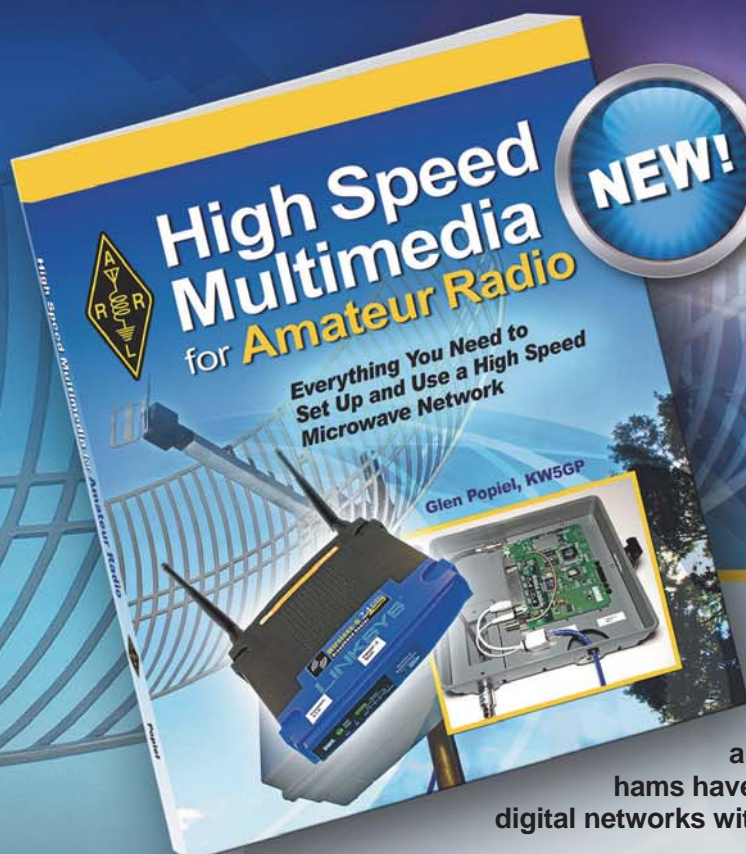
I enjoyed your editorial in the latest *QEX*. It seems like common sense to me. You just put the problem into perspective in a very pleasant and informative way. Thanks for doing that. — Lou McFadin, W5DID.



**NEW!**

# High Speed Multimedia for Amateur Radio

By **Glen Popiel, KW5GP**



## Build a High Speed Amateur Radio Microwave Network

Using commercial off-the-shelf equipment and developing their own software, groups of hams have created high speed wireless Amateur Radio digital networks with wide area coverage.

The possible uses for these high speed data networks in the Amateur Radio community are endless. Virtually any service that works on the regular Internet can be adapted to an Amateur Radio high speed multimedia (HSMM) network, including video conferencing, instant messaging, voice over Internet protocol (VoIP), network sensors and cameras, remote station control, and many other services. With the capability to send real-time video and data files, the public service and disaster support aspects of Amateur Radio are expanded tremendously.

This book introduces HSMM networking, explains the basics of how it works, and describes the various technologies in use today. Later chapters explain in detail how to deploy your own HSMM network, along with various applications to put it to work. Well illustrated step-by-step instructions will guide you through the process of installing and configuring software needed to get your HSMM network up and running.

### Includes:

- Introduction to High Speed Multimedia
- High Speed Multimedia Technologies
- HSMM Equipment for Amateur Radio
- TCP/IP for HSMM
- HSMM Applications
- Security and Filtering
- Backup and Redundancy
- Deploying HSMM Networks
- The Future of HSMM

High Speed Multimedia for Amateur Radio  
ARRL Item No. 0529

**Member Price! Only \$24.95** (retail \$27.95)



**ARRL** The national association for  
**AMATEUR RADIO®**



[www.arrl.org/shop](http://www.arrl.org/shop)

Toll-Free US 888-277-5289 or  
elsewhere +1-860-594-0355

# Quicksilver Radio

# Test Equipment

## USB Microscope



Up to 500X magnification. Captures still images and records live video. Built in LED Lighting. A must for working on surface mount components.

## Wireless Relay Switch



200'+ Range. We have single, four, and eight channel models.

## GO-PWR Plus™



Portable power to go or backup in the shack. Includes Powerpoles, bright easy to read meter, and lighted switch. For U1 size (35 ah) and group 24 (80 ah) batteries.



## Digital Voltmeter/ Ammeter

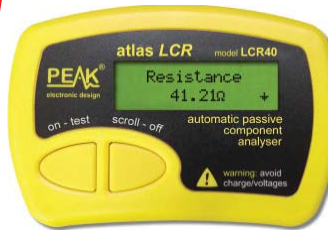
Two line display shows both current and voltage. Included shunt allows measurement up to 50A and 99V. Snaps into a panel to give your project a professional finish.

## LCR and Impedance Meter



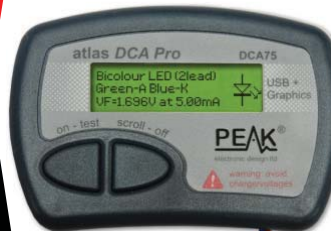
Newest Model. Analyzes coils, capacitors, and resistors. Indicates complex impedance and more.

## Automatic Passive Component Analyzer



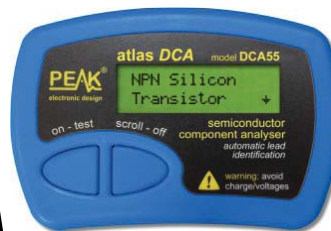
Analyzes coils, capacitors, and resistors.

## Advanced Semiconductor Component Analyzer



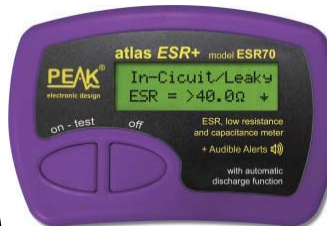
Analyzes transistors, MOSFETs, JFETs, IGBTs, and more. Graphic display. Enhanced functionality with included PC software.

## Semiconductor Component Analyzer



Analyzes transistors, MOSFETs, JFETs and more. Automatically determines component pinout.

## Capacitance and ESR Meter



Analyzes capacitors, measures ESR.

Get All Your Ham Shack Essentials at Quicksilver Radio Products. Safe and Secure Ordering at:

[www.qsradio.com](http://www.qsradio.com)



